Atmospheric Transport and Fate of Mercury and its Impacts on New York State

Final Report 05-05
July 2005

New York State
Energy Research and
Development Authority

NYSERDA

NYSERDA

The New York State Energy Research and Development Authority (NYSERDA) is a public benefit corporation created in 1975 by the New York State Legislature. NYSERDA's responsibilities include:

- Conducting a multifaceted energy and environmental research and development program to meet New York State's diverse economic needs.
- Administering the **New York Energy $mart**[SM] program, a Statewide public benefit R&D, energy efficiency, and environmental protection program.
- Making energy more affordable for residential and low-income households.
- Helping industries, schools, hospitals, municipalities, not-for-profits, and the residential sector, including low-income residents, implement energy-efficiency measures.
- Providing objective, credible, and useful energy analysis and planning to guide decisions made by major energy stakeholders in the private and public sectors.
- Managing the Western New York Nuclear Service Center at West Valley, including: (1) overseeing the State's interests and share of costs at the West Valley Demonstration Project, a federal/State radioactive waste clean-up effort, and (2) managing wastes and maintaining facilities at the shut-down State-Licensed Disposal Area.
- Coordinating the State's activities on energy emergencies and nuclear regulatory matters, and monitoring low-level radioactive waste generation and management in the State.
- Financing energy-related projects, reducing costs for ratepayers.

NYSERDA administers the **New York Energy $mart**[SM] program, which is designed to support certain public benefit programs during the transition to a more competitive electricity market. Some 2,700 projects in 40 programs are funded by a charge on the electricity transmitted and distributed by the State's investor-owned utilities. The **New York Energy $mart**[SM] program provides energy efficiency services, including those directed at the low-income sector, research and development, and environmental protection activities.

NYSERDA derives its basic research revenues from an assessment on the intrastate sales of New York State's investor-owned electric and gas utilities, and voluntary annual contributions by the New York Power Authority and the Long Island Power Authority. Additional research dollars come from limited corporate funds. Some 400 NYSERDA research projects help the State's businesses and municipalities with their energy and environmental problems. Since 1990, NYSERDA has successfully developed and brought into use more than 170 innovative, energy-efficient, and environmentally beneficial products, processes, and services. These contributions to the State's economic growth and environmental protection are made at a cost of about $.70 per New York resident per year.

Federally funded, the Energy Efficiency Services program is working with more than 540 businesses, schools, and municipalities to identify existing technologies and equipment to reduce their energy costs.

For more information, contact the Communications unit, NYSERDA, 17 Columbia Circle, Albany, New York 12203-6399; toll-free 1-866-NYSERDA, locally (518) 862-1090, ext. 3250; or on the web at www.nyserda.org

Atmospheric Transport and Fate of Mercury and its impacts on New York State

Final Report

Prepared for the

New York State Energy Research and Development Authority

Albany, NY

www.nyserda.org

Mark R. Watson

Senior Project Manager

Prepared by

Atmospheric Sciences Research Center

State University of New York

Albany, NY

Chris Walcek

and

Atmospheric Modeling and Weather Forecasting Group

University of Athens

Athens, Greece

George Kallos

NYSERDA
Report 05-05

NYSERDA 6488

July 2005

PREFACE

The New York State Energy Research and Development Authority (NYSERDA) is pleased to publish "Atmospheric Transport and Fate of Mercury and its Impacts on New York State." This report was prepared by the Atmospheric Sciences Research Center, located in Albany, NY. This project was funded as part of the New York Energy $mart^{SM} Environmental Monitoring, Evaluation and Protection (EMEP) program and represents one of several studies focusing on air quality issues associated with the generation of electricity. More information on the EMEP program may be found on NYSERDA's website at: www.nyserda.org/programs/environment/emep/.

NOTICE

This report was prepared by the Atmospheric Sciences Research Center in the course of performing work contracted for and sponsored by the New York State Energy Research and Development Authority (hereafter the "Sponsor"). The opinions expressed in this report do not necessarily reflect those of the Sponsor or the State of New York, and reference to any specific product, service, process, or method does not constitute an implied or expressed recommendation or endorsement of it. Further, the Sponsor and the State of New York make no warranties or representations, expressed or implied, as to the fitness for particular purpose or merchantability of any product, apparatus, or service, or the usefulness, completeness, or accuracy of any processes, methods, or other information contained, described, disclosed, or referred to in this report. The Sponsor, the State of New York, and the contractor make no representation that the use of any product, apparatus, process, method, or other information will not infringe privately owned rights and will assume no liability for any loss, injury, or damage resulting from, or occurring in connection with, the use of information contained, described, disclosed, or referred to in this report.

ACKNOWLEDGMENTS

NYSERDA appreciates the input of EMEP Program Advisors and Science Advisors for their review of this project report.

TABLE OF CONTENTS

FIGURES

TABLES

EXECUTIVE SUMMARY

A speciated inventory of mercury emissions, based on the 1996 EPA mercury emissions inventory, has been prepared and implemented into two comprehensive atmospheric mercury models in order to assess the fate of mercury in New York State. A model for assessing policies designed to mitigate undesirable mercury effects in New York State has been delivered to the New York State Department of Environmental Conservation (NYSDEC).

This NYSERDA research initiative facilitated collaboration between researchers at the NYSDEC and the State University of New York (SUNY) Atmospheric Sciences Research Center (ASRC) in developing a comprehensive inventory of speciated mercury emissions for eastern North America. This mercury emission inventory represents a consolidation of information gathered by the U.S. Environmental Protection Agency (EPA), Canadian authorities, and the Electric Power Research Institute (EPRI), and speciation profiles for each individual point source in the inventory have been extrapolated from all available speciation measurements. Past mercury emission inventories reported only total mercury emissions, and speciation was performed during the modeling phase using ad hoc assumptions about partitioning among less reactive gaseous Hg(0) or more reactive gaseous mercury [RGM or Hg(2)] and particulate Hg_p based only on a single "anthropogenic" speciation profile not specific to each individual point source.

Two regional-scale models of atmospheric mercury were used to simulate a 1997 13-day summertime episode in eastern North America. This research effort initiated a scientific collaboration between the Atmospheric Modeling group at the University of Athens with established expertise in mercury modeling and the NYSDEC air pollution modeling group. NYSDEC scientists gathered all available mercury concentration and wet deposition measurements in the eastern U.S. for the initial assessment and evaluation of the mercury models used by Dr. Kallos' Atmospheric Modeling group at University of Athens (UA).

Simulated mercury wet deposition using the improved mercury emission inventory developed during this research effort in two UA mercury models showed reasonable agreement (within a factor of two) with available wet deposition measurements, although clearly there were inadequate measurements to perform a comprehensive model evaluation. Significant discrepancies were noted between the two atmospheric mercury models in this study. These differences are related to the treatment of parameterized microphysics and scavenging used by the models, suggesting a need for further evaluation and refinement of atmospheric mercury models. However, measurements of mercury deposition are altogether too sparse and intermittent to make robust conclusions about the accuracy of these state-of-the-science models. Measurements are only

available at isolated sites for restricted time periods using weekly-accumulated precipitation, while it is well known that accurate assessments of model performance would require considerably higher time and space resolution, and longer term comparisons between model simulations and measurements.

Additional modeling results showed that in-state mercury emissions contributed 11-21% of total accumulated wet deposition of mercury to the Adirondacks area during a 13-day summertime period, highlighting the influence of mercury sources outside New York State to mercury impacts in the state. The relatively low local (in-state) contribution to mercury deposition in New York State results from the extremely long residence time of mercury in the atmosphere, a feature that renders mercury pollution a global-scale phenomenon. Further "influence function" studies showed extremely fine-scale structure to the upwind areas impacting mercury concentrations and deposition at individual sites in New York State, suggesting the need for high-resolution models of the fine-scale air flows in New York State in order to accurately assess mercury impacts resulting from in-state emission sources.

The following report provides a more detailed description of the accomplishments of this research effort, and is divided into five sections:

1. Emission Inventory Development
2. Regional Scale Mercury Modeling Studies
3. Influence Function Analysis
4. Project Approach and Overview
5. Recommendations for Future Efforts

Section 1
EMISSION INVENTORY DEVELOPMENT

In order to develop effective environmental policies to reduce the release of mercury in the environment and monitor progress over time, it is necessary to develop an accurate quantification of mercury emissions for use in air quality models. Models of atmospheric mercury constitute an essential tool for estimating concentrations and deposition of atmospheric mercury resulting from anthropogenic emissions, and assessing the relationship between undesirable impacts and controllable emissions. The inventory generated here is extracted from point and area source inventories of mercury emissions within eastern North America archived by U.S. and Canadian environmental protection agencies, augmented with source information provided by the Electric Power Research Institute (EPRI), a research agency supported by U.S. electric generating utilities.

Past emission inventories for mercury have been prepared based on relatively sketchy country-total emission reporting information. For example, Global Emissions Inventory Activity (GEIA 1998) presented a global inventory of 1990 mercury emissions that has been used in previous modeling studies (Shia et al., 1999). The 1990 GEIA global inventory was constructed largely from individual countries reporting total emissions without specifying precise source locations. In order to spatially distribute country totals, the 1990 GEIA inventory used population density distributions to spatially locate mercury emissions within each reporting country. In the inventory described here, mercury emissions are spatially distributed using point source locations reported by individual states to the EPA.

Under the 1990 U.S. Clean Air Act, the EPA has developed a National Toxics Inventory (NTI) of Hazardous Air Pollutant (HAP) emissions. The NTI represents a consolidation of reports submitted by states that is updated every three years. In this study the 1996 EPA inventory was used, although a 1999 inventory became available late in 2002, slightly before the end of this research effort. In addition to reporting emission amounts for various HAPs, the inventory documents source characteristics and stack information that is used for subsequent speciation and placement of mercury emissions.

Mercury emissions reported in the NTI were assigned to three chemical forms of mercury: unreactive gaseous mercury [Hg(0)], reactive gaseous mercury [Hg(2)], and particulate mercury [Hg_p]. Source-specific speciation proportions were assigned to each mercury point and area source defined in the NTI archive based on available stack measurements, laboratory studies, and EPA recommendations. Considerable effort also went into quality assuring the stack information provided for point sources. Numerous inconsistencies were noted in the stack diameters, exhaust temperatures, and flow velocities that apparently resulted from

ambiguous reporting requirements in place at the time the NTI was collected from individual states and local air pollution control agencies.

Figure 1 shows total [Hg(0) + Hg(II), gaseous + particulate] emissions over eastern North America. The highest areas of mercury emissions in eastern North America are just west of Washington D. C., near New York City, and two locations in Florida, although mercury emissions are spread widely throughout the area, with some localized emission peaks in the Ohio River Valley, and other local emission peaks associated with some urbanized areas. Local extremes in total mercury emissions are associated with individual especially strong point sources. West of Washington D.C., the large point source is associated with a cement production facility there. The two large source areas in Florida are associated with waste incinerators in the Tampa and Miami areas. Several large municipal waste incinerators combine to produce the high just to the east of New York City.

This inventory was compared with an earlier GEIA 1990 inventory, and significant discrepancies were found (Walcek et al., 2003). Total emissions in this updated inventory over eastern North America are about 64% of the emissions reported in the 1990 GEIA inventory. Some of this discrepancy can be attributed to emission changes between 1990-1996, but most of these discrepancies result from the lack of quality point source data in the earlier inventory.

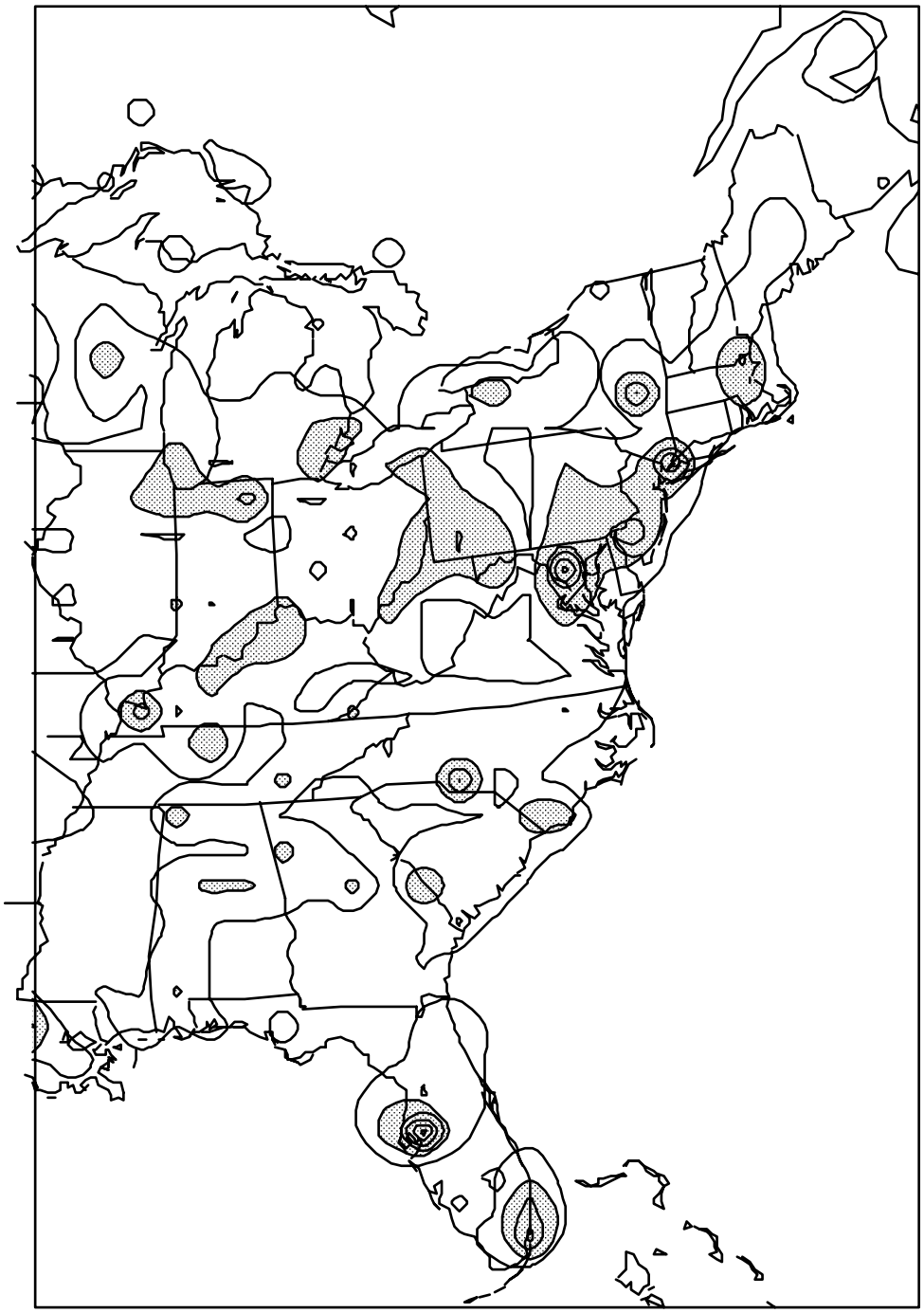

Figure 1: Spatial distribution of total gaseous + particulate, Hg(0) + Hg(II) emission rates in eastern North America. Emissions are summed over Lambert-conformal 80x80 km^2 areas, and contours are drawn at 90%, 70%, 50%, 30%, 10% and 1% of the maximum emission rate (west of Washington D. C.) of 23215 moles Hg per year per 80x80 km^2 area. Total emissions in domain = 5.26×10^5 moles $year^{-1}$.

Section 2
REGIONAL-SCALE MODELING STUDIES

The emissions information described above was incorporated into two atmospheric mercury models: Regional Atmospheric Modeling System (RAMS) and University of Athens regional Eta meteorology model (Skiron/Eta), which simulated the transport, transformation and deposition of mercury in eastern North America, and focused on impacts in New York State. The RAMS is a highly sophisticated, computationally-intensive model capable of two-way interactive nesting of any number of grids, allowing for extremely high resolution simulations, which is considered necessary for studying near-source dispersion of mercury species. RAMS also includes an advanced cloud microphysical process algorithms and detailed parameterizations of surface processes. In contrast, the Skiron/Eta model is less computationally intensive, using one-seventh to one-eighth the computer resources of RAMS. Skiron/Eta uses a more coarse fixed-resolution grid, provides reasonably accurate meteorology, and incorporates a viscous sub-layer formulation that is necessary for description of mercury fluxes from the sea surface. Both models are flexible and can be applied in any part of the world. The use of two atmospheric models, in conjunction with available measurements, allows for the inter-comparison of the results and therefore, improved understanding on the discrepancies in our current understandings of atmospheric processes related to mercury.

CALCULATED MERCURY CONCENTRATIONS AND DEPOSITION

Figure 2 shows an example of the meteorological information used to assess the transport and fate of mercury by these regional-scale atmospheric models. Three-dimensional wind fields at high time resolution simulate the transport, precipitation patterns and surface physics necessary to quantify dry and wet deposition, as well as concentrations of all species of mercury.

Both models simulated a 13-day episode 14-26 August 1997 during which observations of mercury concentration and deposition are available (this 13-day period was selected since it was the identical period chosen for a previously-published regional-scale modeling study of mercury in the northeast United States). Model calculations and measurements are compared for two different emission scenarios:

1) All mercury emissions in eastern North America are included; and

2) Simulations where New York State mercury emissions are not included.

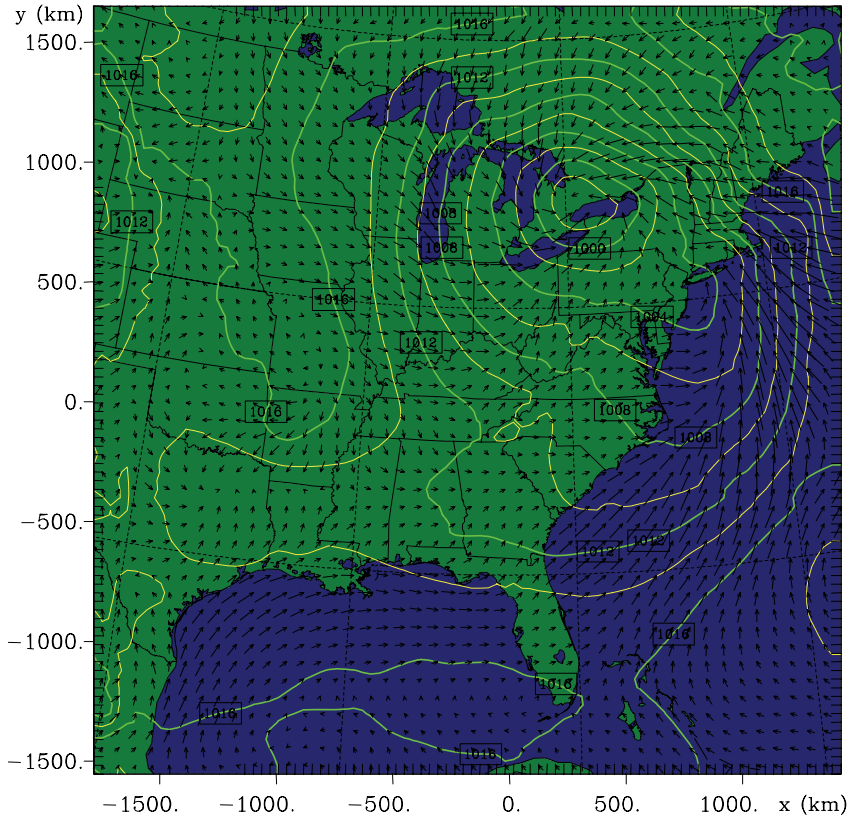

Figure 2: Mean Sea Level Pressure and total winds at 1200 UTC, on 21 August 1997 from RAMS model. Contour increment: 2 mbar.

The first set of simulations allows us to evaluate the models' performance relative to the available measurements. The second set of simulations allows us to make quantitative assessments of the impact of mercury at sensitive receptor areas in New York State that can be attributed to mercury emissions within New York State. Presumably these New York emissions are subject to potential statewide regulation, and therefore the efficacy of state-level mitigation efforts can be assessed.

Figure 3 shows the calculated wet deposition of Hg(2) during the 13-day simulation period over the eastern U.S. domain. The greatest wet deposition occurs in regions of highest precipitation, which is a highly irregular pattern, superimposed on the field of mercury downwind of the large local point sources, another complex pattern shown in Figure 1. A strong southern flow was established over the northeastern U.S. during the beginning of this 13-day period. On 21 August 1997, a deep low-pressure system extended over New York State, inducing considerable precipitation in central Pennsylvania and a strong northeastern flow

in eastern New York, with strong northwest winds over the Canadian borders into New York State. The increasing temperature as well as the strengthening southwesterly flow during this time period are important parameters that influence the dispersion and diffusion of mercury over New York State. These conditions can support the transfer of mercury from the eastern seaboard towards New York State.

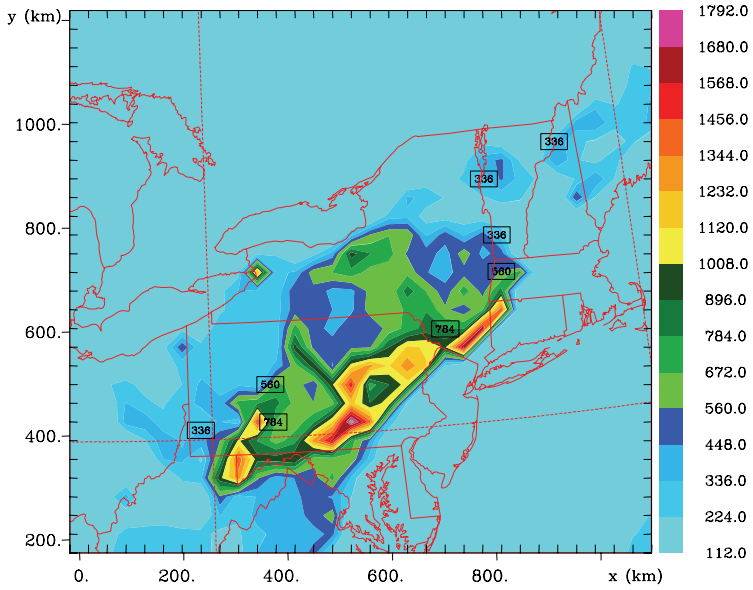

Figure 3: Accumulated wet deposition of Hg^2 (in ng/m^2) at 0000 UTC on 26 August 1997 after 13 days of simulation, estimated using the RAMS model.

The accumulated rainfall calculated by the RAMS and the Eta models during the 13-day simulation exhibit considerable differences that can be attributed to the behavior of the convective scheme used in each model. Skiron/Eta model uses the Betts-Miller-Janjic precipitation scheme, which tends to overestimate precipitation areas, without overestimating the precipitated water. On the contrary, the RAMS microphysical scheme calculates higher amounts of precipitation in more restricted areas, leading to local peaks. These differences in moisture physics of current generation meteorological models are expected and represent a key area of uncertainty that strongly influences our ability to accurately simulate mercury and impacts.

Figure 4 shows the accumulated total mercury deposition [dry + wet, Hg(0) + Hg(2)] to New York State during this 13-day period calculated by the two regional-scale pollution models used in this study (RAMS-Hg & Skiron/Eta). In general, the agreement between the calculated total deposited amounts is quite good, indicating that these models are reasonably consistent and can be used as tools for assessing longer-term impacts of concentration and deposition.

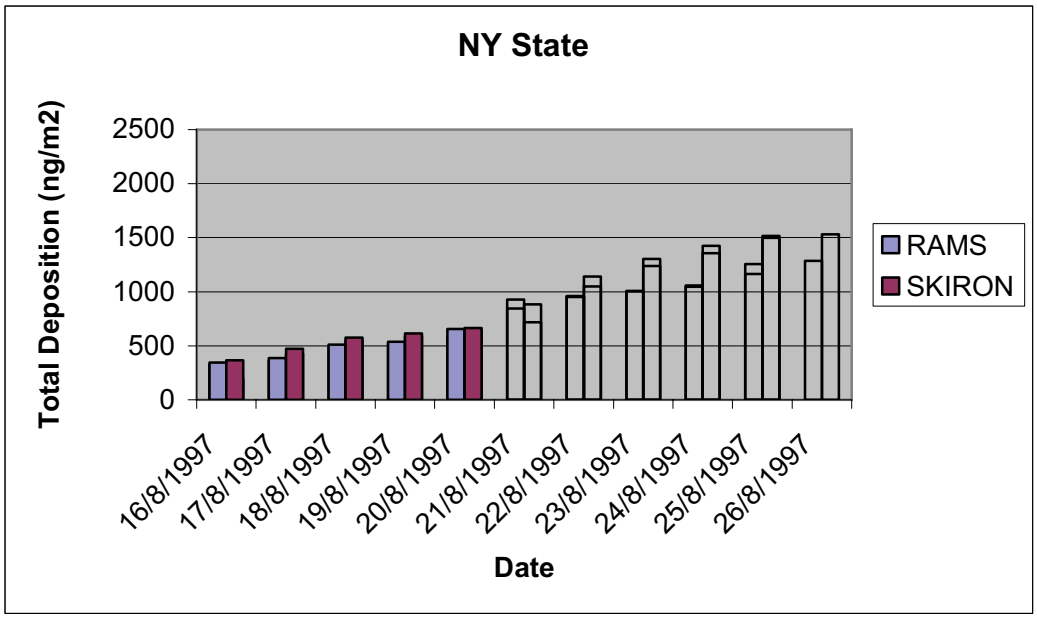

Figure 4: Accumulated deposition of mercury (ng/m^2) calculated from RAMS and Skiron/Eta systems averaged over New York State from 14 to 26 August 1997.

COMPARISONS WITH OBSERVATIONS

In order to evaluate the models' performance, calculations of Hg(2) wet deposition were compared with available wet deposition measurements from the Mercury Deposition Network (MDN). Deposition measurements are available from several locations in the northeast U.S. upwind and downwind of New York State only, and no measurement sites were located in New York State during this time period. MDN deposition observations at selected sites close to New York State (Allegheny Portage in Pennsylvania; Dorset and St. Andrews, Canada; Bridgton, Acadia and Greenville, Maine) have been compared with the accumulated wet deposition of mercury from both models. Deposition observations performed within the Regional Environmental Monitoring and Assessment Program (REMAP) site at Underhill, Vermont are also used. The available observations represent weekly accumulations of wet deposition of all mercury species, for the periods 12 to 19 August 1997 and 19 to 26 August 1997. Therefore only two deposition "observations" are available for the model simulation period for many of these sites.

Figure 5 shows a typical example of the comparison between model calculations and observations of wet deposition. Both models tend to overestimate wet mercury deposition during this period. The observations seem to be higher for the 12 to 19 August 1997 period compared to the model calculated values. On the contrary, when observations for the periods 12 to19 August and 19 to 26 August are accumulated, they are

lower than the model-calculated total deposited amount. The overestimated deposited quantities of mercury from both models are within acceptable limits, considering the uncertainties and possible errors in the observations, the limitations to observations because of weekly sampling, as well as differences of both models' convective and precipitation schemes. It is worth mentioning that even a small shift (temporal or spatial) in the model estimated rain pattern during the observation period, can strongly influence the model deposition calculations. Also it is well known that precipitation patterns show a high structure for weekly periods, and the models used here calculate precipitation averaged over larger areas of several hundreds of square kilometers. Individual collections of rainfall are known to differ appreciably from the "average" falling to a larger area surrounding the sampling site, and individual sites are often not "representative" of actual deposition to larger-scale areas for a number of physical reasons.

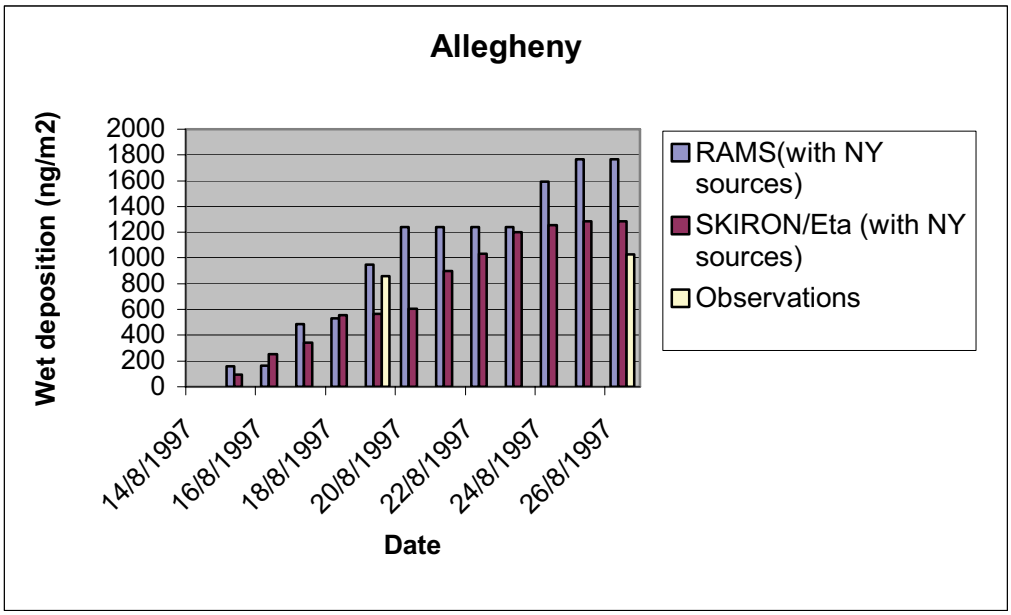

Figure 5: Comparison of observations of wet deposition of mercury (ng/m^2), RAMS and Skiron/Eta outputs at Allegheny Pennsylvania from 14-26 August 1997. RAMS and Skiron/Eta outputs are accumulated since the initial time of the simulation, while the observations correspond to weekly-deposited mercury.

ASSESSMENT OF IN-STATE VS. OUT-OF-STATE CONTRIBUTIONS

One of the goals of this research effort was to quantify the contribution of mercury emitted WITHIN the state of New York to mercury deposition at sensitive receptors in New York State. In order to quantify this contribution, two sets of simulations were performed using both Skiron/Eta and RAMS/Hg models: one

simulation included ALL mercury sources in the domain, while another set of simulations was performed with the emissions in New York State omitted from the Hg emission inventory. By subtracting the results of these two simulations, the relative contribution of in-state Hg sources can be assessed. This methodology provides an estimation of the relative contribution of in-state versus long-range transport to mercury deposition at specific locations.

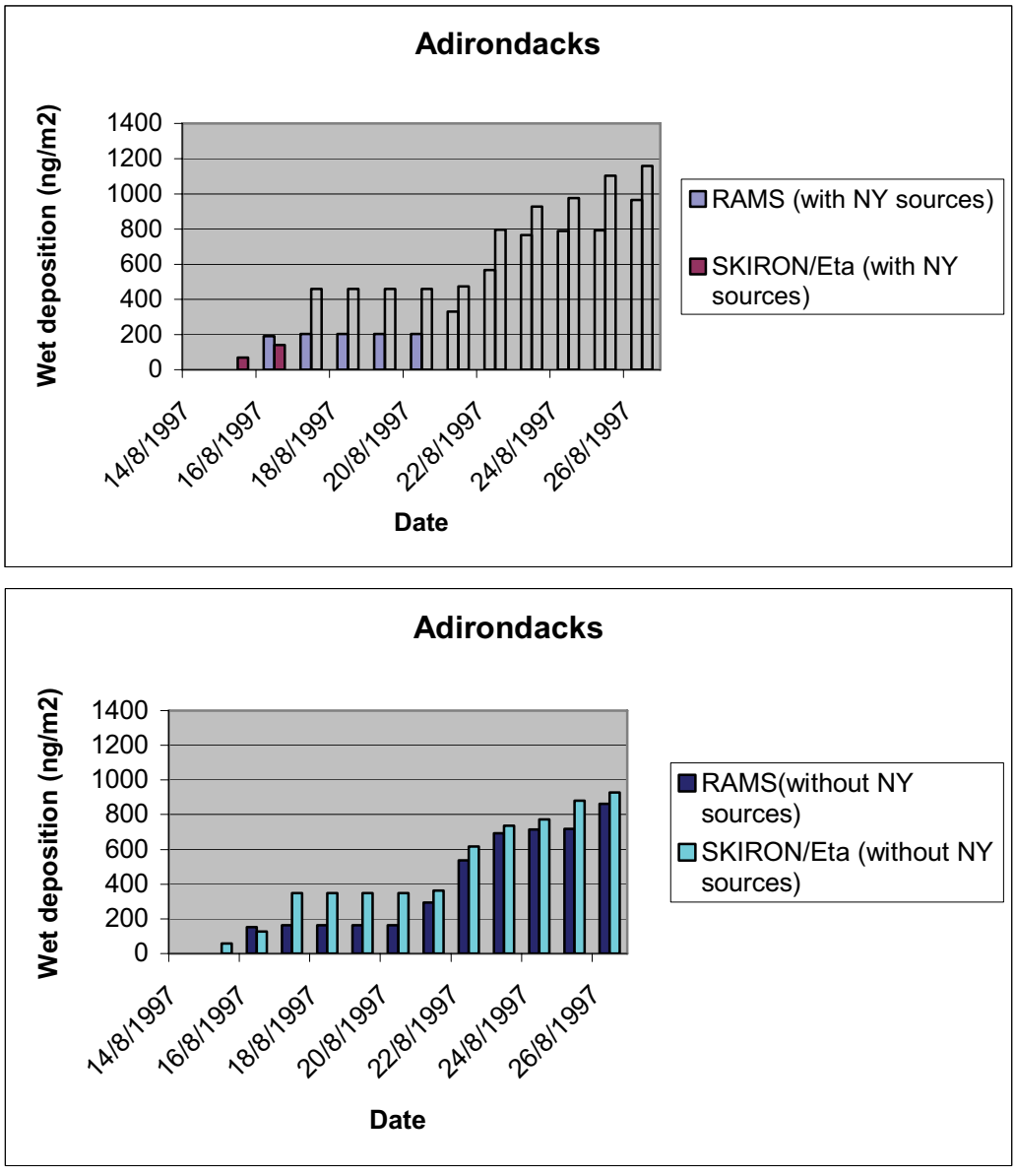

Figure 6: Accumulated wet deposition of mercury (ng/m^2) calculated from RAMS and SKIRON/Eta models with (top) and without (bottom) New York State emissions at a location in the Adirondacks from 14 to 26 August 1997.

Figure 6 compares the calculated total wet deposition of mercury at one site in New York (the Adirondack Mountains) for two simulations (with and without New York emission sources). Total wet deposition to this location in the Adirondack Mountains is reduced by up to 11% when New York mercury sources are removed during this period according to the RAMS models, while the corresponding reduction according to the Skiron/Eta models is 21%. Both of these percent reductions represent the in-state contribution to the deposition at that site. The differences between these models arise due to the different precipitation parameterizations employed by the models and the prevailing weather conditions during the simulation, especially after the 21st of August 1997.

Preliminary results comparing the two sets of simulations with and without the local in-state mercury emissions showed that across New York State, between 10-20% of the wet deposition of mercury could be attributed to mercury emissions from within the state of New York, and these contributions fluctuated during individual days of the simulation. During individual storm events the Skiron/Eta model calculated that up to 40% of the deposition could be attributed to in-state mercury emissions, while the RAMS modeling system generally calculated somewhat lower in-state contributions due to the more sophisticated cloud physics and wet deposition parameterizations included in that model.

Section 3
INFLUENCE FUNCTION ANALYSIS

In addition to these simulations, influence function calculations have been performed in order to identify the recent transport history of the air masses arriving at specific locations. These influence functions are essentially "upwind plumes" calculated backward in time from a receptor site at a particular time. Numerous backward "plumes" are calculated using the Lagrangian Particle Dispersion Model (LPDM, Uliasz and Pielke, 1991) that follows trajectories of an ensemble of particles including the influences of turbulent mixing on particle movement. Since LPDM includes a treatment of the effects of planetary boundary layer turbulence on trajectory calculations, it more realistically identifies upwind regions of influence than classical Lagrangian trajectories that ignore turbulence and its influence on air parcel movements.

Figure 7 shows an overlay of the regions influencing a site in the Adirondack Park for parcels arriving at 7AM and 7PM local time (0 and 12 GMT) followed back in time for 48 hours for the period 19-26 August 1997. The magnitudes of the numbers plotted on Fig. 7 are relative, but show that extremely small plumes or swaths of areas contribute to the concentrations of pollution in the air at this site in upstate New York. Many of the individual "paths" of influence are extremely narrow (several tens of kilometers in width), and some follow terrain features in the complex terrain of upstate New York. Clearly, the influence of individual point sources in and around New York State will be strongly influenced by small-scale

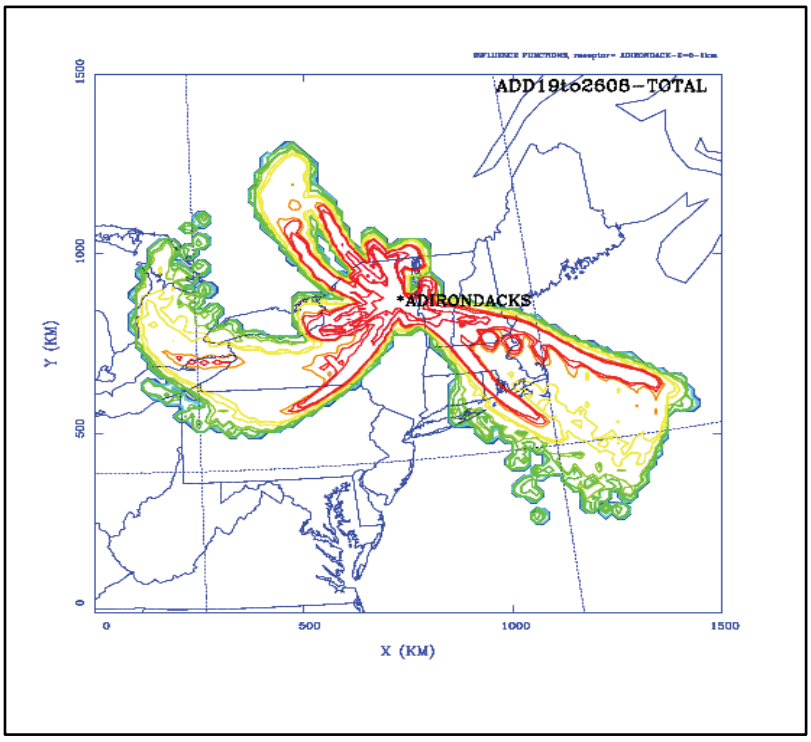

Figure 7: Addition of the influence functions for the experimental period 19 to 26 August 1997. The frame represents a 12h interval. Receptor area: Adirondacks (44.0N, 74.00W). Contours are in logarithmic normalized units (number of particles of unit mass per cubic meter).

meteorological features influencing the transport within and around New York State. These results suggest that fairly high-resolution simulations would be required to accurately assess impacts of individual mercury sources on impacts in New York State.

Section 4
PROJECT APPROACH AND OVERVIEW

Table 1 summarizes the tasks as envisioned in the original research effort proposal for this project. During this research effort, comprehensive and quality-assured emissions inventories were compiled over eastern U.S. and Canada, and observations of mercury concentration and deposition were gathered. Two sets of high-resolution meteorology fields were generated using the RAMS and the Eta meteorology models. Two atmospheric mercury models were then used to simulate concentrations and deposition of atmospheric mercury during a 13-day episode 14-26 August 1997.

Table 1. Project Tasks

Task	Description
1	Gather comprehensive US mercury emissions for 1996
2	Process and quality assure Canadian mercury emissions
3	Process emissions inventory to identify major emission sources
4	Gather and analyze available mercury concentration and deposition measurements
5	Generate detailed meteorology for 1996 episode
6	Run mercury models for episode
7	Compare modeled mercury with concentration and deposition measurements
8	Perform influence function, source-receptor analysis
9	Compare ETA-Hg and AER model
10	Sensitivity studies of mercury model to identify important and/or unmeasured parameters
11	Investigate the limitations or benefits that may result from using AER model
12	Deliver RAMS-Hg model to NYSDEC
13	Interim report of 1st 7-8 month's status
14	Final report (this document)

Mercury wet deposition calculations were compared with available measurements to evaluate the models' performance. Diagnostic analyses of these comprehensive simulations were performed to produce influence function analysis for selected receptor areas. This analysis method calculates the contributions from upwind regions influencing mercury concentrations at particular receptors during individual time periods, showing complex time-varying sequences of upwind influence.

The National Acid Deposition Program/Mercury Deposition Network (NADP/MDN) wet deposition measurements were used for evaluation of model performance. There are eight NDAP/MDN sites in the study domain during this episode period: two in Pennsylvania; three in Maine; and three in Canada. In addition, the Connecticut Department of Environmental Protection (CT-DEP) reports ambient particulate and gaseous mercury, as well as wet deposition at eight sites in Connecticut. Comparisons between model calculations and measured concentrations and wet deposition show satisfactory and semi-quantitative agreement. However, critical gaps in the current understanding of regional-scale transport, deposition and fate of mercury in New York State still exist despite the improved modeling capabilities and understanding of mercury as an air pollutant. In particular, the use of weekly-averaged wet deposition measurements at only a few measurement sites is not adequate to quantitatively assess episodic model performance.

NYSERDA also sponsored a global-scale mercury modeling research effort using the TEAM model of Atmospheric and Environmental Research (AER) in parallel with this regional modeling work (see *Contributions of Global and Regional Sources of Mercury Deposition in New York State,* NYSERDA project 6485, July 2002). One task requested comparisons between these two models. Preliminary comparisons of these modeling results with the AER annual aggregations presented at the October 2002 Blue Mountain Lake meeting show semi-quantitative agreement. For annual aggregation periods, the AER model shows in-state mercury emissions contributing 11-21% of the mercury deposition within the state, and this in-state contribution decreases towards the north. While it is difficult to directly compare the episodic simulations here with the annual-average results of AER, we find that both models' calculations are reasonably consistent with available and sparse measurements, and both models suggest that the in-state Hg emissions contribute about 10-20% of the atmospheric mercury deposition at several receptor areas in New York State. The details of the intercomparison between the AER and University of Athens Hg models envisioned during the proposal phase of this research effort proved to be overly optimistic. The simulation period chosen for analysis (August 1997) was incompatible with the mercury simulation performed with the AER model that simulated the entire year of 1998. The August 1997 period was chosen here to accommodate the available Hg measurements and maintain reasonable consistency with the Hg emission inventory, and the AER simulation period was not yet selected when we made the choice to simulate August 1997. Furthermore, a quantitatively rigorous and accurate comparison of two different comprehensive mercury models like the AER model with the RAMS/Hg or Skiron/Eta models would

require considerably greater resources than were made available for this research effort. Such a comparison requires focused commitments by the authors of the models being compared for several months of dedicated time, in addition to careful planning of the overall comparison protocol. These crucial steps were not taken prior to the funding for both the AER and SUNY projects.

By comparing the RAMS-Hg and Skiron/Eta models, we have identified some of the key physical process areas affecting mercury impacts in New York State. It was found that the underlying reason for the differences between the RAMS-Hg and Skiron/Eta model results predominantly from differences in the cloud physics, cloud processes, and wet deposition parameterizations. The RAMS modeling system generally calculates somewhat lower in-state contributions to total mercury impacts than the Skiron/Eta model due to the more sophisticated cloud physics and wet deposition parameterizations included in that model. Therefore we conclude that calculated mercury impacts are extremely sensitive to the parameterizations employed to simulate cloud processes, which are highly variable and uncertain in any current-generation air pollution modeling system.

There are several benefits and limitations of using the AER mercury model relative to using the regional-scale RAMS-Hg and Skiron/Eta models. One benefit of using the AER model for assessing mercury concentrations and deposition in New York State is that the AER model considers a global domain and explicitly simulates longer-term (annual) time periods. Both of these features are highly desirable for mercury modeling because the extremely long residence time of mercury in the atmosphere (~year) leads to its presence on a global scale. Unfortunately, due to the complex nature of processes influencing mercury concentrations in the atmosphere, all comprehensive mercury models are forced to make serious compromises of the veracity of one or more areas of concern and importance in the life cycle of mercury. The Skiron/Eta and the RAMS-Hg models sacrifice the global scale and long-term time domain so that more sophisticated and accurate treatment of the cloud physics and high-resolution transport can be achieved. In contrast, the AER model uses coarse resolution meteorology and more simplified treatments and parameterizations of cloud processes in order to maintain a global domain.

One of the key differences between the AER model and the models used here is the underlying horizontal resolution of the meteorology used by the mercury models. The Skiron/Eta and RAMS-Hg use horizontal resolutions varying from 4-20 km, while the AER model uses gridded 100 km resolution meteorology. Results of the highest-resolution version of the RAMS-Hg model show that several large mercury point sources in New York State frequently form plumes that horizontally grow in size only to several times the depth of the planetary boundary layer (4-10 km) while they are resident in New York State. Furthermore, these plumes are contorted into shapes by wind fields that are strongly influenced by topography (mountains and valleys) having scales of less than several tens of kilometers in size. For example, often

plumes flow along the major river valleys (Hudson, Mohawk) during some time periods. Clearly, the 100 x100 km^2 averaged winds used by the AER model will not accurately simulate the true directions and spread of pollution impacts on shorter time scales from the individual large incinerator and cement production facilities identified in New York State.

The RAMS-Hg and SUNY emission processing models have been delivered to the NYSDEC and set up to run on their LINUX parallel-networked computer cluster. NYSDEC staff have been trained in the implementation of these modeling systems on their local computer network and have performed the setup runs comparing the calculations for test cases and confirmed that results are consistent with the model's setup on the native machines at University of Athens.

Results of this research effort have been summarized at two NYSERDA-sponsored meetings (Fall 2001 and Fall 2003), and published in two international Journals. One paper,

> Walcek, C., S. DeSantis & T. Gentile, 2002: Preparation of mercury emissions for eastern North America. **Environmental Pollution, 123**, 375-381,

summarizes the methods for incorporating the latest EPA mercury emissions inventories into the air quality models used in this research effort. Another paper will be presented at an upcoming NATO Air Pollution symposium:

> Kallos G., A. Voudouri, I. Pytharoulis, and C. Walcek, 2003: Some preliminary results concerning the Hg budget estimates for the State of New York. Abstract accepted for presentation and publication at the 26th NATO/CCMS International Technical Meeting on Air Pollution and its Application, being held in May 2003 in Istanbul, Turkey.

The NATO series of air pollution conferences are published as textbooks following the meetings.

Section 5
RECOMMENDATIONS FOR FUTURE EFFORTS

EMISSIONS EFFORTS

Accurate management of HAP emissions, including mercury, requires a standardization of HAP emission reporting for use by EPA, state, industry and research institutions. The inconsistencies we found in this study apparently result from the lack of coordination between state environmental agencies and the EPA on inventory reporting requirements found in various parts of the Clean Air Act. In May 2000, the EPA proposed the Consolidated Emissions Reporting Rule (CERR) that would reduce and harmonize emission reporting requirements for criteria and hazardous air pollutants (HAPs) on a national basis. However, under current regulations the Office of Management and Budget does not include the collection of HAP-specific data, so the rule has not been promulgated. While the collection of HAP data is considered important, many states express the need for additional details on the HAP reporting requirements and a formal public proposal and discussion before EPA moves forward on finalizing this part of the CERR (STAPPA, 2000). The inventory errors and discrepancies discovered during the aggregation of these emissions data will continue until there is a central repository of HAP data with clearly defined requirements on reporting parameters.

MERCURY MODELING

The modeling systems used here provide useful tools for policy makers and can be used in assessing the impacts of mitigating or reducing mercury emissions. However, these model results and comparisons with observations suggest that there is a need for performing at least an explicit one-year simulation period using a comprehensive model in order to quantitatively evaluate the models using the available measurements, and to derive reasonable conclusions about the in/out-of-state contributions to mercury deposition in New York State. Furthermore, we find that the existing database on mercury deposition (weekly values at a few sites in the Northeast U.S.) and concentration measurements (particulate mercury and gaseous HG(0) at a few sites in NE U.S.) is extremely deficient in making definitive statements about the consistency of the models being used to simulate mercury and the measurements used to evaluate these models. Clearly more and better measurements would be highly desirable, and greatly improve the credibility of any models used to assess mercury transport and fate in New York State.

REFERENCES

GEIA (1998) http://www.ortech.ca/cgeic/DownLoad/Mercury.txt; http://www.ortech.ca/cgeic/DownLoad/Mercury.zip

Shia, R.-L., Seigneur, C., Pai, P., Ko, M., Sze, N. D., 1999. Global simulation of atmospheric mercury concentrations and deposition fluxes. Journal of Geophysical Research, 104, 23747-23760.

STAPPA, 2000. State and Territorial Air Pollution Program Administrators and the Association of Local Air Pollution Control Officials (ALAPCO) Docket Letter #A9840, July 7, and August 12, 2000. 444 N. Capitol St., NW, Suite 307, Washington DC.

Walcek, C., S. DeSantis & T. Gentile, 2003: Preparation of mercury emissions for eastern North America. Environmental Pollution, 123, 375-381.

Uliasz, M., and R. A. Pielke, 1991: Application of the receptor oriented approach in mesoscale dispersion modeling. In Air Pollution Modeling and Its Application VIII, van Dop, H. and D. G. Steyn, Editors, Plenum Press, New York, 338-408

Kallos Publications of Mercury Modeling Work

Journals

Pirrone N., R. Ferrara, I. Hedgecock, G. Kallos, Y. Mamane, J. Munthe, J. Pacyna, I. Pytharoulis, F. Sprovieri, A. Voudouri and I. Wangberg, 2003: Dynamic processes of mercury over the Mediterranean region: results from the Mediterranean Mercury Cycle System (MAMCS) project. Atmos. Env., 37, 21-39.

Voudouri A., I. Pytharoulis and G. Kallos, 2004: Mercury budget estimates for the State of New York. Environmental Fluid Mechanics, in press.

Conferences

Kallos, G., A. Voudouri, I. Pytharoulis and C. Walcek, 2002: Mercury budget estimates for the state of New York based on the RAMS and Skiron/Eta modeling systems. 5th RAMS workshop and related applications. Santorini, Greece. pp. 11

Kallos G., A. Voudouri, I. Pytharoulis and O. Kakaliagou, 2001: Modelling framework for atmospheric mercury over the Mediterranean region: model development and applications. In: Margenov S., J. Wasniewski and P. Yalamov (Eds.), ICLSSC, LNCS 2179, Springer-Verlag, Berlin pp. 281-290

Kallos G., A. Voudouri, I. Pytharoulis and O. Kakaliagou, 2001: Modelling the mercury cycle in the Mediterranean: similarities and differences with conventional air pollution modelling. Proceedings of the 25th ITM of NATO/CCMS on Air Pollution Modelling and its Application, Belgium, 15-19 October 2001, pp. 67-74

Kallos G., N. Pirrone, A. Voudouri, I. Pytharoulis, F. Sprovieri and M. Gensini, 2001: Source-Receptor relationship for atmospheric mercury in the Mediterranean region. 6th International Conference on Mercury as a Global Pollutant. 15-19 October, 2001, Minamata, Japan. pp. 39

Kallos G., N. Pirrone, A. Voudouri, I. Pytharoulis and O. Kakaliagou, 2001: Characteristic paths and scales of mercury transport and deposition in the Mediterranean region. 6th International Conference on Mercury as a Global Pollutant. 15-19 October, 2001, Minamata, Japan. pp. 65

Kallos G., N. Pirrone, A. Voudouri, I. Pytharoulis, O. Kakaliagou, E. Mavromatidis, M. Varinou, F. Gofa, P. Katsafados, F. Sprovieri and P. Costa, 2001: Atmospheric mercury in the Mediterranean Region. A source-receptor relationship study. 4th ELOISE conference, 5-7 September, 2001, Rende, Italy. Proceedings, pp. 96

Kallos G., N. Pirrone, A. Voudouri, I. Pytharoulis, O. Kakaliagou, I. Hedgecock, G. Trombino and M. Gensini, 2001: Atmospheric modelling of the mercury cycle in the Mediterranean: Is it possible to use conventional air pollution modeling techniques? 4th ELOISE conference, 5-7 September, 2001, Rende, Italy. Proceedings, pp. 74

Kallos G., O. Kakaliagou, A. Voudouri, I. Pytharoulis, N. Pirrone, L. Forlano and J. Pacyna, 2001: Modelling of the mercury cycle in the atmosphere. In: Gryning and Schiermeier (Eds.), 24th ITM of NATO/CCMS on Air Pollution Modelling and its Application, Kluwer Academic Publishers, pp. 247-254

Pirrone N., G. Kallos, G. Trombino, I. Hedgecock, A. Voudouri, I. Pytharoulis and J. Pacyna, 2001: Eulerian modelling framework for atmospheric mercury over the Mediterranean region: model development and application. 6th International Conference on Mercury as a Global Pollutant. 15-19 October, 2001, Minamata, Japan. pp. 38

Voudouri A. and G. Kallos, 2004: New developments on RAMS-Hg model. 27th ITM of NATO/CCMS on Air Pollution Modelling and its Application, October 25 - 29, 2004 in Banff, Canada, accepted.

Voudouri A., I. Pytharoulis, G. Kallos and C. Walcek, 2004: Some preliminary results concerning the Hg budget estimates for the State of New York. In: Borrego and Incecik (Eds.), 26th ITM of NATO/CCMS on Air Pollution Modelling and its Application, Kluwer Academic Publishers, pp. 271-278

APPENDIX

IASA

UNIVERSITY OF ATHENS
SCHOOL OF PHYSICS, DIVISION OF APPLIED PHYSICS
ATMOSPHERIC MODELING & WEATHER FOREACASTING GROUP
University Campus, Bldg PHYS-V
Athens 15784, Greece

Atmospheric Transport and Fate of Mercury and its Impact on New York State

SUBAWARD# 01-9
RF PTAEO#1015266-20439-1

FINAL REPORT

Prepared for
New York State Energy Research and Development Authority
(NYSERDA) #6488

Prepared by
The Atmospheric Modeling and Weather Forecasting Group
G. Kallos, A. Voudouri, I. Pytharoulis,
O. Kakaliagkou, M. Astitha

JULY 2002

Atmospheric Transport and Fate of Mercury and its Impact on New York State

SUBAWARD# 01-9

RF PTAEO#1015266-20439-1

FINAL REPORT

Prepared for

New York State Energy Research and Development Authority

(NYSERDA) #6488

Prepared by

The Atmospheric Modeling and Weather Forecasting Group

G. Kallos

A.Voudouri

I.Pytharoulis

O. Kakaliagkou

M. Astitha

JULY 2002

ACKNOWLEDGMENTS

We would like to thank all the members of the participating groups for the excellent cooperation we had during this project. Particularly we would like to thank all the NYSERDA personnel and Dr. C. Walcek who prepared the emissions database. Dr. S. T. Rao is kindly acknowledged for the useful discussions we had during the project, as well as for his suggestions on mercury modeling issues. Special thanks are also due to Dr. C. Tremback of ATMET Inc. (USA) for his assistance on the RAMS model development.

The sea-surface temperatures, and the orography data sets were obtained from the National Center for Atmospheric Research (NCAR), Boulder, Colorado, which is sponsored by the National Science Foundation of USA. The gridded model analyses were received from the European Center for Medium range Weather Forecasts (ECMWF), Reading, United Kingdom. The availability of these data sets from NCAR and ECMWF was very important for the prompt execution of the project tasks.

Publications acknowledging this project

Kallos, G., A. Voudouri, I. Pytharoulis, O. Kakaliagou (2001): Modeling framework for atmospheric Mercury over the Mediterranean region: model development and applications, 3rd International Conference on Large-Scale Scientific Computatations, 6-19 June 2001, Sozopol, Bulgaria, pp 281-290.

Kallos, G., A. Voudouri, I. Pytharoulis, O. Kakaliagou (2001): Modeling the mercury cycle in the Mediterranean: similarities and differences with conventional air pollution modelling, 25th NATO/CCMS International Technical Meeting on Air Pollution Modelling and its Application, 15-19 October 2001, Louvain-la-Neuve, Belgium, pp 67-74.

Kallos, G., N. Pirrone,A. Voudouri, I. Pytharoulis, O. Kakaliagou, E. Mavromatidis, M. Varinou, F. Gofa, P. Katsafados, F. Sprovieri and P. Costa (2001): Atmospheric mercury in the Mediterranean region: A source-receptor relationship study. 4th ELOISE Conference, 5-7 September 2001, Rende, Italy.

Kallos, G., N. Pirrone,A. Voudouri, I. Pytharoulis, O. Kakaliagou, I. Hedgecock, G. Trombino and M. Gensini (2001): Atmospheric modelling of the mercury cycle in the Mediterranean: Is it possible to use conventional air pollution modelling techniques? 4th ELOISE Conference, 5-7 September 2001, Rende, Italy.

Kallos, G., A. Voudouri, I. Pytharoulis, O. Kakaliagou and C. Walcek (2001) Atmospheric Transport and Fate of Mercury in New York State – Preliminary model results (Project NYSERDA #6488), September 2001, Albany, New York, USA.

Kallos, G., A. Voudouri, I. Pytharoulis (2002), Modeling of the mercury budgets for the State of New York. Presentation at the 5th RAMS Workshop and Related Applications Atmospheric Modeling From Microscale to Global, 29 September- 3 October 2002, Santorini, Greece.

CONTENTS

1. INTRODUCTION

Mercury is a toxic metal classified as a "hazardous pollutant" because of its potentially harmful effects on ecosystems and human health. The physical and chemical processes involved in the mercury cycle in the atmosphere are very complicated and need special treatment.

The harmful effects of mercury on human and animals are associated with its ambient concentration and deposition, and thus they are directly linked to the mercury amounts released in the atmosphere. According to recent estimates the annual amounts of mercury released into the atmosphere by human activities are between 50 and 75 percent of the total yearly emissions.

Sources of mercury due to human activity include power plants (burning coal and oil), chemical plants (e.g. alkal-cloral plants), waste incinerators, ferrous foundries, non-ferrous metal smelters, refineries, and cement kilns. Important fluxes of mercury include not only the anthropogenic emissions (e.g. from coal-fired power plants and incinerators) but also the emissions from water surfaces (i.e. ocean and lakes), soil and plants. Mercury emitted and deposited on land and water bodies in the past can evaporate and be re-emitted. Soils and vegetation near former industrial sources of atmospheric mercury emissions are re-emission sources. Complex biological and chemical interactions, such as methylation and elementary mercury production and volatilization, prolong the lifetime of mercury cycle and affect releases to the atmosphere. Mercury accumulating in soils is released only slowly to terrestrial waters. Mercury deposited in open ocean waters is being removed in relatively short time-scales (10-20 years).

In contrast mercury deposited to a watershed remains and its loading effects may persist, affecting fish in fresh waters and estuarine/coastal regions for long periods. The highly toxic methylmercury compounds are entered in the aquatic nutrition chain and, therefore, in the food chain. High concentrations of mercury have been found even in fish taken from remote lakes throughout the world that receive no direct pollutant discharge. Currently, 25 lakes in upstate New York have health advisories on fish consumption because of high mercury levels. Many of these lakes are remote with no local sources of mercury. Power plant emissions currently constitute about 25% of total anthropogenic emissions of mercury in the United States. The EPA

recently determined that it is necessary to reduce mercury emissions from coal-fired power plants.

The harmful effects of mercury on people have been well known since the poisoning incidence in Minamata, Japan in the 1950s. Dozens of people were victims of methylmercury poisoning after consuming fish contaminated by chemical plant effluents in Minamata Bay (Harada, 1966). In the 1950s and 1970s, three separate epidemic poisonings occurred in Iraq (Marsh et. al, 1980, 1981, 1987; Clarkson et. al, 1975), with 459 deaths attributed to mercury-contaminated grain. The concern of National Wildlife Federation and most health agencies in the U.S. stems from the effects of mercury exposure on children, when they are exposed uterine, as a result of their mothers' consumption of mercury-contaminated fish. These exposure levels are generally much lower than the poisoning events in Japan or Iraq. However, lower levels are not synonymous to any danger for the public health. Elevated mercury levels in the U.S. are thought to put up to 166000 pregnant women at risk of exposing their foetuses to harmful mercury levels in a given year.

Two types of models are usually used to study the mercury problem, namely source-based and receptor-based models. The source-based models require detailed emissions and meteorological data and can represent the dispersion, transformation, and deposition of mercury. Mercury budgets can be simulated with them. The receptor-based models include the trajectory and factor analysis methods.

A summary of the source-based mercury atmospheric models used in previous studies was made by the Electric Power Research Institute (EPRI) group and is given in Appendix 1 (EPRI TR-107695, 1996). A common feature of nearly all these models is that they were originally developed to study sulfur dioxide, sulfate and acid rain, and they were modified to include mercury transformation and deposition. Although effort was devoted in these models in order to represent the mercury cycle realistically, most of them take into account only a limited number of mercury chemistry processes. The gas-phase chemistry in these models is represented on a more or less adequate way but the gas-to-particle conversion and, in general, the particle treatment is almost absent. Moreover, the meteorology is either inadequately represented or absent in these models. Many of them use coarse horizontal and/or vertical resolution grids of limited vertical extent. Also, all of them do not even employ a full-physics meteorological model. So, the above models are not able to provide an accurate representation of many meteorological processes such as

convective or large-scale precipitation, large-scale subsidence and drying, etc. Many of these processes are very important for the transformation and deposition of mercury and they need to be taken into account at each time step. For example, good representation of turbulence is important for dry deposition of adsorbed elemental mercury, while wet deposition of the various mercury species is strongly dependent on the microphysical scheme used in the meteorological model. In most of the conventional model there is a poor representation of the precipitation leading to a wet deposition of mercury of low accuracy. Thus, the meteorological processes need to be well modeled if an accurate study of mercury is desired.

In this project, the transport, transformation and deposition of mercury in New York State was studied using and comparing atmospheric models. Two major model developments took place. These two developments were constructed within two well-known atmospheric models: the Regional Atmospheric Modelling System (RAMS; Pielke et al. 1992) and the SKIRON/Eta (Kallos et al. 1997 and references therein). The use of two atmospheric models allowed the inter-comparison of the results and, therefore improved understanding on the mercury modelling.

There are several reasons for performing the development of the mercury modelling within these two specific models. The main reason for using RAMS is its unique capability of two-way interactive nesting of any number of grids, which is considered as absolutely necessary for studying near-source dispersion of mercury species. Additional capabilities include the incorporation of the most advanced cloud microphysical process algorithms, the detailed parameterization of surface processes and the use of the non-hydrostatic assumption. On the other hand, the main reason for using the SKIRON/Eta model for development is that it provides very accurate meteorological fields without being computationally expensive (7-8 times less computer resources compared to RAMS). Moreover, it has a unique capability of describing the dust cycle (uptake, transport, deposition) and it incorporates a viscous sub-layer formulation that is necessary for description of mercury fluxes from the sea surface. The configuration of both models is very flexible and they can be used in any part of the world.

This report summarizes the main results from the simulations performed using RAMS and SKIRON/Eta meteorological modeling systems. Models have been run for an individual episode during which the highest quality and comprehensive emissions, observations of mercury concentration and deposition were available. An accurate

assessment of our current understanding of atmospheric mercury (as quantified in current regional-scale air pollution models) requires both high-quality measurements of concentrations and deposition together with accurate estimates of Hg emissions**.** Model calculations and measurements have been compared during the 14 to 26 August 1997 simulation period for two different scenarios:

(a) when robust Hg measurements were available in and around NY State and

(b) when Hg emissions in NY State were not considered.

The Mercury Deposition Network (MDN) provides wet deposition measurements, but sites are upwind and downwind of New York State only.

The aim of this project was to identify and quantify critical gaps in the current understanding of regional-scale transport deposition and fate of mercury in New York State, improve modeling capabilities and understanding of mercury as an air pollutant, and provide a tool for policy makers in mitigating the impacts of mercury pollution.

2. MODEL DESCRIPTION AND SET-UP

2.1 Model description

2.1.1 RAMS

RAMS is a highly versatile numerical code developed by scientists at Colorado State University and ASTER Inc., for simulating and forecasting meteorological phenomena (Walko and Tremback, 1996; Pielke et al., 1992). It is considered as one of the most advanced modeling systems available today. It is a merger of a non-hydrostatic cloud model (Tripoli and Cotton, 1982) and a hydrostatic mesoscale model (Mahrer and Pielke, 1977). It has been developed in order to simulate atmospheric phenomena with resolution ranging from tens of kilometers to a few meters. There is no lower limit to the domain size or to the mesh cell size of the model finite difference grid. A general description of the model and its capabilities is given in Pielke et al. (1992). However, some RAMS features are summarized in the following:

- Two-way interactive nesting with any number of either telescoping or parallel fine nest grids (Clark and Farley, 1984).
- Terrain following coordinate surfaces with Cartesian or polar stereographic horizontal coordinates.
- Non-hydrostatic or hydrostatic time-split time differencing.
- Cloud microphysics parameterization at various levels of complexity.
- Various turbulence parameterization schemes.
- Radiative transfer parameterizations (short and long wave) through clear and cloudy atmospheres.
- Various options for upper and lateral boundary conditions and for finite operators.
- Varying levels of complexity for surface-layer parameterization (soil model, vegetation etc.).

- Horizontally homogeneous or variable initialization (isentropic analysis). ECMWF and National Center for Environmental Predictions (NCEP) analysis files can also be used for initialization.
- It is highly portable and runs on several types of computers.
- A fully parallelized code is currently available for efficient use in high performance computers.

RAMS is a very useful tool and can be used either for research or operational purposes. There are more than 1000 publications during the last twenty years and more than 400 locations worldwide where RAMS is being used.

Its major components are:

- an atmospheric model which performs the actual simulations.
- a data assimilation package which prepares initial and boundary conditions for the atmospheric model from observed meteorological data and/or other models.
- a post-processing package for visualization and output processing. It helps also for interfacing the atmospheric model with a large variety of other models and applications (e.g. air quality modeling, wave or oceanographic modeling, hydrological applications etc).

In general, RAMS is a highly versatile tool that can be used in air quality studies and in a wide variety of other atmospheric phenomena.

2.1.2 SKIRON/ETA

The SKIRON/ETA is a modeling system developed at the University of Athens by the Atmospheric Modeling and Weather Forecasting Group (Kallos et al., 1997, Papadopoulos et al., 2002). It is based on the ETA model, which was originally developed by Mesinger (1984) and Janjic (1984) at the University of Belgrade. Major development of ETA model has been implemented by NCEP. As a result of this development, the model is in operational use in the United States, having outperformed all other models because of its superior handling of mountains.

At the framework of project MEDUSE, the SKIRON system has been developed even further and enhanced its capabilities with the unique one to simulate the dust

cycle (uptake, transport, deposition). It has been applied to the Saharan dust transport towards the Mediterranean Basin and USA as well as to the lake Aral and China (Nickovic et al., 1998, 2001). The features of SKIRON system are summarized as follows:

- The model variables are calculated on the Arakawa E-grid. The method, which provides a proper behaviour of the model with variables on the E grid is developed by Mesinger (1973, 1977), Janjic (1974, 1979) for cases of strong physical forcing (e.g. orography influence, convection, turbulence).
- Use of η (eta) as vertical coordinate, which is a generalization of σ-coordinates for a better parameterization of step-like terrain (Mesinger, 1984). The model has as option to operate on σ coordinates.
- Use of a split-explicit time differencing scheme.
- Vertical turbulent mixing between levels in the free atmosphere is performed, by using mixing coefficients of the modified Mellor-Yamada 2.5 level turbulence (Mellor and Yamada, 1974, 1982; Janjic 1994).
- Vertical mixing in the surface layer is performed by a Monin-Obukhov similarity model, combined with the viscous sub layer model.
- Parameterization of the surface processes using the Oregon State University (OSU) model, including surface hydrology.
- Orientation, slope and land cover effects of the surface is taken into the account in the energy budget calculations.
- For the surface-processes calculations, a corresponding set of high resolution ground conditions (soil and vegetation types, topography, sea surface temperature) is included.
- The revised Betts-Miller-Janjic deep and shallow cumulus convection scheme is used in order to represent moist convection (Betts, 1986; Betts and Miller, 1986; Janjic 1994). The convective and large-scale parameterization of precipitation does not require expensive computer facilities.
- The use of GFDL radiation scheme with random interaction of clouds at various levels.
- Dust uptake, transport and deposition module (Nickovic et al., 1997, 2001).
- A series of pre- and post-processing modules for better utilization of the available input data and model results.

2.1.3 Mercury Modules

The developed modules for the physico-chemical processes of mercury have been incorporated in both modeling systems (RAMS and SKIRON). In each model, basic processes like advection and diffusion are the ones already existing for passive tracers that were modified accordingly. The modules for the various atmospheric and surface processes of mercury species are briefly described below:

a. ***Emissions processor*:** This module deals with the preparation of emissions from anthropogenic and natural sources. It utilizes the data stored in the mercury emission inventory. The various sources are allocated within the model domain (point sources). The modules define emissions according to the land use (area sources), define initial and lateral boundary conditions according to the type of simulation; initial run (cold start) or continuation run (hot start). The entire module is very flexible because the emission inventory can be updated easily and the source allocation is automatic according to the geographic coordinates and the type of sources. Stack characteristics should be added easily in case they are available.

b. ***Chemical-kinetics*:** It is well known that chemical and physical transformations of mercury in the atmosphere with changing meteorological conditions play an important role in the cycle of this contaminant in the environment (Forlano et al., 1999). The chemical and physical transformations of mercury and its compounds in the atmosphere are described in the Chemical-Physical (C-P) module. The C-P module is a merger of a Gas-Solid Partitioning (G-P) model, which is a numerical model developed at the University of Michigan by Pirrone and co-workers (Pirrone and Keeler 1995) in order to evaluate the partitioning of atmospheric mercury during transport, and a Chemical-Kinetics (C-K) model which is based on the previous work done by Munthe, Pleijel and co-workers for the Baltic Sea and North Sea regions (Pleijel and Munthe, 1995; Petersen *et al*., 1996, Pirrone et al., 2002). The G-P and C-K modules are coupled and describe the mechanisms involved in the dynamics of gaseous and particulate phase mercury in the atmosphere. Gas phase reactions include oxidation of elemental mercury (Hg^0) to divalent mercury (Hg^{2+}) by ozone and other oxidants.

- *b.1.1*. The G-P module describes the diffusive uptake or release of a gaseous Hg (Hg° and Hg species) by atmospheric particles. Many assumptions are inherent in the formulation of the G-P model. The particles are spherical and have a non-porous, non-sorbing inner core surrounded by a uniformly porous, sorbing outer shell. In spherical co-ordinates, the diffusion of mercury and mercury species in atmospheric particles is governed by the following partial differential equation

$$\partial S(r) / \partial t = n\, D_m\, [\partial^2 B(r) / \partial r^2 + 2/r\, \partial B(r) / \partial r]$$

where S(r) is the total volumetric concentration of Hg^0 at a radial distance r from the center of a particle, B(r) is the non-adsorbed concentration of Hg^0 in the micropores of a particle, D_m is the molecular diffusion coefficient of Hg^0 in the air, and n is the intraparticle porosity of the porous shell and t is the time. In solving the above equation for Hg^0 several assumptions have been made including local equilibrium between the adsorbed Hg^0 and Hg^0 in the gas phase.

- *b.1.2.* The C-K module accounts for all the major chemical reactions of atmospheric mercury in the gas phase, particulate phase and aqueous phase (i.e. cloud droplets, aqueous phase adsorbed in the total suspended particulate) during the transport of air masses on local and regional scale. As showed in recent studies of atmospheric deposition and transport of mercury non local-urban scales, the contribution of airborne mercury to the overall budget of mercury released from the atmosphere to water and terrestrial receptors may be substantial, although the concentration of atmospheric mercury in particle phase is low compared to that in the gas phase.
- *b.2 Dry deposition module*: This module consists of two sub-modules in order to account for dry deposition over water surface and over land. The model proposed by Williams (1982) and modified later by Pirrone et al. (1995a, b) for trace metals and semi-volatile organic pollutants is used to calculate the deposition fluxes over water surfaces. The model of Slinn and Slinn (1981) is used for deposition over soil and vegetation. These modules consider super micron particle eddy diffusivity, gravitational settling and particle inertia as the main mechanisms influencing the deposition to terrestrial receptors. Finally, the model combines this term with the terminal settling velocity and

Brownian diffusion to predict deposition velocities. In order to reduce the uncertainty associated with the deposition fluxes of atmospheric mercury to terrestrial receptors the suggestions of Hicks *et al*. (1985) have been adopted. Other formulations (e.g. Giorgi, 1986) have been coded and are incorporated in the models as alternatives.

- *b.3. Wet deposition module***:** A state-of-the-art wet deposition module has been developed and linked with the other modules and the atmospheric model. The wet removal process concerns the soluble chemical species (Hg^2 and its compounds, and some Hg^0), and also particulate matter scavenged from below the precipitating clouds. The wet deposition module has been validated and calibrated by using a long-term record of mercury in rainfall precipitation collected in Europe during the last decade.

All the above-described modules have been included in the original atmospheric models (Pirrone et al., 2002).

The processes involved in mercury transport and transformation are rather complicated and require special treatment. Due to the small concentrations of some mercury species and the processes involved, especially the gas to particle conversion, stiff differential equations solvers were used. This requires significant computer resources, which makes the simulations for long periods and high resolution very difficult. In addition, the aqueous phase processes are very important and the atmospheric models must include detailed cloud microphysical algorithms, which require also significant amount of computer power. The two atmospheric models used for the development (RAMS and SKIRON/Eta) have such capabilities through different approaches. RAMS has a detailed cloud microphysical scheme and the two-way interactive nesting capabilities, which make it appropriate for simulations near the sources and simultaneously over larger areas. The computer power required for long-term simulations is beyond the limits of the conventional workstations and servers available and requires parallel computations. For this reason, most of the simulations performed so far are in a rather coarse grid. The SKIRON/Eta system has a microphysical scheme which is less demanding in computer resources but accurate enough for precipitation calculations. Therefore, it is preferable for several sensitivity calculations of several days. The inter-comparison of the results between the two models is an absolutely necessary process in order to avoid systematic errors since

there are no systematic measurements available for the mercury species in several locations for performing inter-comparison studies.

2.1.4 LPDM model

The Lagrangian Particle Dispersion Model (LPDM) is a simulation tool used to investigate pollution dispersion over complex terrain. LPDM allows the simulation of releases of pollutants from arbitrary emission sources, by tracking the motion of particles (Uliasz and Pielke, 1991). The unique feature of the LPDM is its ability to use two different options for dispersion calculations:

The traditional source-oriented approach, which consists of solving model equations forward in time for given emission sources. The basic concept behind source–oriented approach is the determination of the impact of a particular source upon its surroundings. The result of this approach is to obtain a time and space distributed concentration field.

The receptor-oriented approach, based on the calculation of influence functions from backward trajectories of particles. The proposed methology is based on a Lagrangian type of dispersion, taking into account turbulence in the calculations (particles are released from the receptor during the sampling time). This is considered to be the main advantage compared to simple back trajectory calculations, showing the non-linear paths of the air masses during the desired travelling time. This approach results in the definition of the origin of the air masses monitored at specific locations (receptor area) and times. It is important to denote that this approach gives a qualitative definition of the areas of influence and does not provide quantitative information for specific pollutants.

2.2 Models setup

2.2.1 RAMS

a. Model set-up

The simulation performed with both models started at 0000 UTC on 14 August 1997 and ended at 0006 UTC 26 August 1997. One grid has been selected with the following configuration:

- 90x90x30 points and 36 km horizontal grid increment. The coordinates of the center of the domain were at 36.926 ^{o}N and 85.037 ^{o}W
- For the model domain, thirty vertical levels following the topography were used at: 69, 195, 325, 458, 559, 775, 994, 1269, 1611, 2040, 2576, 3250, 4059, 4916, 5766, 6616, 7466, 8316, 9166, 10016, 10866, 11716, 12566, 13416, 14266, 15116, 15966,16816 and 17666 m. This configuration is considered adequate for the present study and the computer resources available for the project.

b. Input data

-*Topography files.*

A detailed data set of 30 arc-second was used. This data set has a global coverage and is available from EROS Data Center (Sioux Falls, SD 57198). From the above topography data set the land-water percentage was extracted.

-*SST files.*

The Sea Surface Temperature (SST) data set was retrieved from the National Center for Atmospheric Research (NCAR) and consists of mean climatological monthly values with a resolution of 1 degree.

-*Vegetation and land use files*

The specification of the type of vegetation was in gridded form with a resolution of 30 arc-seconds and global coverage. The vegetation data have been retrieved from NOAA/NGDC.

-*Meteorological fields*

The initial data for the atmospheric model were prepared by the isentropic analysis package. The model was initialized with gridded data sets containing horizontal velocity components, temperature, geopotential height and relative humidity as a function of pressure. More specifically, the data were obtained from the European Center for Medium Range Forecasting (ECMWF). Their horizontal increment is 0.5 degree, and they are available every 6 hours (0000, 0600, 1200 and 1800 UTC). The initialized analysis data sets were used instead of non-initialized analysis data in order to avoid unnecessary local effects. The horizontal resolution of this data set is comparable with the RAMS grid used.

c. Initialization procedures

-*Topography*

The terrain height data, which are to be present on the model grid, has been set to 4, indicating the shortest mode with respect to the model grid.

-*Meteorological fields*

The gridded data sets contain horizontal velocity components, temperature and relative humidity as a function of pressure at the following 12 pressure levels: 1000, 925, 850, 700, 500, 400, 300, 250, 200, 150,100 and 50 hPa. These data are objectively analyzed using RAMS on isentropic surfaces from which they are interpolated to the RAMS grids. These initialization fields are used in order to supply a time series of observational data for the atmospheric model to assimilate during execution. The lateral boundary region of the coarser grid is nudged toward the initialization file values every 900 s, while there is no relaxation time scale at the center of the domain.

-*Soil moisture information*

Six levels were active in the soil model at a depth of 0.50, 0.35, 0.20, 0.10, 0.05 and 0.0 m.

Apart from these settings, the simulations were set to be non-hydrostatic. The lateral boundary conditions on the outer grid followed the Klemp-Lilly condition which is a variant of the Orlanski condition, in which the gravity wave propagation

speeds computed for each cell in the Orlanski condition are averaged vertically, with the single average value being applied over the entire vertical column. The horizontal diffusion coefficients were computed as the product of horizontal deformation rate and a length scale squared, based on the original Smagorinsky formulation. The vertical diffusion coefficients were computed according to the Mellor and Yamada parameterization scheme, which employs a prognostic turbulent kinetic energy. For both short wave and long-wave radiation parameterizations, the scheme described by Mahrer and Pielke (1977) has been used.

The roughness length is defined according to the vegetation cover. The simulation was also performed by activating condensation of water vapor to cloud water and the microphysical parameterization of any species of liquid or ice. The mean rain, snow, aggregates, graupel or hail droplet diameter was specified from the default value in RAMS code and the number of concentration is diagnosed automatically from this mean diameter and the prognosed mixing ratio.

2.2.2 SKIRON/Eta

a. Model set-up

The selected model area for the present study extends 48.8 ^{o}N to 21.5 ^{o}N and from 107.3 ^{o}W to 63.8 ^{o}W, centered at 36.9 ^{o}N and 85 ^{o}W, and covers the USA. This area cover the same area with the one used for RAMS with minor differences attributed to the SKIRON/Eta horizontal projection.

b. Input data and model initialization

The SKIRON/Eta model uses the following set of input data:

-*Topography files.*

In this study a topographical data set with a global coverage at a horizontal grid spacing of 30-arc seconds (approximately 1 kilometer) provided by the US Geological Survey (USGS) was used.

The model while processing the topography file, records the average elevation in each grid cell. The model land/sea mask is derived from the topographical data. If half

of the points contained in each grid box are over land, then this grid box is defined as a land point, and in the opposite case it is defined as a sea point.

-*Sea Surface Temperature Sea (SST) files.*

For Sea Surface Temperature Sea (SST) there are three options: the latitudinal variation of pre-defined SST, the climatological 1x1 degree data from NCAR (mean monthly values) and the ECMWF gridded fields. In the present study climatological values are used.

-*Soil texture.*

Soil textural data classes are available with a global coverage at resolution of 2x2 min. Two global sets with different resolutions are used in order to derive the finer textural classes:

a. The Staub and Rosenzweig Zobler Near-Surface Soil Texture data set at 1x1 degree resolution consists of 7 textural classes plus water, organic matter and land ice.

b. The UNEP/GRID Gridded FAO/UNESCO Soil Units at 2x2 min resolution consisting of soil units with 134 legends (indicating the soil types, ocean, rocks, salt and inland water).

-*Vegetation types*

For the geographical vegetation distribution, an empirical correspondence is specified between the Olson World Ecosystems with 59 classes at 10x10 min resolution with a global coverage and the 13 SSIB vegetation types required by the SKIRON/ETA model. Alternatively a data set with higher resolution namely 30”x30” latitude-longitude is available. In this study the higher resolution data set was used.

-*Soil moisture information*

Soil moisture and temperature was calculated in six levels at a depth of 0.50, 0.15, 0.28, 0.50, 1.00 and 2.55 m. In addition, the slopes and the azimuths of the sloping surfaces were computed and the used for the calculation of the incoming solar radiation over the sloping terrain. Albedo variations are also calculated.

-*Meteorological fields*

For the initialization and boundary conditions either analysis and/or forecast fields from the European Center for Medium Range Forecasting (ECMWF) or from the National Center for Environmental Predictions (NCEP) Washington can be used. In the present study analysis fields from the ECMWF every 6 hours (0000, 0600, 1200 and 1800 UTC) were used. The data sets consist of the parameters velocity

components, specific humidity and geopotential height at 12 pressure levels namely at: 1000, 925, 850, 700, 500, 400, 300, 250, 200, 150, 100 and 50 hPa. The data for the simulations covered the area from 80.0^{o}N to 10.0^{o}S and from 40.0 ^{o}W to 70.0 ^{o}E, with grid spacing 0.5^{o}, similar to the data set used by RAMS model.

2.2.3 Mercury modules.

a. Emissions data

The emissions data used in both models were obtained from all counties as well as point sources provided by the New York State Department of Environmental Conservation (Chris Walcek, personal communication). The database provided information for each point source such as the location of the source, latitude and longitude, stack height, information on the emission type (Hg^0, Hg^2 and Hg^P) and type of plant. The locations of sources (area and point) in the USA are illustrated in Fig. 2.1. A second simulation was performed without using the New York State sources as displayed in Fig. 2.2.

Re-emission involves gaseous evasion of previously deposited mercury in water and soil and is also considered in both models. Fluxes of mercury from soil and water are taken into account. These values are defined in the pre-processing module. SKIRON model reads the defined values from the pre-processing module and fluxes are calculated, which contribute to the overall emission. RAMS model reads the defined values and calculates the emissions per volume unit.

A parameterization of the mercury fluxes from the sea is included in the mercury modelling system. The fluxes are approximated by a hyperbolic empirical function that mainly depends on the wind speed at 10m height and the sea-surface temperature. This function was formulated in such a way so that the fluxes of mercury from the sea to lie within the range reported or inferred by the literature (e.g. Lindqvist et al. 1991; Jackson 1997; Xu et al. 1999). The concentration of mercury in the top layer of the sea (namely above the thermocline) and its seasonal variability was also considered in the calculation of the mercury fluxes from the sea-surface. In the literature, the average observed concentrations of Hg^0 in lakes and oceans range significantly from about 20 ng/m^3 to 2000 ng/m^3 (e.g. Brosset 1984; Vandal et al. 1993; Fitzerald et al.

1997). In general, there is a large uncertainty about the spatial and temporal variations of elemental mercury concentration in surface water (Xu et al. 1999). Also, the work of Xu et al. (1999) indicated that it is unclear how important are the emissions from the water bodies (lakes and oceans) relative to the anthropogenic or plant emissions. A detailed parameterisation of air-water exchange of mercury may be required in case the emissions from water bodies appear to be important for the mercury concentrations.

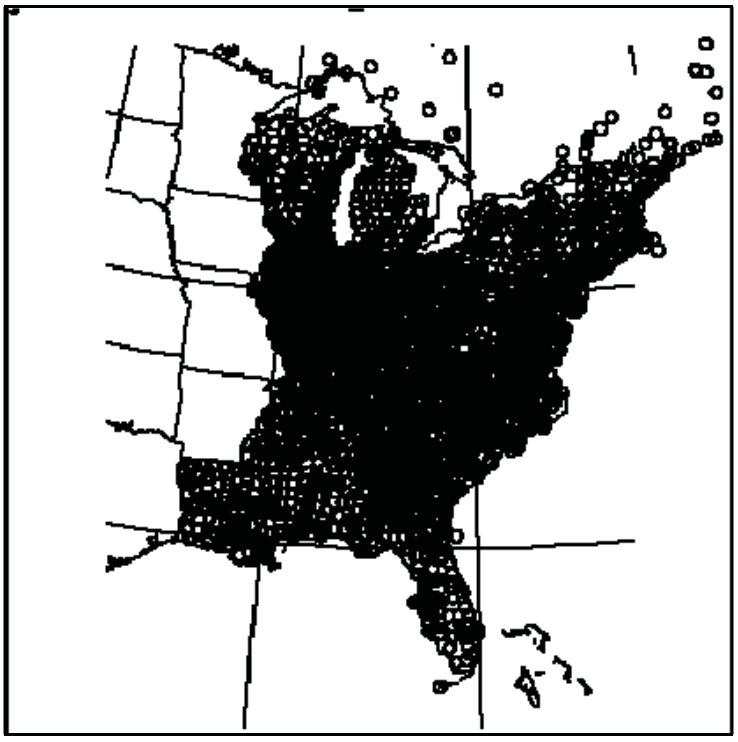

Figure 2.1: Sources location over eastern US.

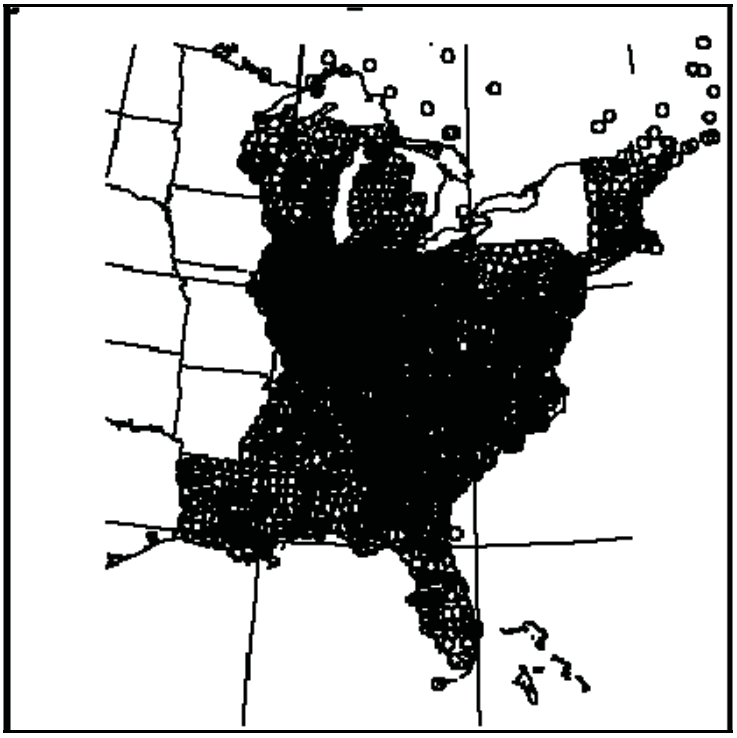

Figure 2.2: Sources location over eastern US without the New York State sources.

b. Initial and boundary conditions for Hg^0, Hg^2 and Hg^P

Horizontally homogeneous initial and boundary conditions are used for the three mercury species. The boundary concentrations of all species are fixed throughout the simulations. Constant initial and lateral boundary concentrations of 1.4 ng/m^3, 80 pg/m^3 and 10 pg/m^3 are used for Hg^0, Hg^2 and Hg^P respectively, in the lowest 2 km (EPRI TR-107695, 1996). Moreover, Shannon and Voldner (1995) estimated the background concentration of Hg^P to be equal to 10 pg/m^3 near the ground.

The initial and lateral boundary concentrations of the three species decrease with height. Hg^0 decreases linearly with height above 2 km, reaching the 70% of its low-level concentration at 6 km. At this height, the background concentration of Hg^0 becomes equal to 0.92 ng/m^3. From 6 km to the model upper limit, the background concentration of Hg^0 decreases linearly to 0 ng/m^3. The background concentration of Hg^2 and Hg^P decreases rapidly with height above 2 km, practically vanishing at about 6 km.

c. Wet deposition and dry deposition initialization

c1. Wet deposition

Wet deposition of Hg^P, Hg^2 and Hg^0 adsorbed in rain droplets is activated if there is precipitation. For Hg^P and Hg^2, the whole concentrations are deposited from that layer where condensation occurs, while for the Hg^0 adsorbed, the concentration that is deposited depends on the amount of water present in the model layers.

c2. Dry deposition of Hg^P

The deposition scheme, described earlier in this report, is applied in the first model level. The deposition velocities are calculated over land and sea for 15 different particle sizes. At the end of the calculation, one deposition velocity is used that represent on a weighted way from the 15 different sizes. Due to the greater deposition velocities in regions with high humidity, as the size of the particles is becoming larger in this case, great difference in deposition values over land and sea are calculated.

c3. Dry deposition of Hg^2

Dry deposition scheme for Hg^2 is applied in the first model level. The deposition velocity of Hg^2 was fixed in time and space in the model runs. Deposition velocities within this range have been measured for SO_2 (Sehmel 1980), which exhibits similar transport and deposition characteristics with mercury, and used in previous studies of mercury (e.g. Petersen et al. 1995). The value of 0.005 m/s was used in the model integrations. This value is in good agreement with Hg^2 deposition velocities used in previous studies (e.g. Shannon and Voldner 1995; Pai et al. 1997).

c4. Dry deposition of Hg^0 adsorbed

The gaseous flux of Hg^0 from air to land/water surface is assumed to be zero in several studies (Pai et al., 1997). However, a non-negligible flux of gaseous Hg^0 is taken into account by the gas-particle module. In fact, due to the diffusion of Hg^0 to the particulates, a small fraction of Hg^0 remains trapped in and then deposited with the aerosol particle. This process, which has been neglected in all other models so far, is not always negligible.

The deposition velocity of Hg associated with particles, (Hg^P), was calculated by distributing its mass according to a lognormal particle size distribution, as it has been described above (see §2.1.3b). The deposition velocity for Hg^0 adsorbed in aerosol is calculated following the same procedure as for Hg^P (Seinfeld, 1986). Dry deposition

scheme for Hg^0 adsorbed in aerosols was applied, over land and water in the first model level.

After applying the wet and dry deposition schemes the concentration of Hg^0 adsorbed is not considered anymore. The reason for the obvious difference in deposition values for Hg^0 adsorbed is the following: Hg^0 adsorbed is created through diffusion only when the relative humidity is less than 70%. In the other case, Hg^0 is transformed through chemical reactions to Hg^2 and then, Hg^2 is adsorbed. The last procedure is currently not used in the final version of both models (RAMS and SKIRON/Eta) since the computational time for the chemical procedure is extremely high and the values of the calculated Hg^2 adsorbed are in the order of 10^{-10}. Following the fact that Hg^0 adsorbed is created in regions with relative humidity less than 70%, it is expected that the higher values of dry deposition of Hg^0 adsorbed will also appear over these regions.

3. RESULTS AND DISCUSSION

In this section, a description of the meteorological conditions prevailing during the 14 to 26 August 1997 simulation period, as well as mercury concentration and their wet and dry deposition pattern is presented. This description is based on both RAMS and SKIRON/Eta output fields, and it is focused mainly on the State of New York. The analysis of the results is focused on wet and dry deposition of all three mercury species (Hg^0, Hg^2 and Hg^P) and models outputs are compared with all available observations.

3.1 Meteorological conditions

A detailed meteorology has been derived for the 14 to 26 August 1997 simulation period using RAMS and SKIRON/Eta system. Detailed meteorology is critical to improve the mercury concentration estimates, and to define the wet deposition patterns, as the total precipitation is determinative, especially for Hg^2 and Hg^P species. Both models used have the ability to simulate meteorological variables, such as wind, temperature, rain and the prevailing meteorological conditions with good accuracy.

The Geopotential height valid at 1200 UTC 16 August 1997 (note that UTC is EST+5h) is presented in Fig. 3.1. Contours indicate the geopotential height of the 850 hPa surface, expressed in meters. Low geopotential height (compared to other locations at the same latitude) indicates the presence of a storm or trough at mid-troposphere levels. Relatively high geopotential height indicates a ridge and quiescent weather. The mean sea-level pressure valid at 1200 UTC 16 August 1997 is illustrated in Fig 3.2. Contours indicate sea level pressure in hPa (or millibars). High sea level pressure indicates calm weather. Low sea level pressure indicates cyclones or storms near the surface of the earth. Thus, it is evident that a low-pressure system that covered the Grear Lakes region extended over the area of interest (New York State) during the first days of simulation. The ECMWF analyses and RAMS model outputs, presenting the Geopotential height and the wind at 850 mbar, seem to be in good agreement (Fig. 3.3).

Meteorological data, such as temperature, wind speed and direction, derived from RAMS model during the first days of simulation are illustrated in Figs 3.4-5. A strong

southern flow was established over the northeastern US during the first day of simulation while near surface temperature over the northeastern US did not exceed 20 °C. On 21 August 1997, a deep low-pressure system extended over the State of New York inducing a strong northeastern flow (Figs. 3.6-8). Strong southerlies predicted over the Atlantic Ocean reaching the northeastern coast of US. Strong northwestern winds are evident over the Canadian borders (Figs. 3.9-3.10). The increasing temperature as well as the strengthening of southwesterly flow are important parameters that influence the dispersion and diffusion of mercury over the New York State. These conditions can support the transfer of mercury from the eastern seaboard towards the New York State.

The calculated accumulated rain, within the 12 days of simulation is illustrated in Fig. 3.11a,b (focused on the area of interest) from RAMS and SKIRON/Eta systems respectively. It is evident that the total accumulated rain calculated from both models, exhibits differences that can be attributed to the behaviour of the convective scheme used in each model (RAMS and SKIRON/Eta). SKIRON/Eta model uses the Betts-Miller-Janjic precipitation scheme, which tends to overestimate the precipitation areas, without overestimating the precipitated water. On the contrary, the RAMS microphysical scheme calculates higher amounts of precipitation in more restricted areas, leading to local peaks.

These differences on the accumulated rain patterns can strongly influence the mercury wet deposition patterns. Therefore, different wet deposition patterns of all mercury species, calculated using both models should be expected, if modelling is limited to short directions (i.e. episodes). This indicates the need of performing mercury simulations for longer period covering the entire year.

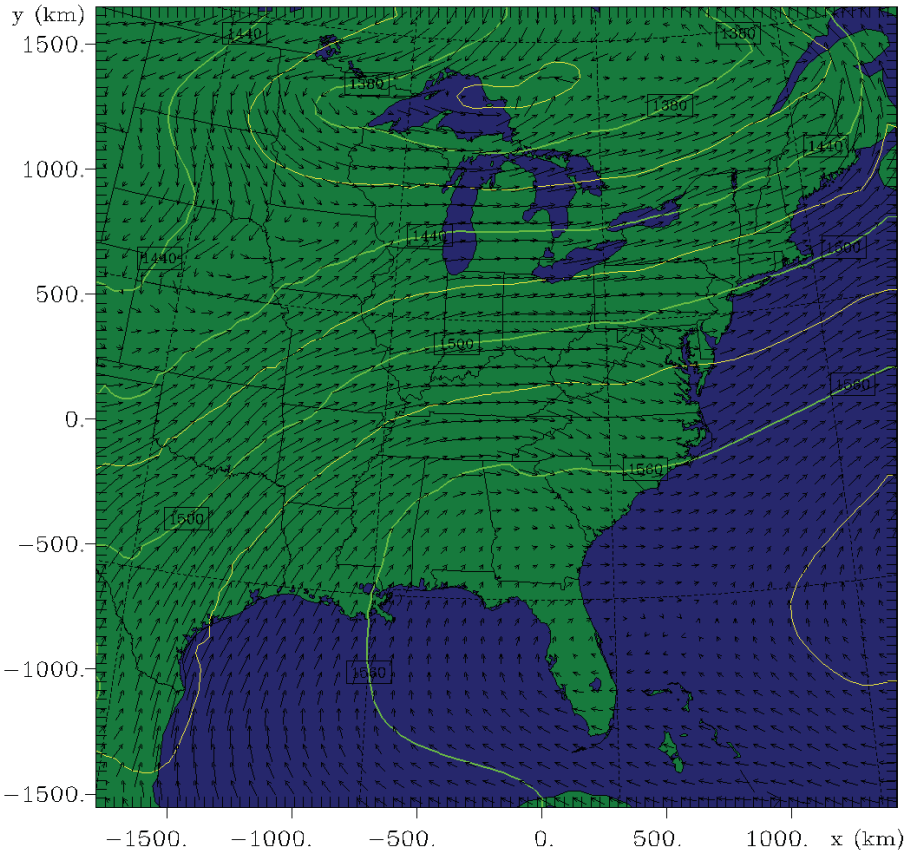

contours	geopotential height (m)	1350.	1590.	30.00	1e 0
vectors	→ 5.0 m/s horiz 5.00 m/s vert				

Figure 3.1: Geopotential heights at 850mb at 1200 UTC, on 16 August 1997 from RAMS model. Contour increment: 30 gpm.

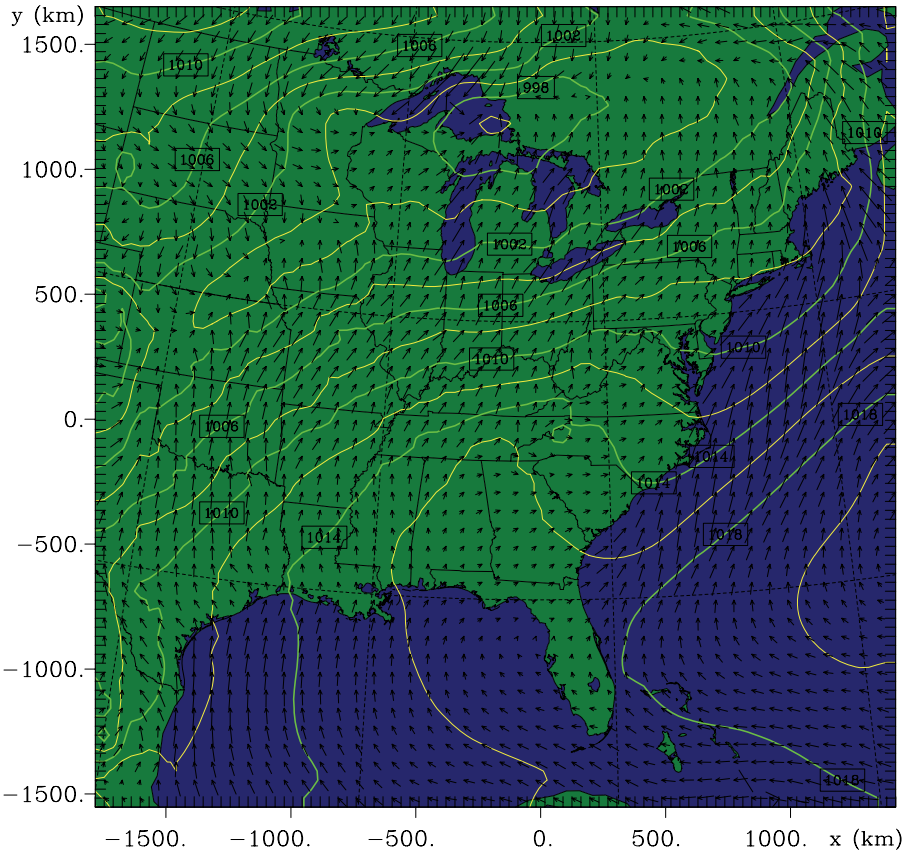

contours	sea level pressure (mb)	996.0	1020.	2.000	1e 0
vectors	→ 5.0 m/s horiz	5.00 m/s vert			

Figure 3.2: Mean Sea Level Pressure and horizontal wind field at 1200 UTC, on 16 August 1997 from RAMS model. Contour increment: 2 mbar.

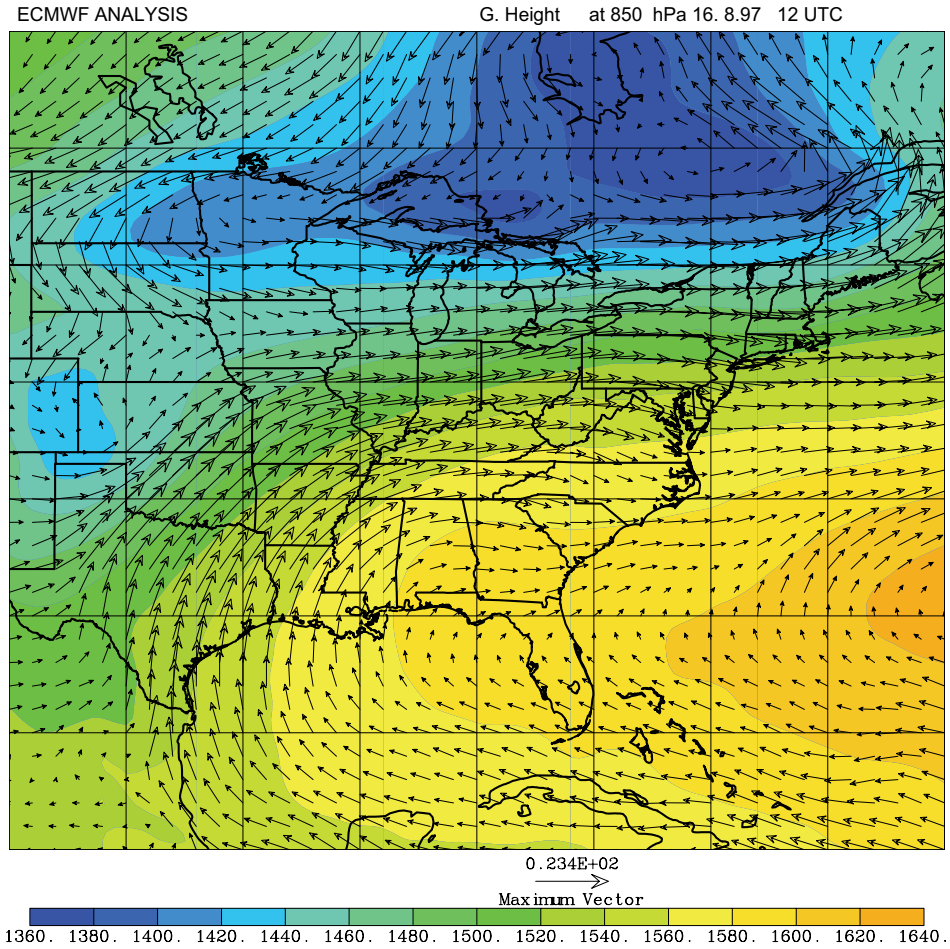

Figure 3.3: ECMWF data analysis of Geopotential height and wind speed and direction at 850 mb, at 1200 UTC, on 16 August 1997. The color scale corresponds to Geopotential height (in m).

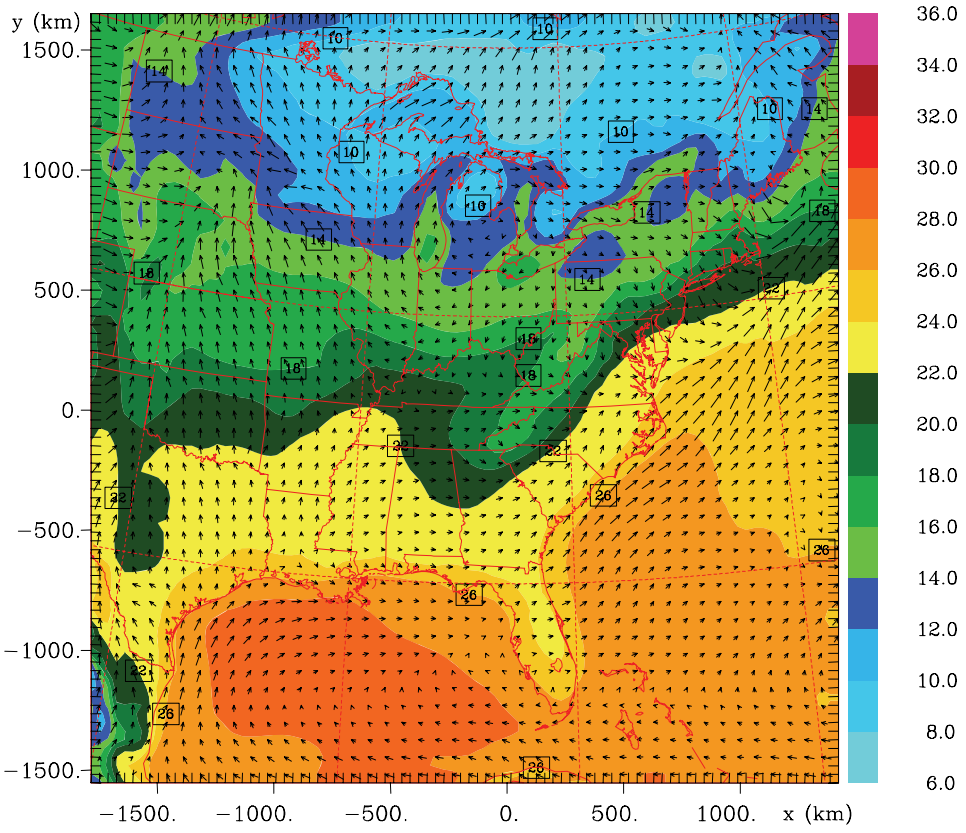

		Grid 1			
z = 69.2 m	1997−08−14−1200 UTC 0 s	min	max	inc	lab*
contours	temperature (C)	8.000	36.00	2.000	1e 0
vectors	→ 5.0 m/s horiz 5.00 m/s vert				

Figure 3.4: Temperature and horizontal wind field at the fist model level (~ 69 m) at 1200 UTC, on 14 August 1997 from RAMS model. The color scale corresponds to temperature (in ^{o}C).

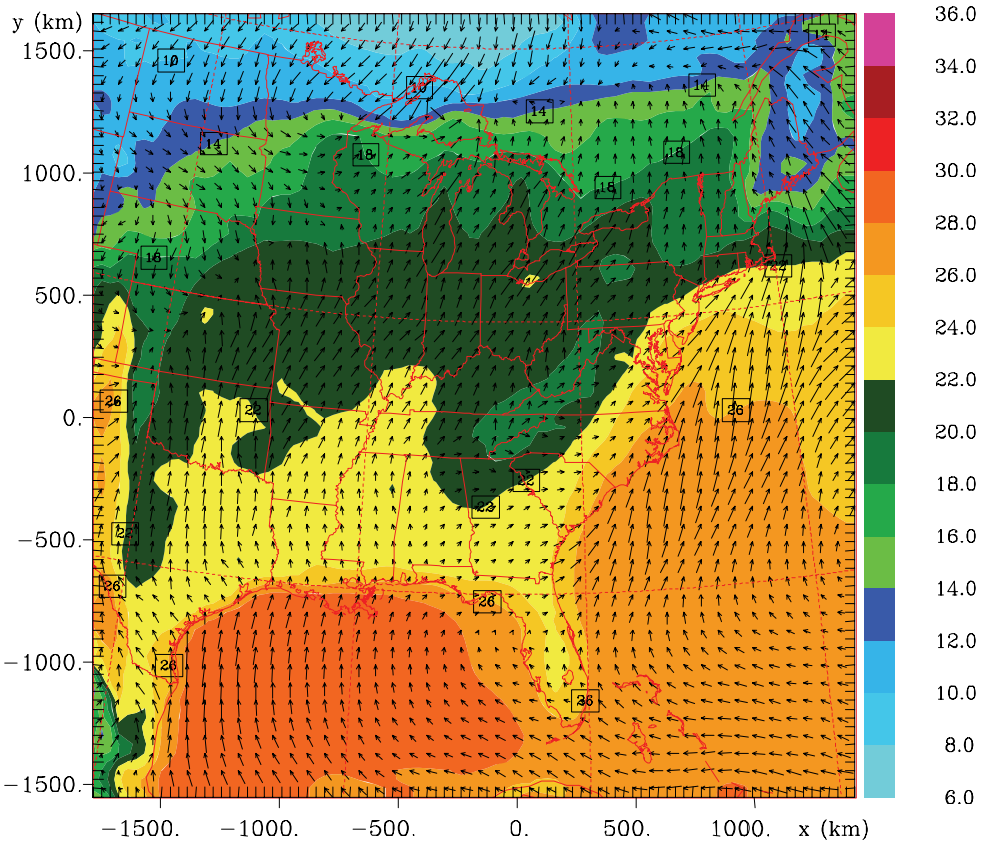

		Grid 1			
z = 69.2 m	1997−08−16−1200 UTC 0 s	min	max	inc	lab*
contours	temperature (C)	8.000	36.00	2.000	1e 0
vectors	→ 5.0 m/s horiz 5.00 m/s vert				

Figure 3.5: Temperature and horizontal wind field at the fist model level (~ 69 m) at 1200 UTC, on 16 August 1997 from RAMS model. The color scale corresponds to temperature (in ^{o}C).

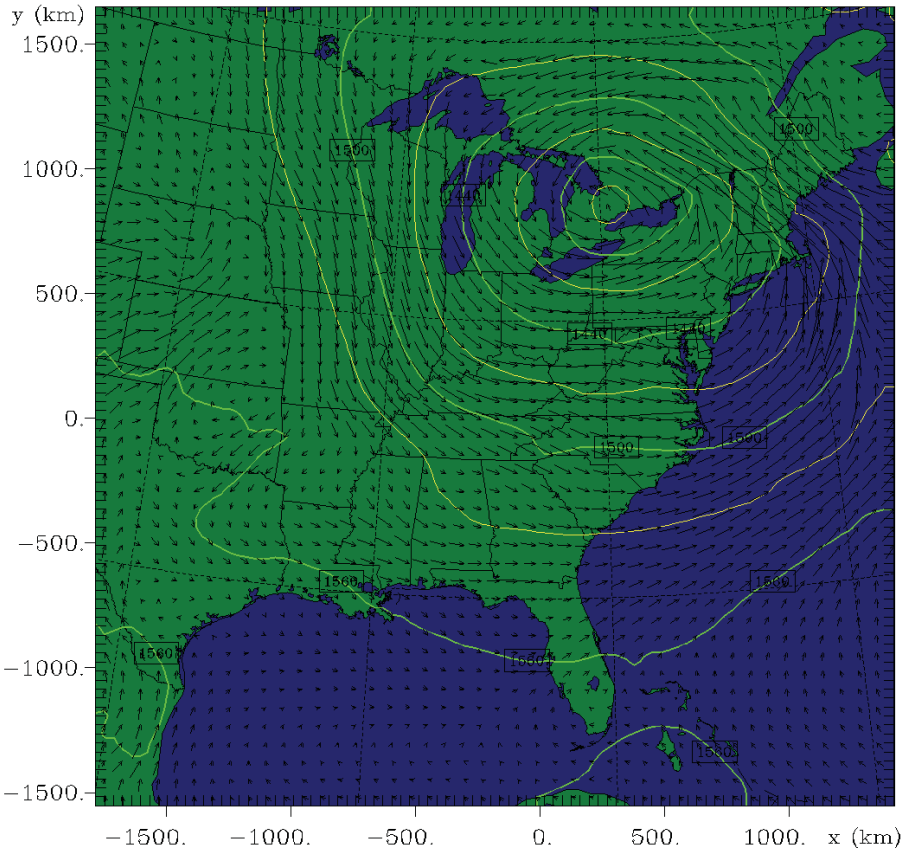

contours	geopotential height (m)	1350.	1560.	30.00	1e 0
vectors	→ 5.0 m/s horiz 5.00 m/s vert				

Figure 3.6: Geopotential heights at 850mb at 1200 UTC, on 21 August 1997 from RAMS model. Contour increment: 30 gpm.

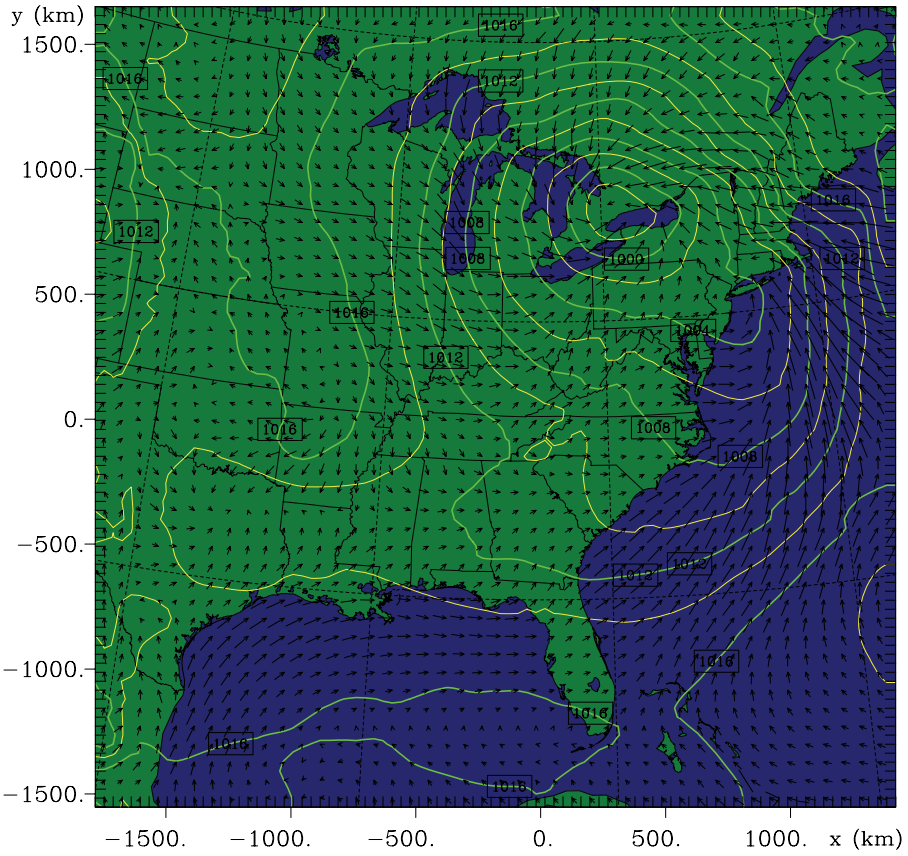

Figure 3.7: Mean Sea Level Pressure and total winds at 1200 UTC, on 21 August 1997 from RAMS model. Contour increment: 2 mbar.

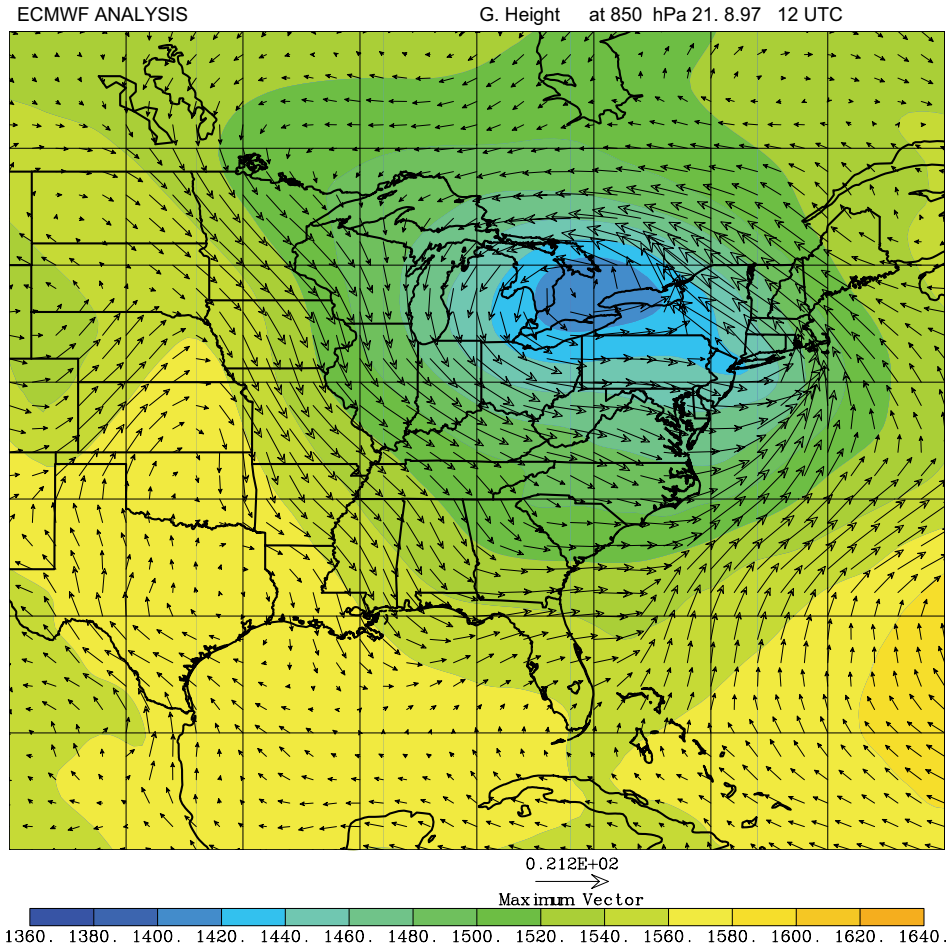

Figure 3.8: ECMWF data analysis of Geopotential height and wind speed and direction at 850 mb at 1200 UTC, on 21 August 1997. The color scale corresponds to Geopotential height (in m).

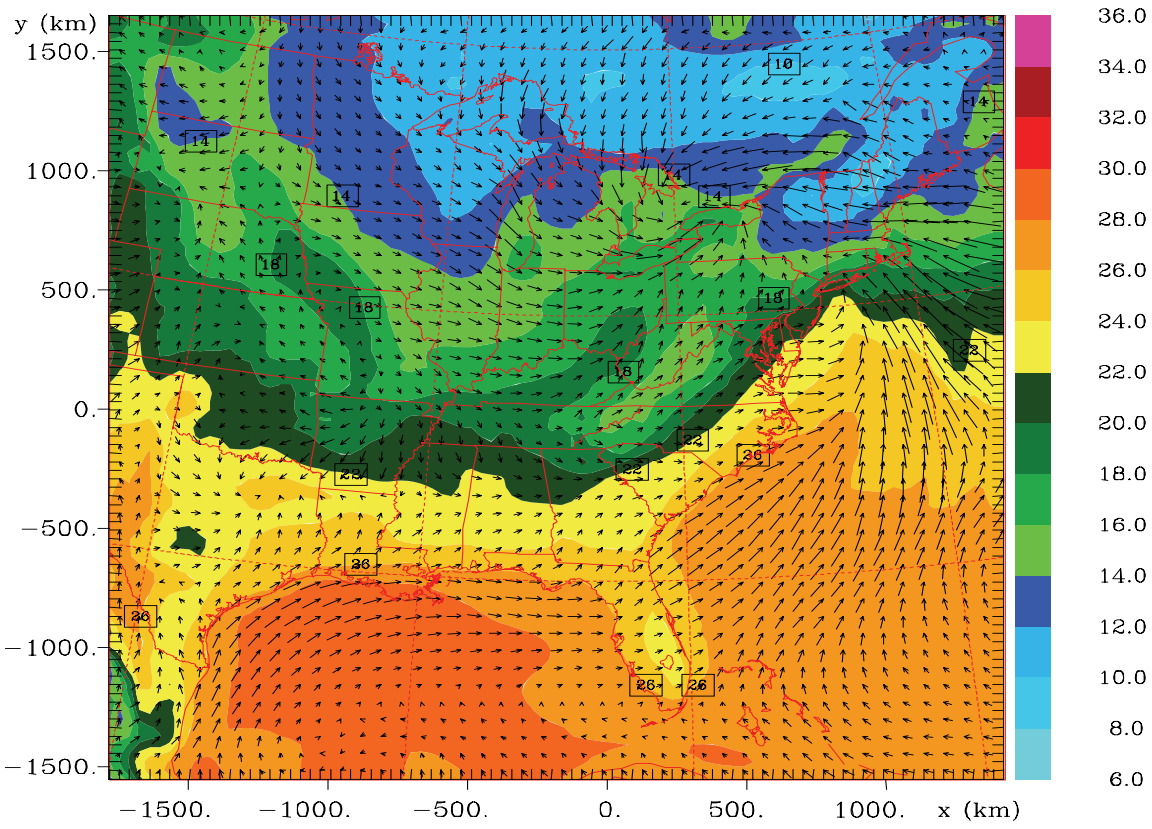

		Grid 1			
z = 69.2 m	1997−08−21−1200 UTC 0 s	min	max	inc	lab*
contours	temperature (C)	8.000	36.00	2.000	1e 0
vectors	→ 5.0 m/s horiz 5.00 m/s vert				

Figure 3.9: Temperature and horizontal wind field at the fist model level (~ 69 m) at 1200 UTC, on 21 August 1997 from RAMS model. The color scale corresponds to temperature (in ^{o}C).

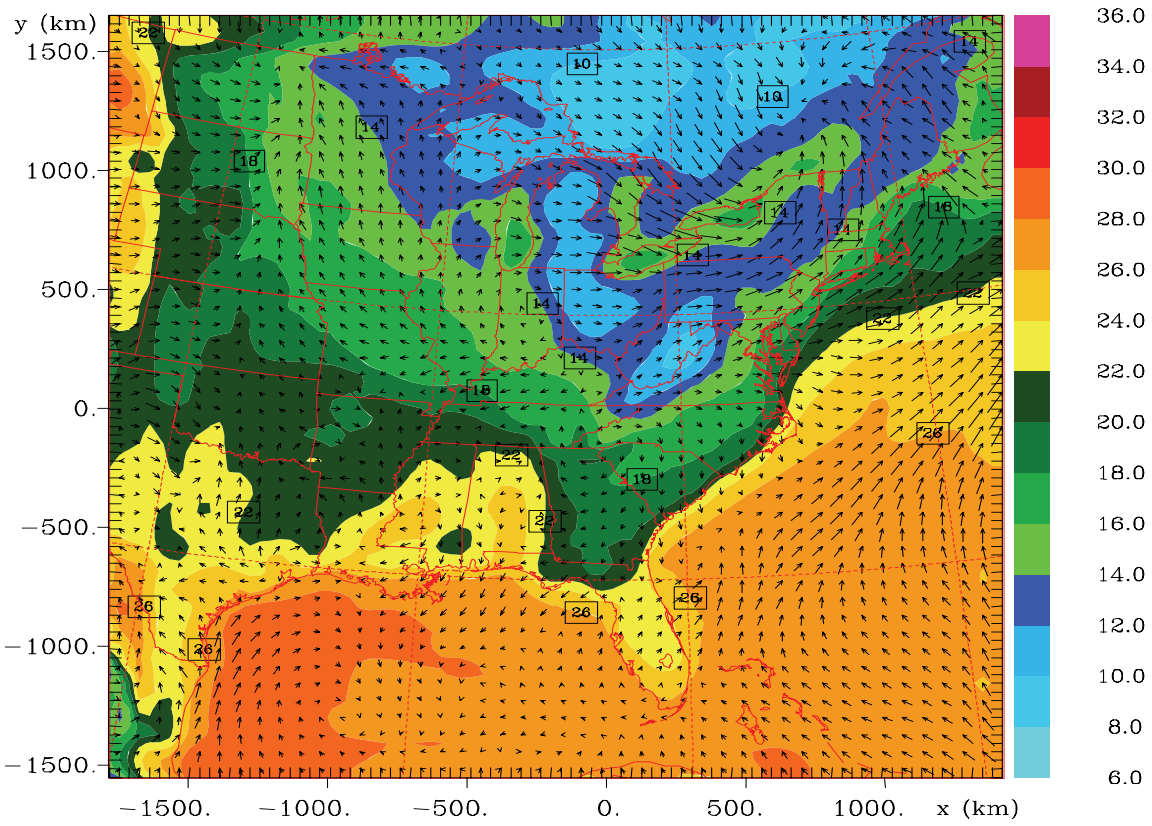

		Grid 1			
z = 69.2 m	1997−08−23−1200 UTC 0 s	min	max	inc	lab*
contours	temperature (C)	8.000	36.00	2.000	1e 0
vectors	→ 5.0 m/s horiz 5.00 m/s vert				

Figure 3.10: Temperature and horizontal wind field at the fist model level (~ 69 m) at 1200 UTC, on 23 August 1997 from RAMS model. The color scale corresponds to temperature (in ^{o}C).

(a)

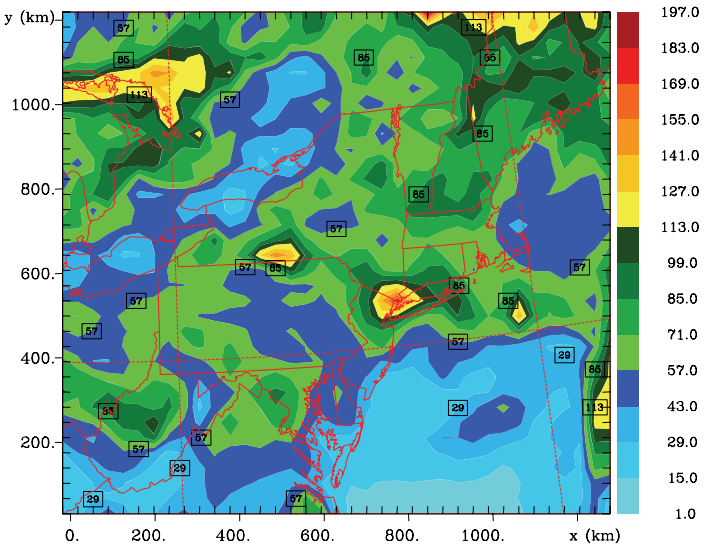

		Grid 1			
	1997-08-26-0000 UTC 0 s	min	max	inc	lab*
contours	total accum precip (mm)	15.00	197.0	14.00	1e 0

(b)

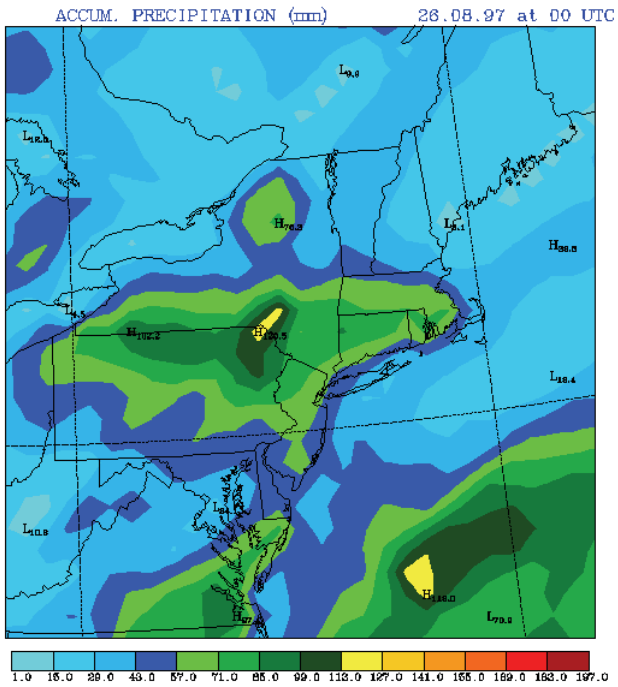

Figure 3.11: 12-days (14-26 August 1997) accumulated rain (mm), from (a) RAMS system (b) SKIRON/Eta system.

3.2 Simulation performed with all sources

The relative contributions of in-state mercury sources and out-state sources to the mercury deposition are an important issue for policy makers in New York State. In this project, we performed two simulations, one with all available sources of NE USA and another without the New York State sources. The location of the sources in both cases with and without the New York State sources is illustrated in Figs 2.1-2 respectively. The concentration of mercury species is dictated by many factors that affect the chemical and physical processes such as atmospheric reactions and deposition. It also depends strongly on flow conditions and source locations (Davies and Notcutt 1996).

The simulation performed with all available sources showed that the Hg^0 concentrations were nearly uniform all over the domain, with higher concentrations near the sources especially during the first few hours of the simulation. Also, Hg^2 and Hg^P concentrations were still high around the sources for selected periods during the day. This can be attributed to the photochemical reactions producing Hg^2 and Hg^P during the daytime and to the poor dispersion conditions prevailing at the time. This is also consistent with the literature (Schroeder et. al 1998), as Hg^0 is known as a long-range transport pollutant, while Hg^2 can be removed in the vicinity of a few tens to a few hundreds of kilometres. In addition Hg^P species are likely to be deposited at intermediate distances depending on the prevailing wash-out mechanisms. These differences on the transport mechanisms for each specie are clearly illustrated in the concentration patterns of Hg^0, Hg^2 and Hg^P presented in Figs 3.12-14, respectively.

It is known that mercury enters the aquatic environment through the deposition processes. Therefore, it is important to estimate the amount of mercury species deposited through different atmospheric processes. The mechanisms used to simulate the transport and deposition of Hg^2 and Hg^P have been described above. An attempt was made to calculate the accumulated deposition patterns for the simulation period. More specifically, the wet and dry deposition patterns of Hg^P, Hg^2 and Hg^0-adsorbed were estimated using both models RAMS and SKIRON/Eta.

The dry deposition patterns of all three mercury species are varying over sea and over land. The transport of mercury species is dependent upon the advective transport by the mean wind and transport by turbulent dispersion. The spatial and temporal variations on the dry deposition patterns can be determined through the similarities

with the conventional pollutants. The dry deposition pattern of Hg^0-adsorbed in Total Suspended Particles (TSPs) is illustrated in Fig. 3.15. During the integration period, the dry deposition values of Hg^0-adsorbed, are generally higher over land. This is attributed to the dry deposition scheme over land and over water (as it is described in §2.2.3) used in both models. In addition, the amounts of Hg^0-adsorbed in Total Suspended Particles (TSP) are lower compared to the other species. However, they are considered important for the mercury concentrations and deposition and, therefore, included and treated separately in both models.

The accumulated (during the 12 days of the simulation) amounts of Hg^P that is deposited through dry processes are greater over the sea than over land as illustrated in Fig. 3.16. The dry deposition patterns of Hg^P and Hg^0-adsorbed depend on the pollutant concentration and the deposition velocity. The deposition velocity of Hg^P used in these simulations is a weighted average of 15 deposition velocities, corresponding to the 15 size intervals at which particles are distributed. Over regions with high humidity (e.g. over sea surface) greater deposition velocities are observed due to the dependence of the deposition velocity with the size of the particles. Particles growth is relatively high under these conditions.

Dry and wet deposition patterns of Hg^2 are illustrated in Figs 3.17-18. The highest amounts of the pollutant are deposited near the sources. This is also consistent with the literature (Schroeder and Munthe 1998). Hg^2 is also highly soluble so it dominates the wet deposition pattern of gaseous mercury. The wet deposition pattern of Hg^2 has several similarities with the wet deposition pattern of Hg^0-adsorbed, but the Hg^2 deposited amounts are higher.

The wet deposition pattern of Hg^0-adsorbed is similar to the Hg^P since the total amount of precipitation is higher over the mountainous areas (see Figs 3.19 and 3.20, respectively).

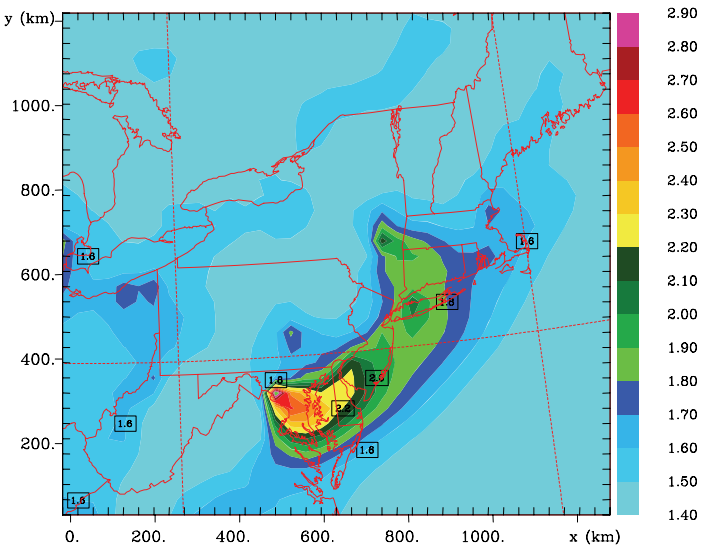

		Grid 1			
z = 69.2 m	1997-08-14-1200 UTC 0 s	min	max	inc	lab*
contours	Hg0 (ng/m3)	1.500	2.900	0.1000	1e 0

Figure 3.12: Hg^0 concentration at the first model level (~ 69 m) at 1200 UTC on 14 August 1997 from RAMS model. The color scale corresponds to concentration (in ng/m^3).

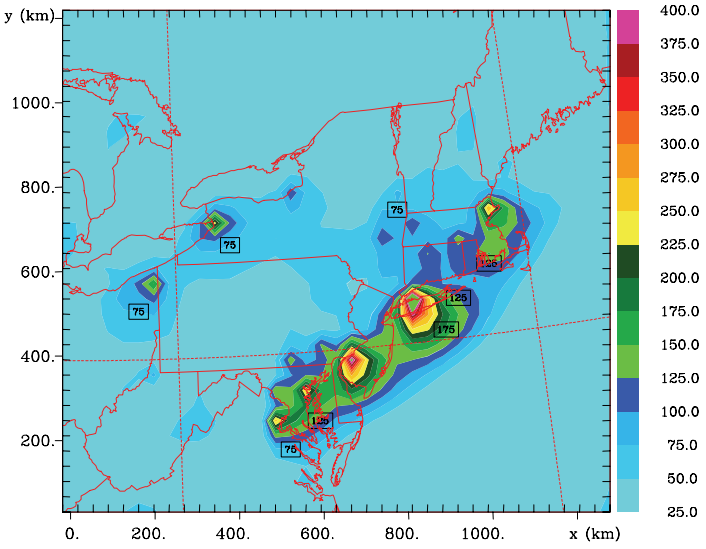

		Grid 1			
z = 69.2 m	1997-08-14-1200 UTC 0 s	min	max	inc	lab*
contours	Hg2 (pg/m3)	50.00	400.0	25.00	1e 0

Figure 3.13: Hg^2 concentration at the first model level (~ 69 m) at 1200UTC on 14 August 1997, from RAMS model. The color scale corresponds to concentration (in pg/m^3).

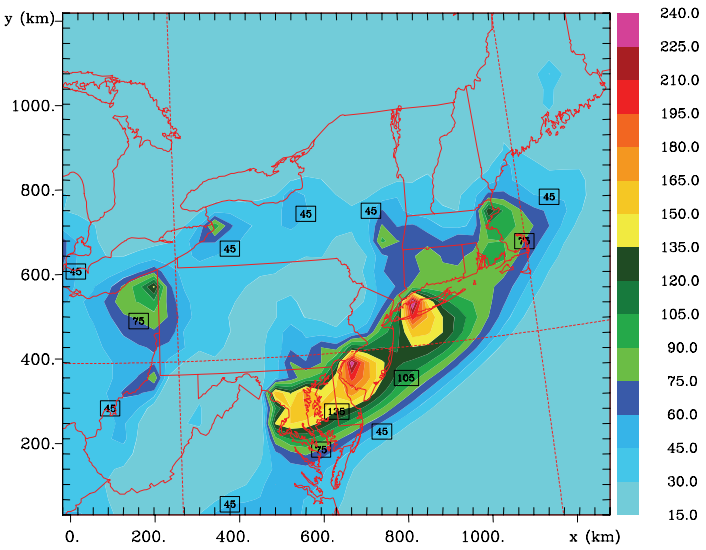

		Grid 1			
z = 69.2 m	1997-08-14-1200 UTC 0 s	min	max	inc	lab*
contours	Hgp (pg/m3)	30.00	240.0	15.00	1e 0

Figure 3.14: Hg^P concentration at the first model level (~ 69 m) at 1200UTC on 14 August 1997 from RAMS model. The color scale corresponds to concentration (in pg/m^3).

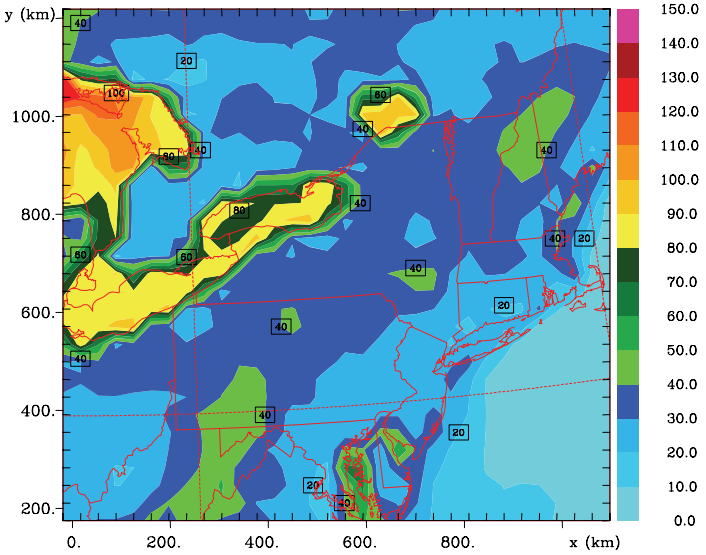

		Grid 1			
	1997-08-26-0000 UTC 0 s	min	max	inc	lab*
contours	Dry dep. Hg0 ads. (pg/m2)	10.00	150.0	10.00	1e 0

Figure 3.15: Dry deposition of Hg^0 adsorbed (in pg/m^2) at 0000 UTC on 26 August 1997 after 14 days of simulation, estimated from RAMS model.

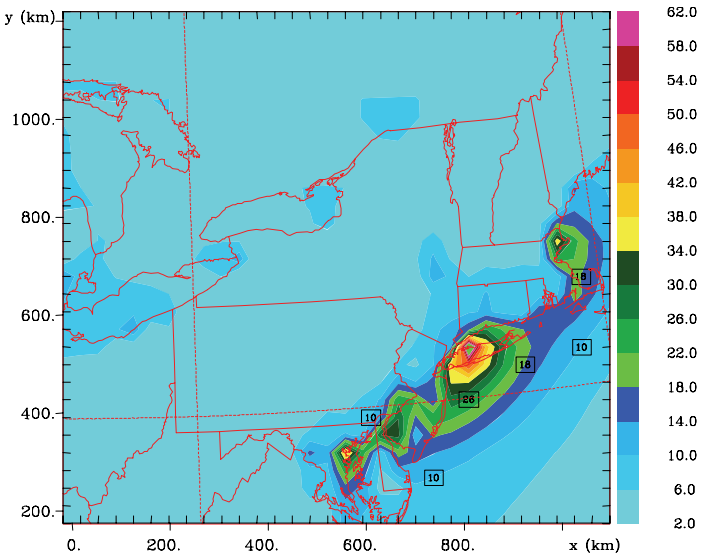

		Grid 1			
	1997-08-26-0000 UTC 0 s	min	max	inc	lab*
contours	Dry dep. of Hgp (ng/m2)	6.000	62.00	4.000	1e 0

Figure 3.16: Dry deposition of Hg^P (in ng/m^2) at 0000 UTC on 26 August 1997 after 14 days of simulation, estimated from RAMS model.

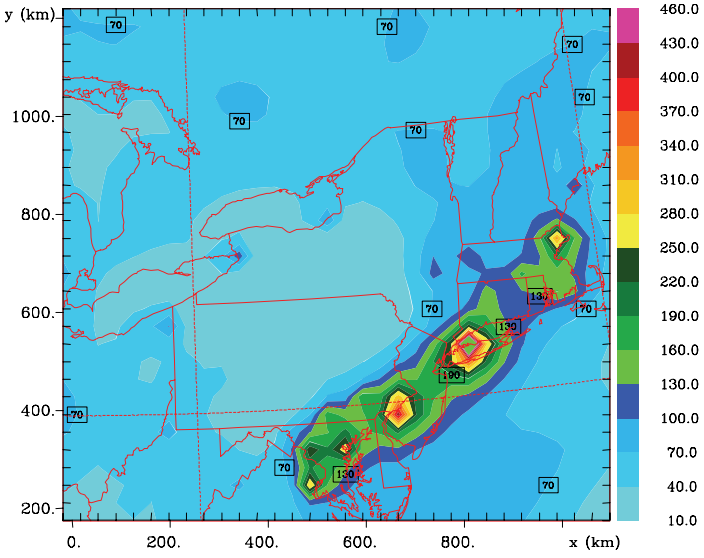

		Grid 1			
	1997-08-26-0000 UTC 0 s	min	max	inc	lab*
contours	Dry dep. of Hg2 (ng/m2)	40.00	460.0	30.00	1e 0

Figure 3.17: Dry deposition of Hg^2 (in ng/m^2) at 0000 UTC on 26 August 1997 after 14 days of simulation, estimated from RAMS model.

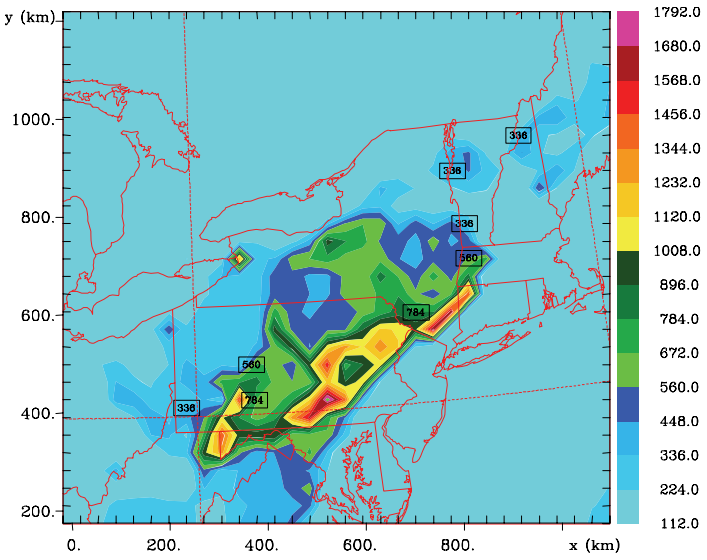

		Grid 1			
	1997-08-26-0000 UTC 0 s	min	max	inc	lab*
contours	Wet dep. of Hg2 (ng/m2)	224.0	1792.	112.0	1e 0

Figure 3.18: Wet deposition of Hg^2 (in ng/m^2) at 0000 UTC on 26 August 1997 after 14 days of simulation, estimated from RAMS model.

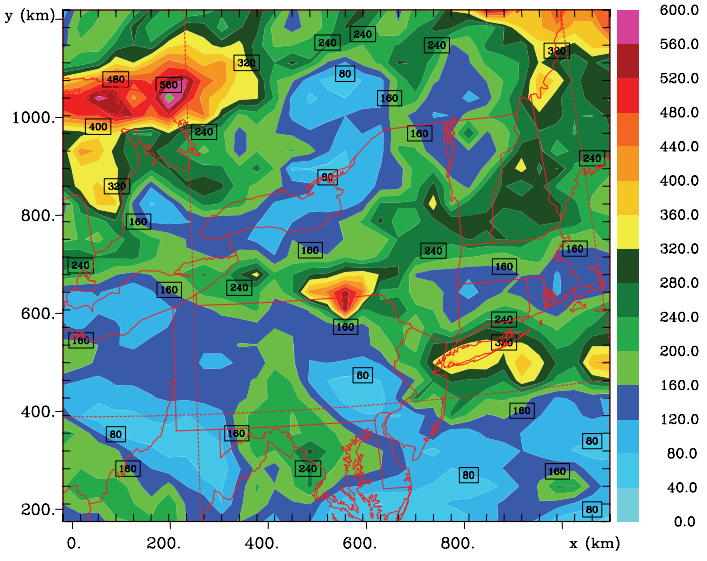

		Grid 1			
	1997-08-26-0000 UTC 0 s	min	max	inc	lab*
contours	Wet dep. of Hg0 ads. (pg/m2)	40.00	600.0	40.00	1e 0

Figure 3.19: Wet deposition of Hg^0 adsorbed (in pg/m^2) at 0000 UTC on 26 August 1997 after 14 days of simulation, estimated from RAMS model.

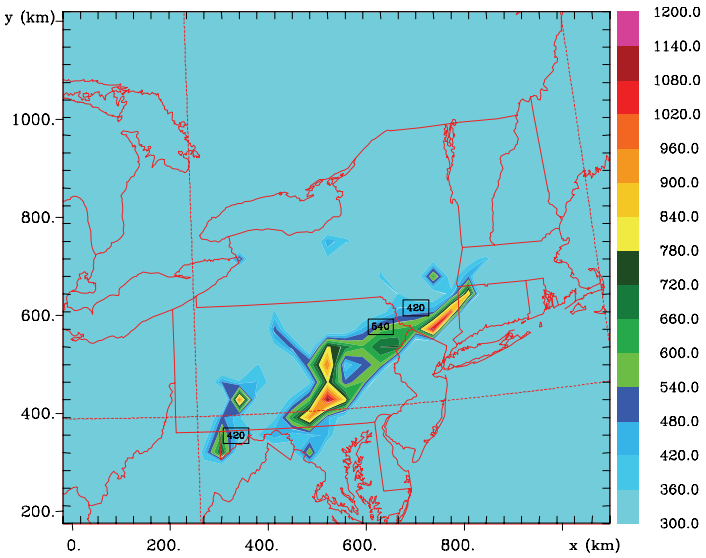

		Grid 1			
	1997-08-26-0000 UTC 0 s	min	max	inc	lab*
contours	Wet dep. of Hgp (ng/m2)	360.0	1200.	60.00	1e 0

Figure 3.20: Wet deposition of Hg^p (in ng/m^2) at 0000 UTC on 26 August 1997 after 14 days of simulation, estimated from RAMS model.

The total deposited mercury (wet and dry) for the simulation performed using all available mercury sources was also averaged over the New York State. More specifically, the wet and dry deposition of Hg^P, Hg^2 and Hg^0-adsorbed were calculated using both modelling systems, namely RAMS and SKIRON/Eta. Dry and wet deposition of all mercury species, accumulated for the simulation period and averaged over the entire domain of the State of New York, is shown in Fig. 3.21. The model results are in good agreement, since the calculated amounts of deposited mercury do not exhibit major differences. However, SKIRON/Eta system calculated consistently higher amounts of wet and dry deposited mercury. The differences in the total (wet and dry) deposited amounts of mercury between the two systems are attributed mainly to the larger amounts of wet deposited mercury calculated from SKIRON/Eta. As mentioned previously in several parts of this report, the wet deposition pattern of mercury is strongly dependent on the precipitation pattern. The Betts-Miller-Janjic precipitation scheme that SKIRON/Eta uses tends to overestimate the precipitation areas, without overestimating the precipitated water. On the contrary, the RAMS microphysical scheme calculates higher amounts of precipitation in more restricted areas, leading to local peaks.

In general, the agreement between the calculated total deposited amounts of both models is quite good (Fig. 3.21). This indicates that they are reliable tools in the study of mercury and that these modelling systems can be used for longer period simulations and estimations of mercury depositions.

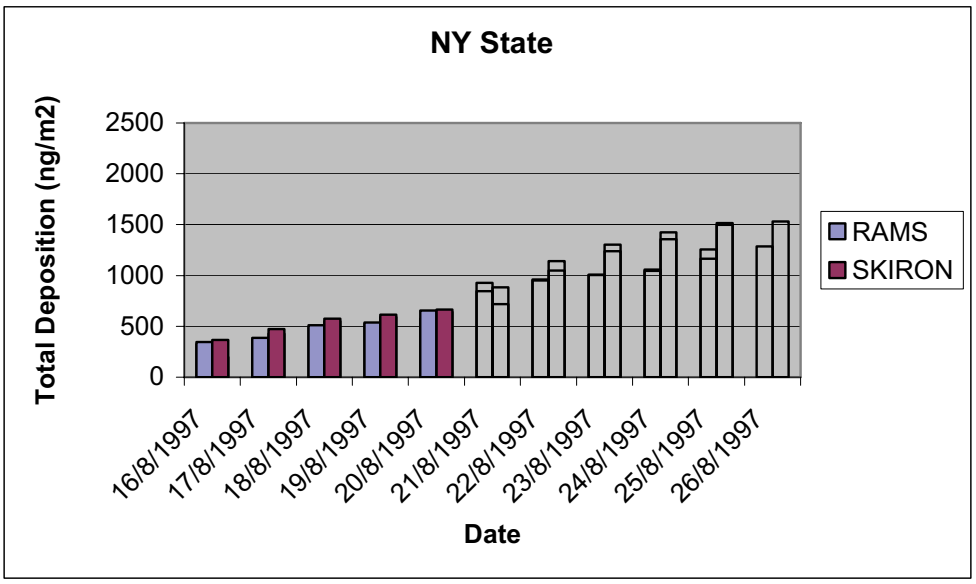

Figure 3.21 Total deposition of mercury (ng/m^2) calculated from RAMS and SKIRON/Eta systems (with NY State emissions) averaged over NY State from 14 to 26 August 1997.

3.3 Simulation without NY State Hg emission sources

In this project a great effort was devoted in an attempt to identify the in out of state contributions of mercury sources to the total deposited mercury over the State of New York. More specifically, simulations were performed for the period 14 to 26 August 1997 without using the sources located in the State of New York.

The mercury concentrations calculated in both cases (with and without the New York State sources) were then compared. The concentrations of all mercury species (Hg^0, Hg^2, Hg^p) when there are no sources over the State of New York are illustrated in Figs 3.22, 3.23 and 3.24 respectively and compared with the Figs 3.12-14. The low concentrations (close to the background value) of all three species in the State of New York, during the first few days of the simulation, indicated the lack of emission sources.

The differences between the Hg^0 concentration patterns appeared mainly downwind the State of New York. As expected the differences in Hg^2 are also evident over the State of New York as Hg^2 can be removed in the vicinity of a few tens to a few hundreds of kilometres downstream of the source. Finally the Hg^P concentrations are different within the State of New York and at intermediate from the sources distances.

In addition, the absence of emission is likely to exert strong influence not only on the concentration pattern of all species but also on their maximum values. Thus, the models can be helpful in estimating the mercury concentration due to the lack of reliable and consistent measuring methods.

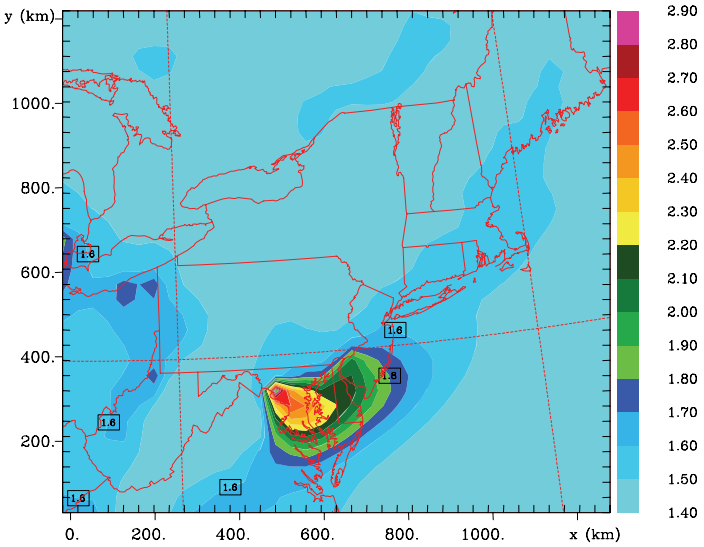

		Grid 1			
z = 69.2 m	1997-08-14-1200 UTC 0 s	min	max	inc	lab*
contours	Hg0 (ng/m3)	1.500	2.900	0.1000	1e 0

Figure 3.22: Hg^0 concentration at the first model level (~ 69 m) at 1200 UTC on 14 August 1997 from RAMS model (without NY sources). The color scale corresponds to concentration (in ng/m^3).

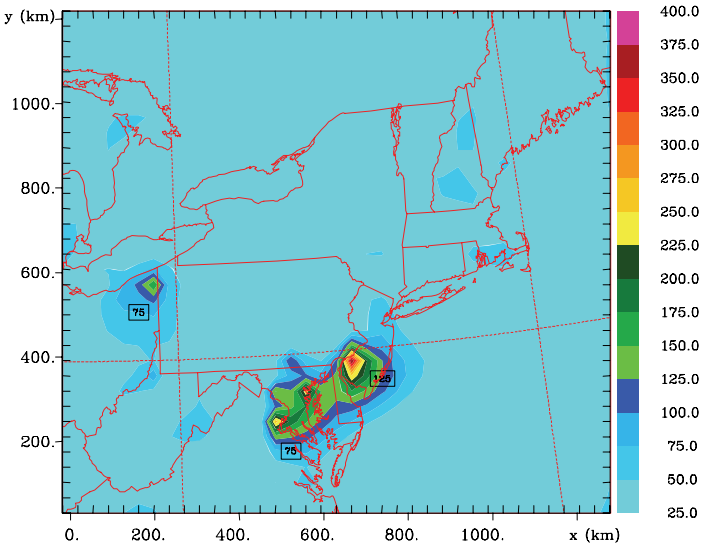

		Grid 1			
z = 69.2 m	1997-08-14-1200 UTC 0 s	min	max	inc	lab*
contours	Hg2 (pg/m3)	50.00	400.0	25.00	1e 0

Figure 3.23: Hg^2 concentration at the first model level (~ 69 m) at 1200 UTC on 14 August 1997 from RAMS model. (without NY sources). The color scale corresponds to concentration (in ng/m^3).

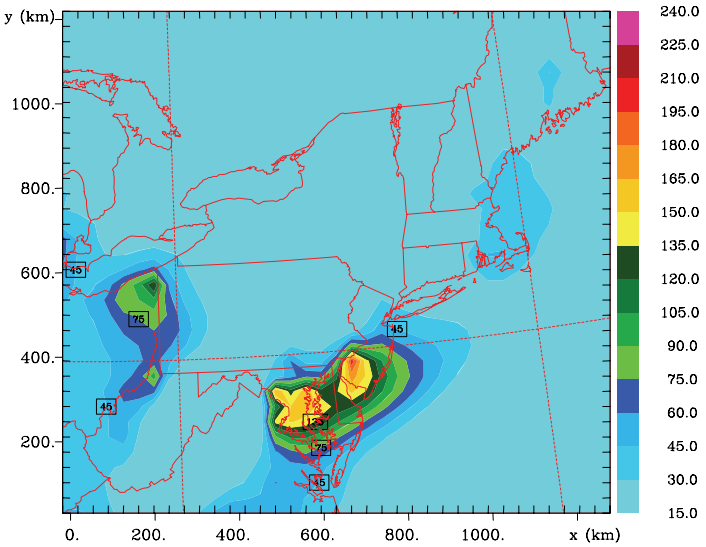

		Grid 1			
z = 69.2 m	1997-08-14-1200 UTC 0 s	min	max	inc	lab*
contours	Hgp (pg/m3)	30.00	240.0	15.00	1e 0

Figure 3.24: Hg^p concentration at the first model level (~ 69 m) at 1200 UTC on 14 August 1997 from RAMS model. (without NY sources). The color scale corresponds to concentration (in ng/m^3).

Wet and dry depositions of all mercury species were also calculated for the second scenario, namely the simulation performed without using the sources available over the State of New York. When sources of mercury are not considered, the dry and wet deposited amount of all species over the selected area of New York is lower (see Figs 3.25-30). The sources of mercury increase the concentration of all species in the State of New York. Therefore, as sources of the pollutant located over the State of New York are excluded for the second simulation scenario, the mercury deposited amount is lower. Major differences between the two simulations are evident for Hg^2 and Hg^P since these species transported in short and intermediate distances respectively.

The two simulations have been also compared for a selected site. This site is Adirondacks, located in the State of New York. This can provide an estimation of the relative contribution of local emissions versus long-range transport to mercury deposition at a specific location. The results of these simulations performed using both models are presented in Figs 3.31 and 3.32. The wet deposition of all three mercury species when the New York State sources are not used, reduced up to 15% . The differences appeared between the two models are lower in the second case without the sources. The differences between the two models increased in both cases (with and without New York State) after the 21st of August. This is due to the precipitation schemes of both models and the prevailing weather conditions during the simulation, especially after the 21st of August 1997.

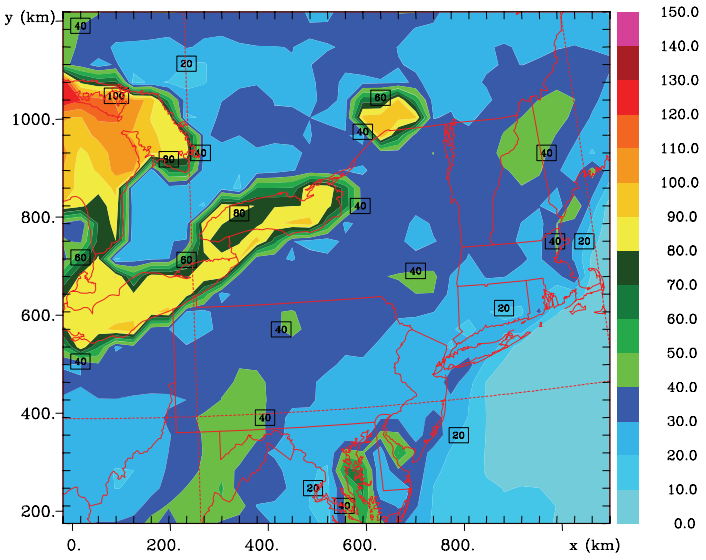

		Grid 1			
	1997-08-26-0000 UTC 0 s	min	max	inc	lab*
contours	Dry dep. Hg0 ads. (pg/m2)	10.00	150.0	10.00	1e 0

Figure 3.25: Dry deposition of Hg^0 adsorbed (in pg/m^2) at 0000 UTC on 26 August 1997 after 14 days of simulation, estimated from RAMS model (without NY sources).

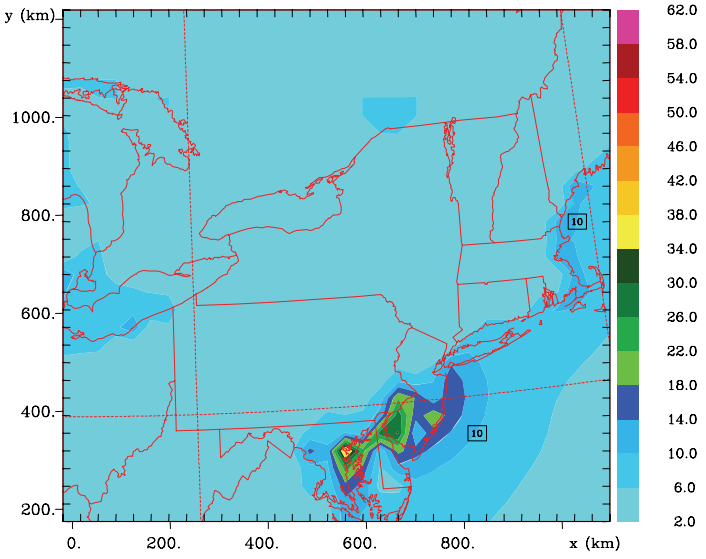

		Grid 1			
	1997-08-26-0000 UTC 0 s	min	max	inc	lab*
contours	Dry dep. of Hgp (ng/m2)	6.000	62.00	4.000	1e 0

Figure 3.26: Dry deposition of Hg^P (in ng/m^2) at 0000 UTC on 26 August 1997 after 14 days of simulation, estimated from RAMS model (without NY sources).

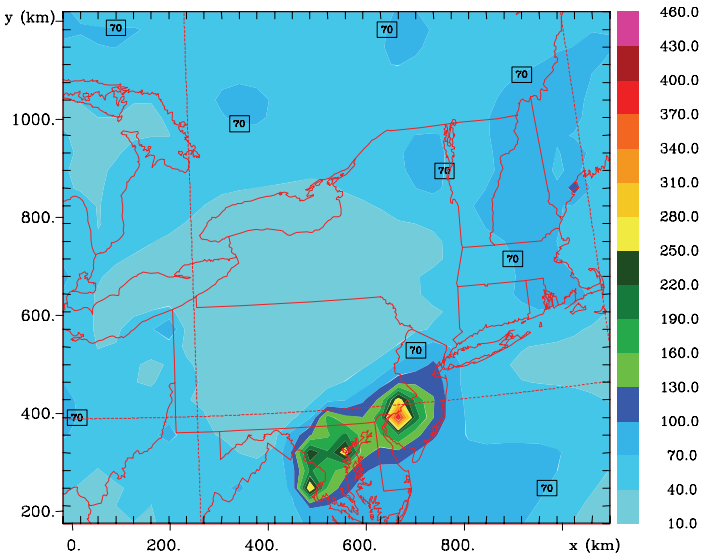

		Grid 1			
	1997-08-26-0000 UTC 0 s	min	max	inc	lab*
contours	Dry dep. of Hg2 (ng/m2)	40.00	460.0	30.00	1e 0

Figure 3.27: Dry deposition of Hg^2 (in ng/m^2) at 0000 UTC on 26 August 1997 after 14 days of simulation, estimated from RAMS model (without NY sources).

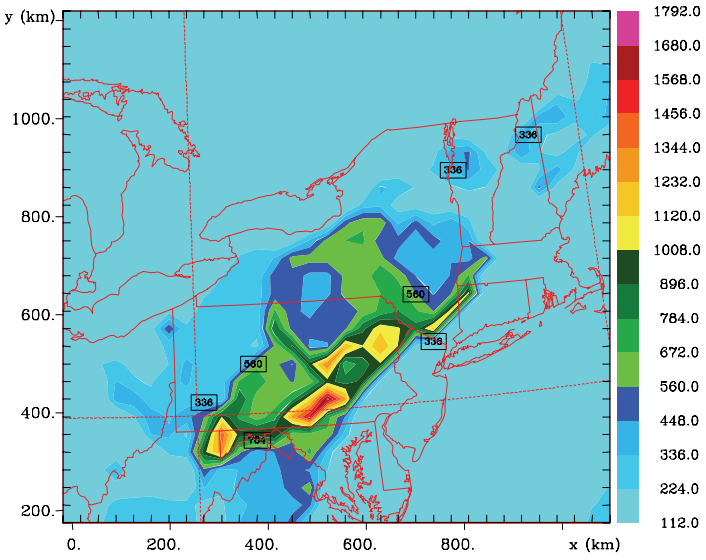

		Grid 1			
	1997-08-26-0000 UTC 0 s	min	max	inc	lab*
contours	Wet dep. of Hg2 (ng/m2)	224.0	1792.	112.0	1e 0

Figure 3.28: Wet deposition of Hg^2 (in ng/m^2) at 0000 UTC on 26 August 1997 after 14 days of simulation, estimated from RAMS model (without NY sources).

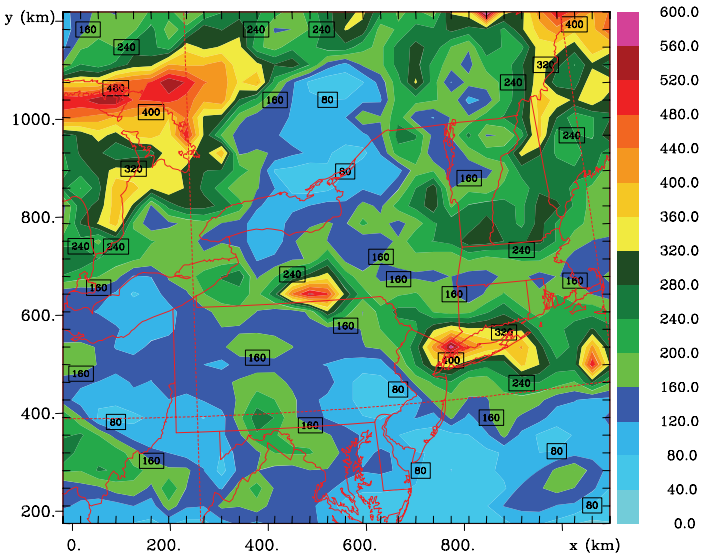

		Grid 1			
	1997-08-26-0000 UTC 0 s	min	max	inc	lab*
contours	Wet dep. of Hg0 ads. (pg/m2)	40.00	600.0	40.00	1e 0

Figure 3.29: Wet deposition of Hg^0 adsorbed (in pg/m^2) at 0000 UTC on 26 August 1997 after 14 days of simulation, estimated from RAMS model (without NY sources).

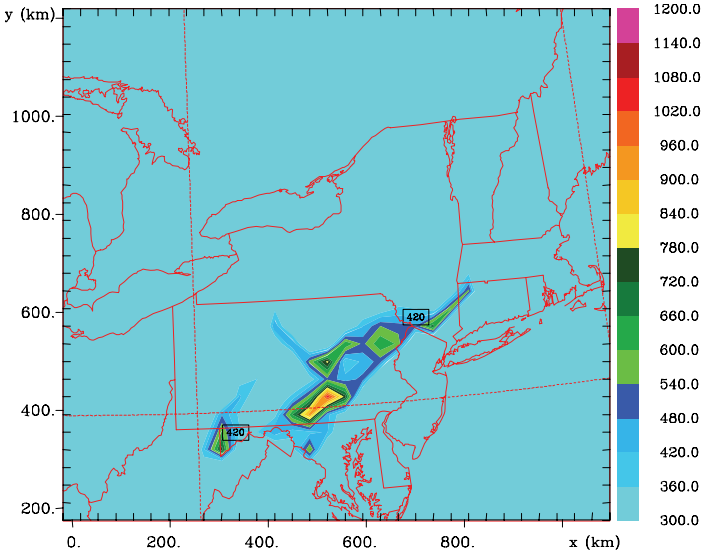

		Grid 1			
	1997-08-26-0000 UTC 0 s	min	max	inc	lab*
contours	Wet dep. of Hgp (ng/m2)	360.0	1200.	60.00	1e 0

Figure 3.30: Wet deposition of Hg^P (in ng/m^2) at 0000 UTC on 26 August 1997 after 14 days of simulation, estimated from RAMS model (without NY sources).

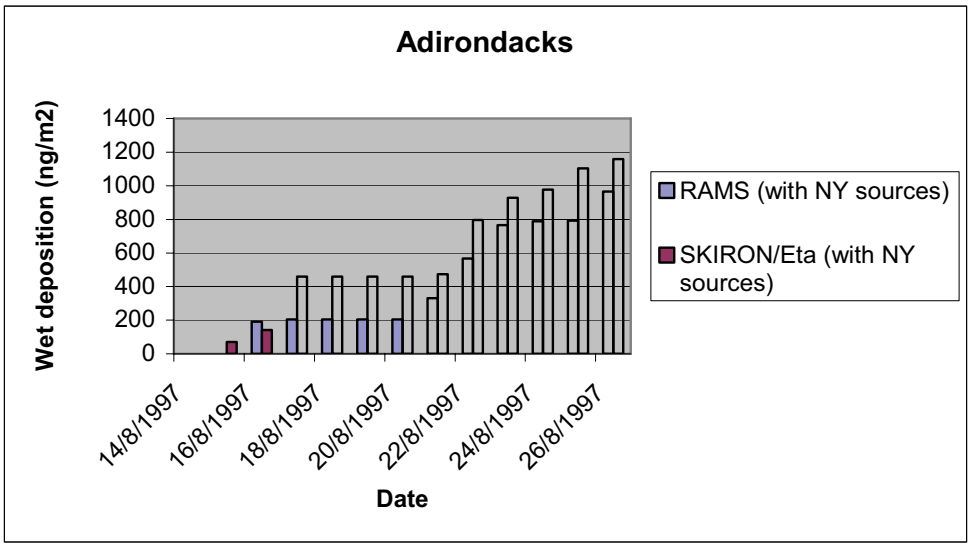

Figure 3.31: Comparison of the accumulated wet deposition of mercury (ng/m^2) calculated from RAMS and SKIRON/Eta models (with NY State emissions) at Adirondacks from 14 to 26 August 1997.

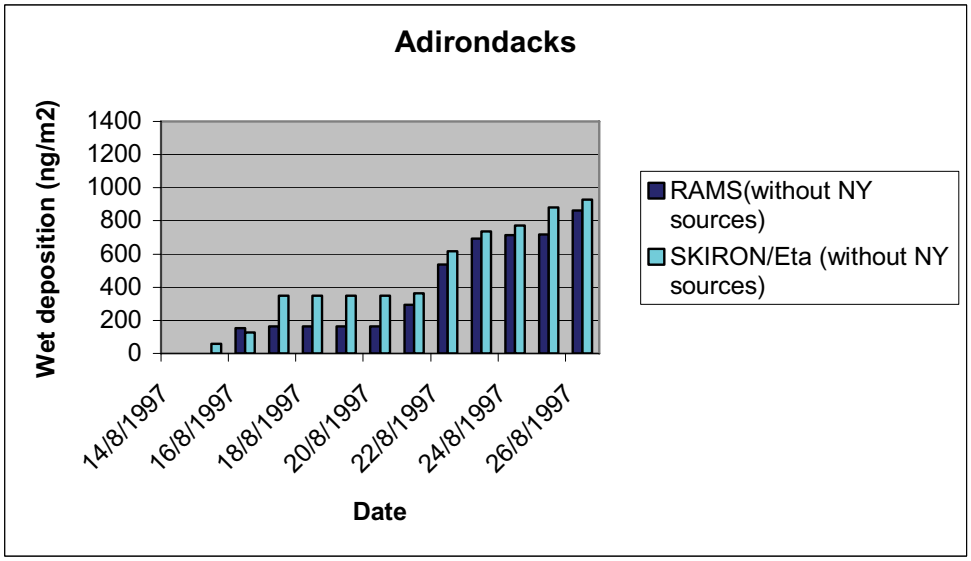

Figure 3.32: Comparison of the accumulated wet deposition of mercury (ng/m^2) calculated from RAMS and SKIRON/Eta models (without NY State emissions) at Adirondacks from 14 to 26 August 1997.

3.4. Source-receptor relationship - LPDM simulations

The purpose of this study is to better understand the source-receptor relationship, through the proposed modelling methodology. In order to achieve this, we performed simulations with the LPDM model for the defined experimental period 14 to 26 August 1997; with RAMS model. The results of this simulation are discussed in this chapter.

In the State of New York, there is a great concern about mercury deposition in locations like Adirondacks area, Catskill Mountains as well as the City of New York and its surrounding region. The combined RAMS-LPDM simulations focused on the calculations of influence functions considering Adirondacks as a receptor area. This study is performed in order to identify the source areas of the pollutant air masses traced at Adirondacks (44.0N, 74.00W) during the experimental period. Influence functions are calculated 48h backward in time, for each day of the period 19 to 26 August 1997, with a 12h time interval, considering Adirondacks as the receptor area. The simulations were performed for the lower part of the troposphere. This approach allows us to identify the location of the air masses during the previous 12h time interval, illustrating the regional transport of the air masses. The 12h time interval is chosen as a representative time period to investigate the transport of air masses in a rather small-sized domain. It is also possible to make the distinction between short range and long-range transport.

A different approach is also presented in this study, in order to compare the results from all the simulations performed for the defined period. This becomes possible by using an ensemble calculation of the influence functions for the seven-day period. The presented methology does not provide a geometric representation of the air masses, but shows the air masses veering according to time, following non-linear paths.

The first simulation started at 1200UTC on 26 August 1997, as shown in Fig.3.33. The first frame in Fig. 3.33 shows the location of the air masses during the previous 12h from the start of the simulation, meaning the time period 0000 to 1200 UTC, for 26 August 1997. The second frame shows the location of the air masses at the time period 1200UTC to 2400UTC, 25 August. Contours are in logarithmic normalized units, presenting the number of particles of unit mass per cubic meter (particles/m^3). It is evident that the air masses were located to the W and SW of Adirondacks area, following the path through the Great Lakes, in a time scale of about 36 to 48h (3^{rd} and 4^{th} frame). The light winds in the area and the poor mixing in the nocturnal boundary layer, do not favor any significant transport, the first 12h of the simulation (1^{st} frame). The second

simulation that started at 2400UTC on 26 August 1997, presents the traveling path of the air masses that reached Adirondacks area, during the day (Fig. 3.34). The path is slightly different, with the air masses traveling through north before reaching Adirondacks, the first 12h of the simulation. Nevertheless, the weak flow field in the area during the first 12h do not allow significant transport of the air masses that reached Adirondacks at 2400UTC. These simulations were performed for each day of the experimental period 19-26 August 1997, and the results are presented in the Appendix 2. It is possible to compare the results for the 0-1km vertical layer and the 1-2km vertical layer, in order to find whether significant vertical mixing occurred or not. As it is well known, land water distribution (Great Lakes region) and complex terrain (Adirondacks Mountains), are some of the features that can result in strong vertical mixing of air masses in the atmosphere. Due to this reason, the regional distances travelled by the air masses can be significantly different. In order to investigate the primary areas of influence, one must examine the plots shown in the Appendix 2. In spite of this, the combination of the influence functions is proposed as a more direct and efficient method, considering the division of the 24h into two parts. In that way, we can investigate the areas of influence for Adirondacks, for two periods, during the day and during the night.

Influence functions provide spatial as well as temporal information on the dispersion of the air masses that reached the receptor area, each day of the simulation period. The methodology used in this simulation is based on the combination of the influence function calculated for the first 12h (0000-1200UTC) of the entire simulation period. These were derived from the 48h simulations done previously. The prevailing traveling path of the air masses that influence Adirondacks area during the night is quite evident in Fig. 3.35. According to Fig. 3.35 distant source areas, that could influence Adirondacks during the 12h interval, are located W and E – SE of the receptor area. Nearby source areas of the air masses, are located to the N of Adirondacks area, where horizontal advection is not significant, due to the weak circulation and the stable conditions in the area. During the day, the pattern of the airflow is different, as shown in Fig. 3.36 (coupling of the 2^{nd} 12h of the entire simulation period- 1200-2400UTC). Distant sources are located mostly to the SE, SW, and NW of Adirondacks area. In addition, the nearby sources are located to the N and W of the receptor area. Comparing the results of Fig. 3.35 and Fig. 3.36, it was found that significant advection occurs during the day, as was expected, and the traveling paths of the air masses appear to be more complicated.

The percentage of contribution of each source area becomes evident with the aid of an ensemble calculation of the influence function, for the entire experimental period (Fig. 3.37). This approach shows the regional transport of the air masses, for the 12h time interval. No separation is made between night and day and only the time interval is constant (12h). As shown in Fig. 3.37, the dominant distant source areas of air masses are located at the W, NW and SE of Adirondacks area. The nearby source areas are located in all directions around Adirondacks, except southward. All of these locations can be treated as potential source areas of pollutant air masses that reached Adirondacks, at the defined experimental period.

The simulation discussed in this report, reveals the usefulness of the methodology to investigate the contribution of a number of sources to air quality at a given receptor. The receptor – oriented approach helps to identify spatially as well as temporally, the origin of the air masses that reach the receptor area in the assumed sampling time, implementing the results of source-oriented modelling approach. The proposed methodology can be very useful in applications such as emission control and planning locations of new emission sources. It is also useful in assessing contributions from different sources to air pollution problems in a defined region.

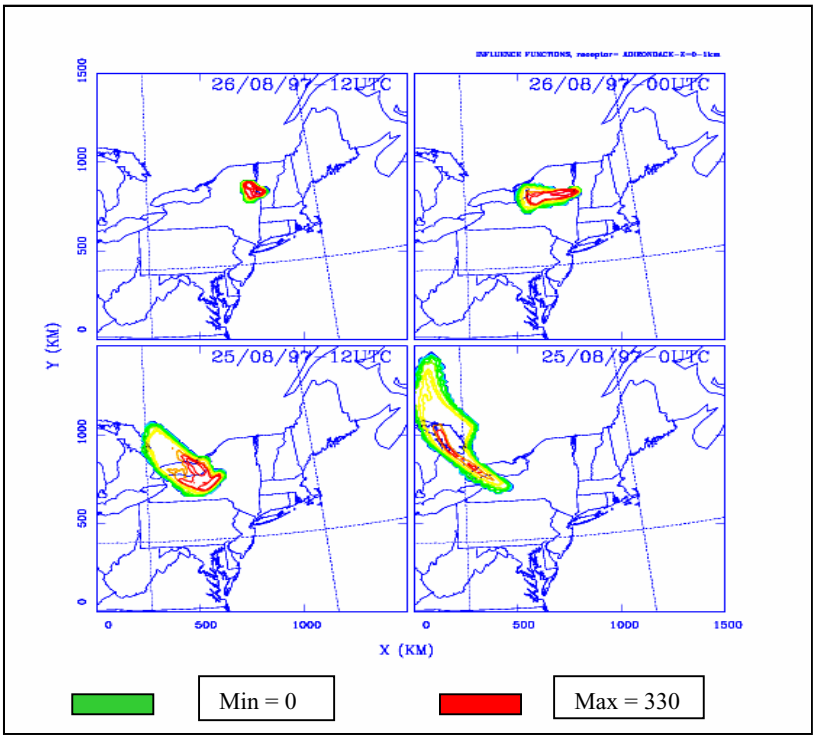

Figure 3.33: Influence functions calculated 48h backward in time for a receptor area centered at Adirondacks area (44.0N, 74.00W). Simulation started at 1200UTC, August 26, 1997. Each frame presents a 12h interval. Contours are in logarithmic normalized units (number of particles of unit mass per cubic meter).

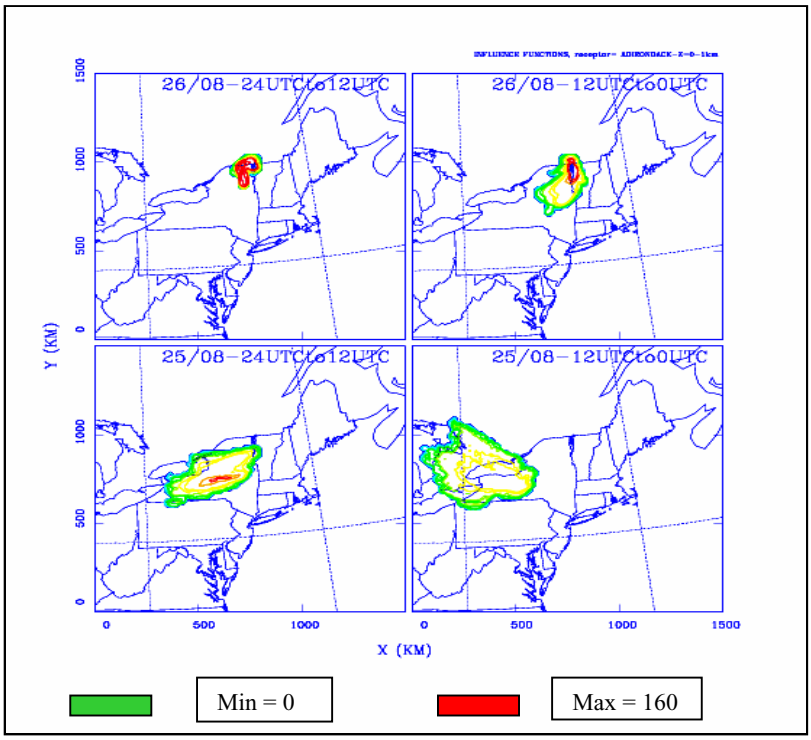

Figure 3.34: Influence functions calculated 48h backward in time for a receptor area centered at Adirondacks area (44.0N, 74.00W). Simulation started at 2400UTC, August 26, 1997. Each frame presents a 12h interval. Contours are in logarithmic normalized units (number of particles of unit mass per cubic meter).

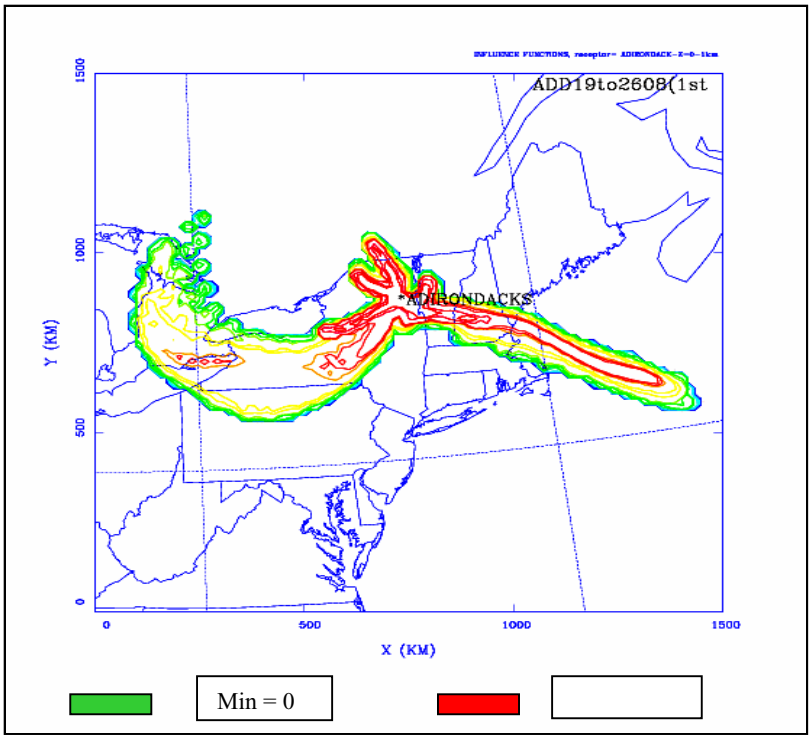

Figure 3.35: Addition of the influence functions for the first 12h (0000 to 1200UTC) of every simulation that started at 1200UTC. Receptor area: Adirondacks (44.0N, 74.00W). Experimental period: 19 to 26 August 1997. Contours are in logarithmic normalized units (number of particles of unit mass per cubic meter).

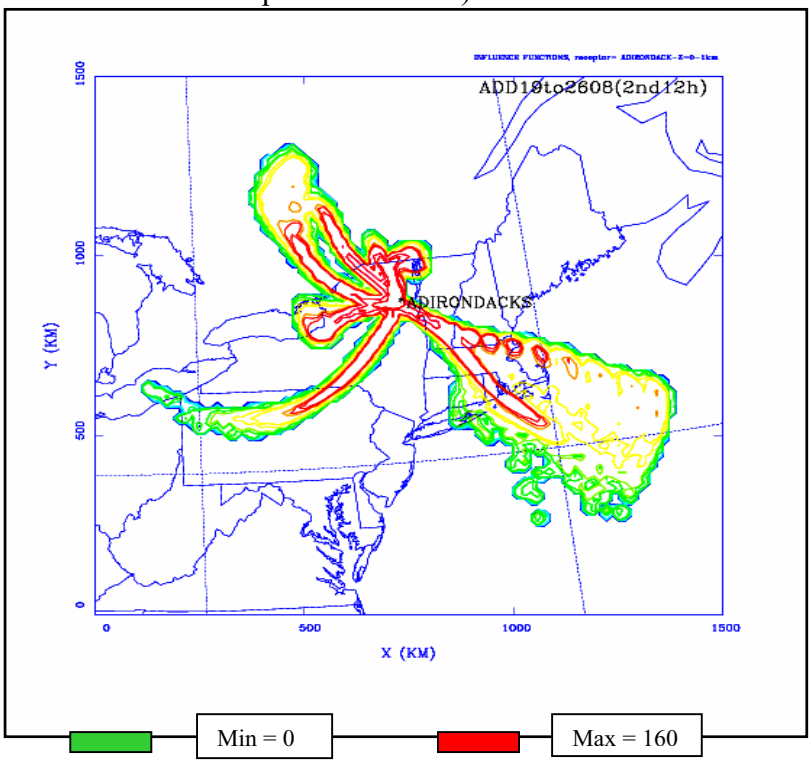

Figure 3.36: Addition of the influence functions for the first 12h (1200 to 2400UTC) of every simulation that started at 2400UTC. Receptor area: Adirondacks (44.0N, 74.00W). Experimental period: 19 to 26 August 1997. Contours are in logarithmic normalized units (number of particles of unit mass per cubic meter).

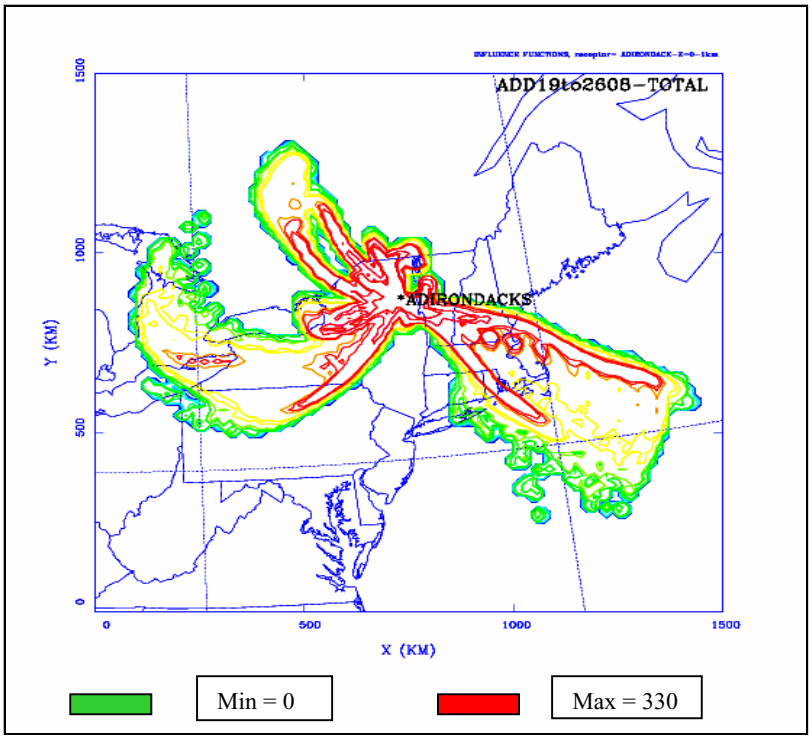

Figure 3.37: Addition of the influence functions for the experimental period 19 to 26 August 1997. The frame represents a 12h interval. Receptor area: Adirondacks (44.0N, 74.00W). Contours are in logarithmic normalized units (number of particles of unit mass per cubic meter).

4. OBSERVATIONS-MODEL CALCULATION INTERCOMPARISON

Deposition measurements are available from several locations of the NE part of the US. More specifically, the Mercury Deposition Network (MDN) provided wet deposition measurements at sites upwind and downwind of NY State only. MDN deposition observations at selected sites within the MDN, namely Allegheny Portage at Pennsylvania, Dorset and St. Andrews at Canada, Bridgton, Acadia and Greenville at Maine have been compared with the accumulated wet deposition of mercury from both models. Deposition observations performed within the Regional Environmental Monitoring and Assessment Program (REMAP) e.g. Underhill at Vermont, have been also compared with the accumulated wet deposition of mercury from both models and the results are illustrated in Figs 4.1-7.

The available observations for these stations represent the weekly measured wet deposition of all mercury species, for the periods 12 to 19 August 1997 and 19 to 26 August 1997. Only two deposition observations are available for the model simulation period. However, an attempt was made to inter-compare model outputs and observations. Since no information for the starting hour during the sampling period is available, the observations have been compared with the 0000UTC model outputs. From the model outputs accumulated wet deposition of all mercury species have been calculated for all 12 days of simulation. The wet deposition values of all three mercury species (Hg^P, Hg^2 and Hg^0-adsorbed) have been accumulated from the initial time of the simulation, for both cases (with and without NY sources) for the entire simulation period. A similar accumulation has also been made for the observations, in order to achieve greater consistency between the observations and model calculations.

The inter-comparison between model calculations and observations was made with both models, for both scenarios. Both models tend to overestimate the deposited amounts of mercury. The observations seem to be higher for the 12 to 19 August 1997 period compared to the model calculated values. On the contrary, when observations for the periods 12 to19 August and 19 to 26 August are accumulated, they are lower than the model-calculated total deposited amount. The overestimated deposited quantities of mercury from both models are within the acceptable limits, taken into account the observation errors, uncertainties of the observation network, weekly measurements, as well as differences of both models convective and precipitation schemes. It is worth

mentioning that even a small shift (temporal or spatial) in the model estimated rain pattern during the observation period, can strongly influence the model deposition values.

When the NY State local emissions were not used during the simulation period, the accumulated wet deposition is (as expected) lower, indicating the strong influence of the emissions at the sites in and around the NY State (see Fig 4.8-14).

In both models, a consistency is evident at most stations. However a longer simulation period combined with a large number of observations is absolutely necessary for more reliable conclusions. Wet deposition observations must be available on a daily basis to compare against modelled values. The difficulties in measuring the wet and dry deposition of mercury make the deposition patterns estimated by the model very useful. Thus, a well-developed numerical model is much cheaper to run, than a dense observation network that is required for high-resolution estimations of the concentration and deposition. From this aspect the developed models should be considered as useful tools for studying the mercury processes and therefore useful to policy makers in accessing various emission control strategies.

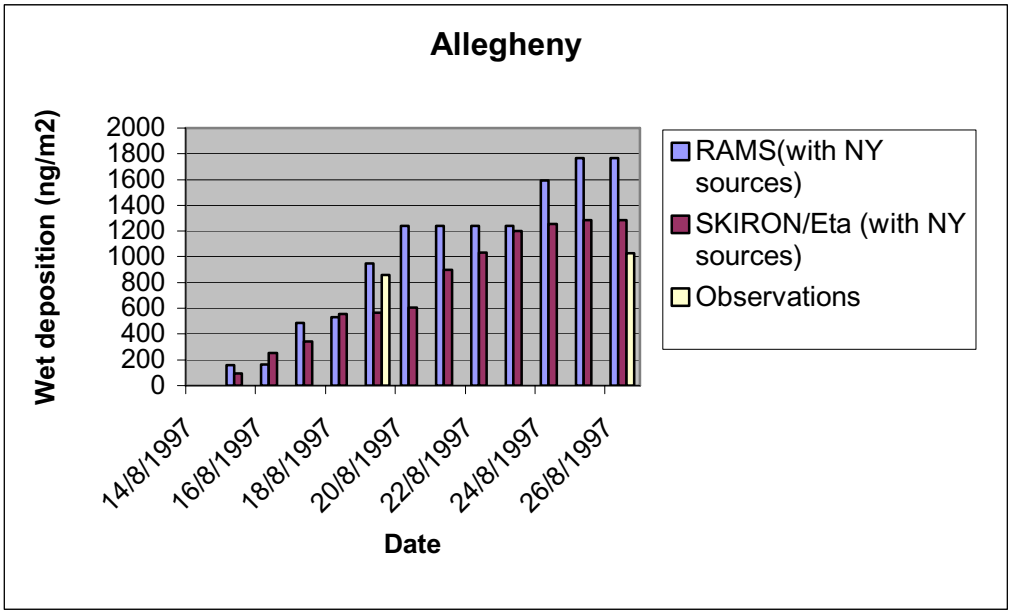

Figure 4.1: Comparison of observations of wet deposition of mercury (ng/m^2), RAMS and SKIRON/Eta outputs (with NY State emissions) at Allegheny from 14 to 26 August 1997. RAMS and SKIRON/Eta outputs are accumulated since the initial time of the simulation, while the observations correspond to weekly-deposited mercury.

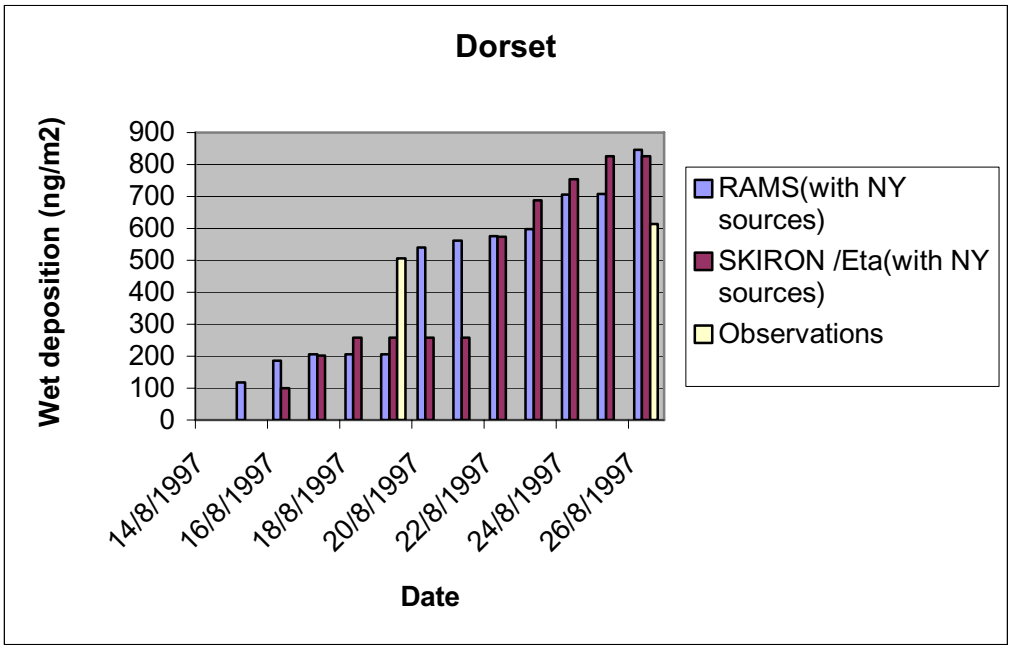

Figure 4.2: Comparison of observations of wet deposition of mercury (ng/m^2), RAMS and SKIRON/Eta outputs (with NY State emissions) at Dorset from 14 to 26 August 1997. RAMS and SKIRON/Eta outputs are accumulated since the initial time of the simulation, while the observations correspond to weekly-deposited mercury

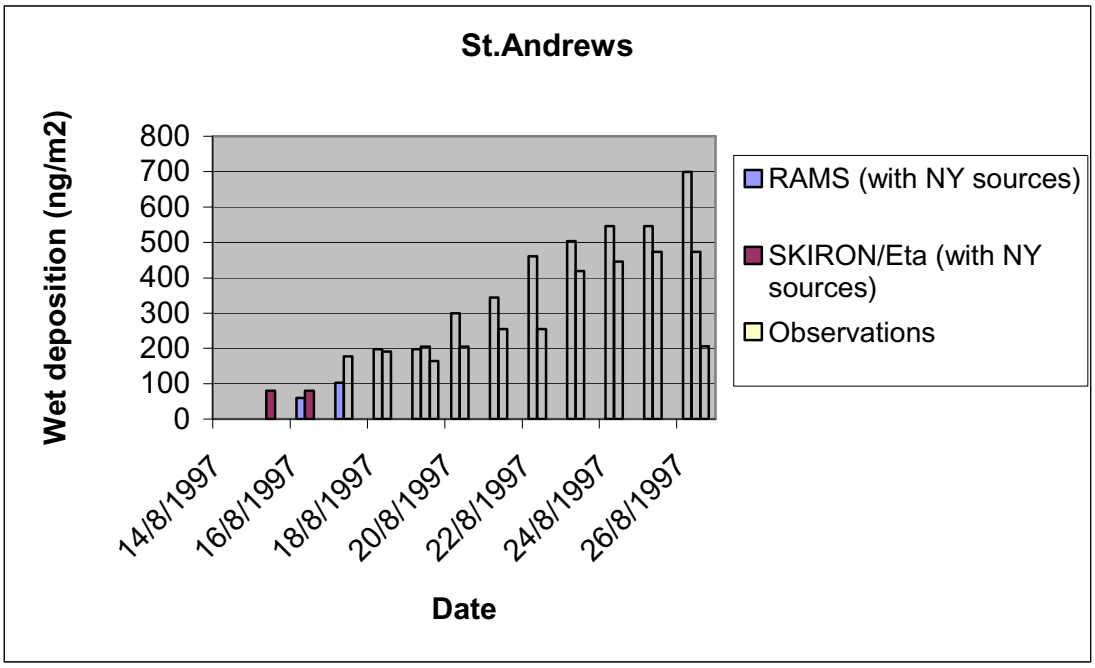

Figure 4.3: Comparison of observations of wet deposition of mercury (ng/m^2), RAMS and SKIRON/Eta outputs (with NY State emissions) at St. Andrews from 14 to 26 August 1997. RAMS and SKIRON/Eta outputs are accumulated since the initial time of the simulation, while the observations correspond to weekly-deposited mercury.

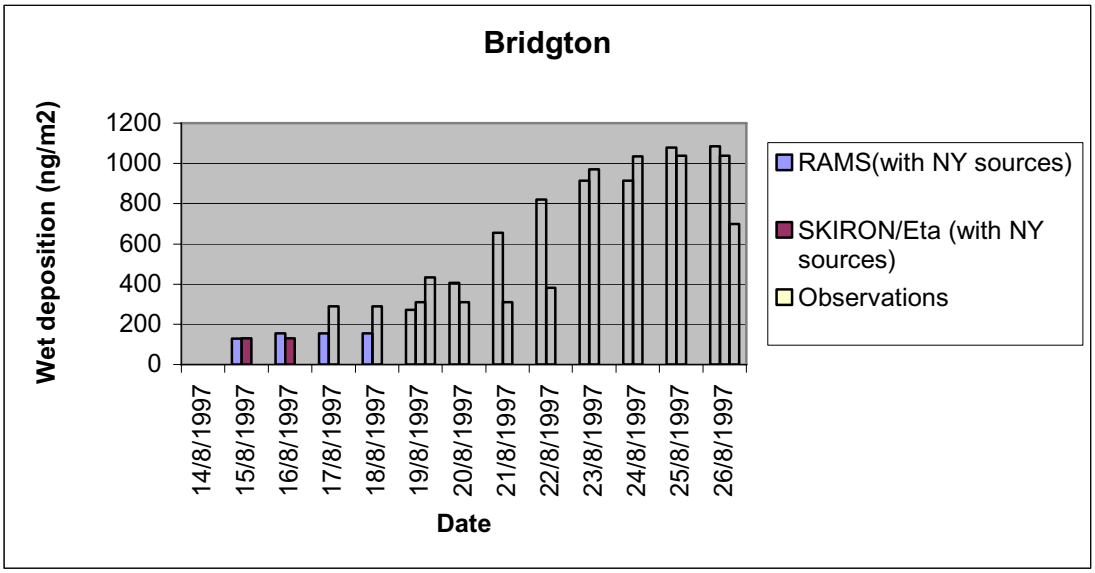

Figure 4.4: Comparison of observations of wet deposition of mercury (ng/m^2), RAMS and SKIRON/Eta outputs (with NY State emissions) at Bridgton from 14 to 26 August 1997. RAMS and SKIRON/Eta outputs are accumulated since the initial time of the simulation, while the observations correspond to weekly-deposited mercury.

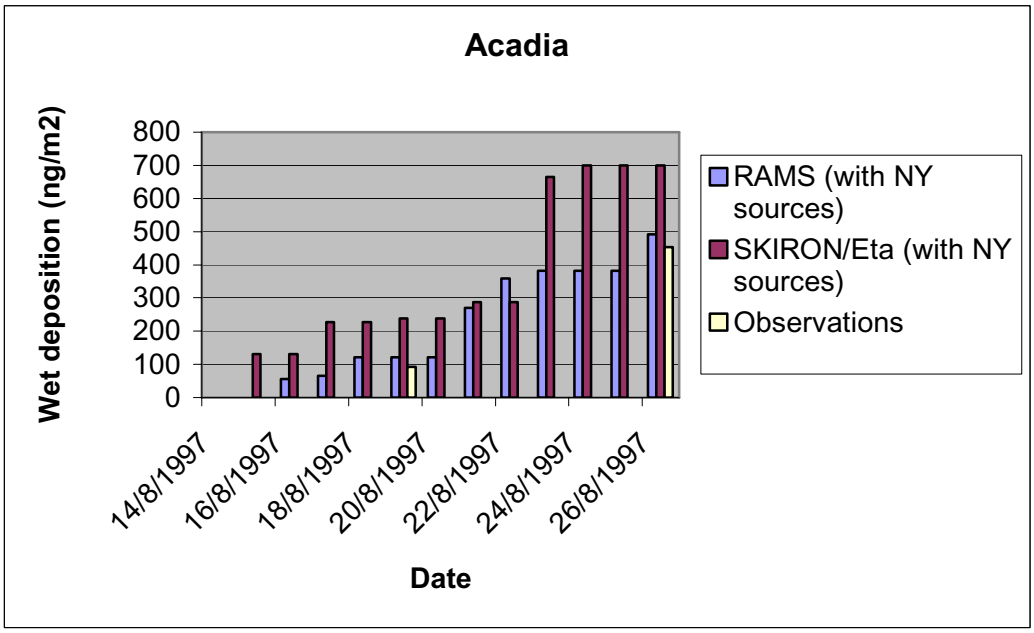

Figure 4.5: Comparison of observations of wet deposition of mercury (ng/m^2), RAMS and SKIRON/Eta outputs (with NY State emissions) at Acadia from 14 to 26 August 1997. RAMS and SKIRON/Eta outputs are accumulated since the initial time of the simulation, while the observations correspond to weekly-deposited mercury.

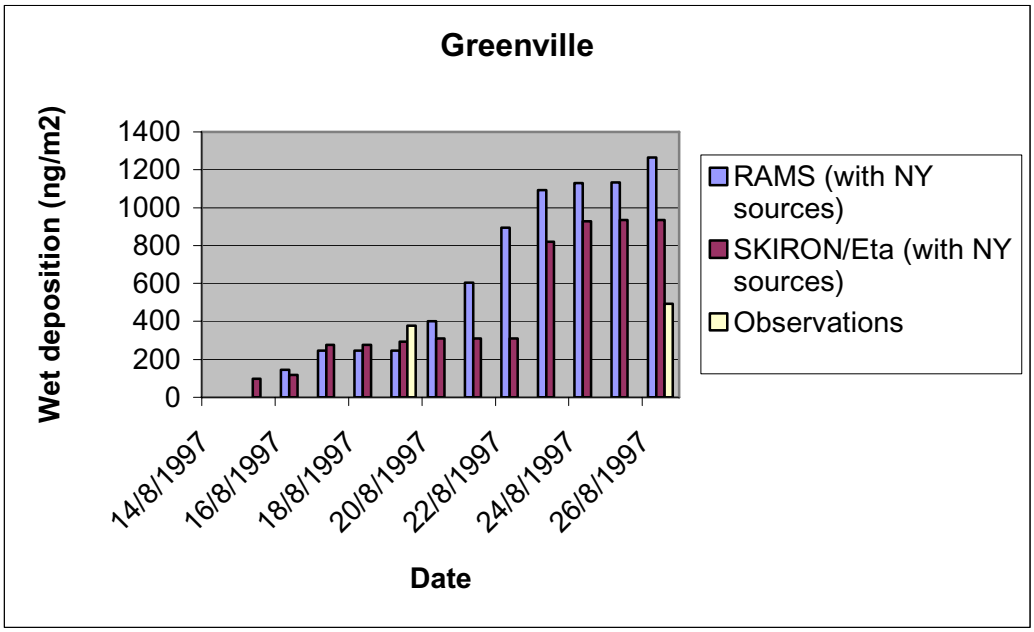

Figure 4.6: Comparison of observations of wet deposition of mercury (ng/m^2), RAMS and SKIRON/Eta outputs (with NY State emissions) at Greenville from 14 to 26 August 1997. RAMS and SKIRON/Eta outputs are accumulated since the initial time of the simulation, while the observations correspond to weekly-deposited mercury.

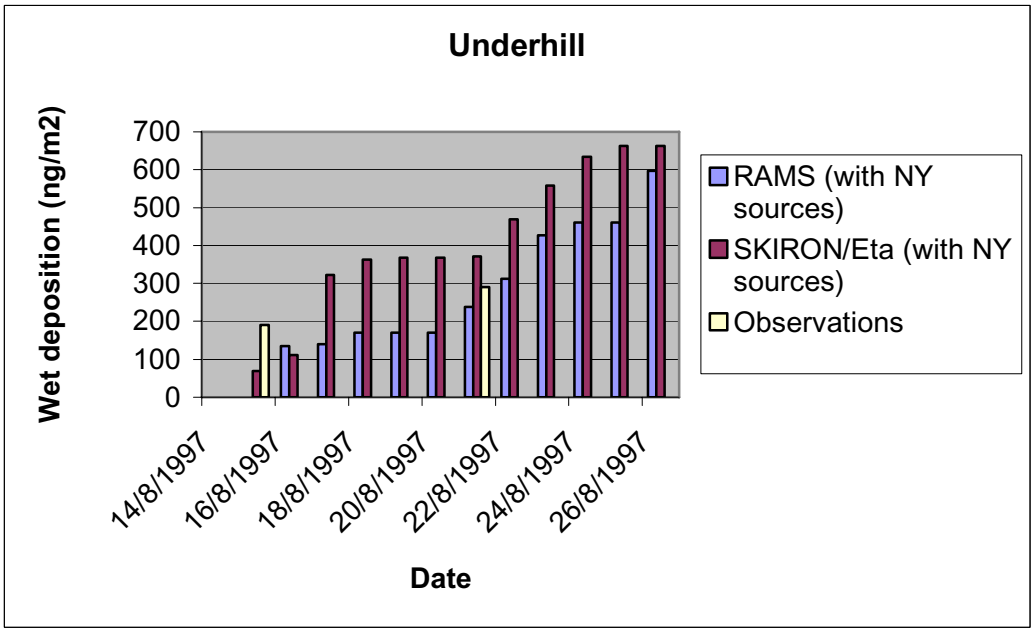

Figure 4.7: Comparison of observations of wet deposition of mercury (ng/m^2), RAMS and SKIRON/Eta outputs (with NY State emissions) at Underhill from 14 to 26 August 1997. RAMS and SKIRON/Eta outputs are accumulated since the initial time of the simulation, while the observations correspond to weekly-deposited mercury.

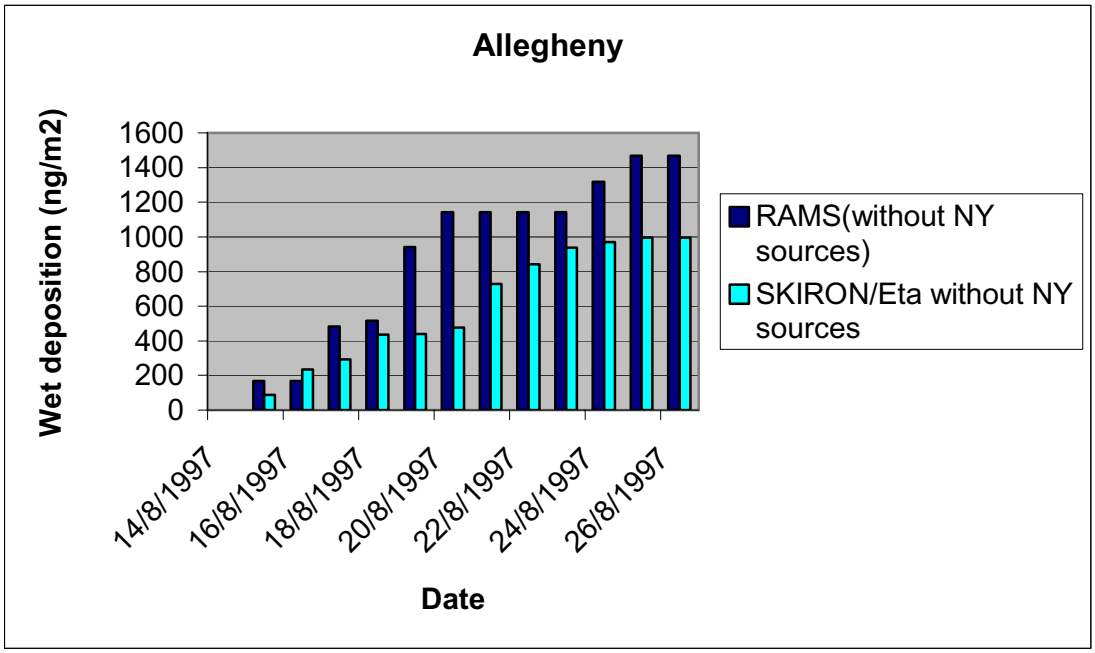

Figure 4.8: Comparison of wet deposition of mercury (ng/m^2) extracted from RAMS and SKIRON/Eta outputs (without NY State emissions), at Allegheny during 14-26 August 1997 simulation period. RAMS and SKIRON/Eta outputs are accumulated from the initial time of the simulation.

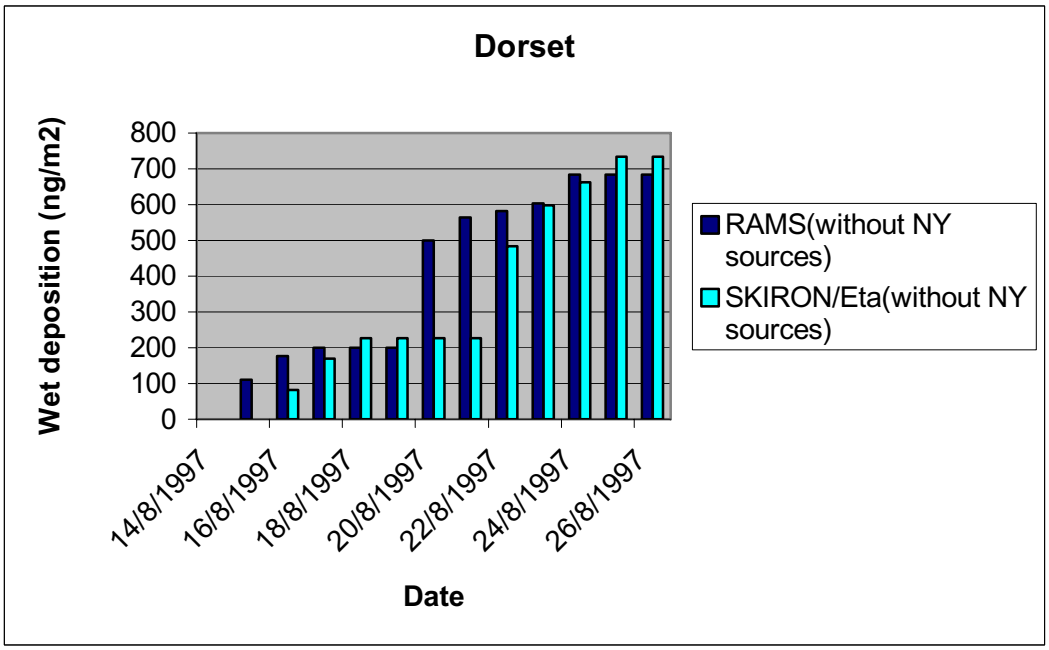

Figure 4.9: Comparison of wet deposition of mercury (ng/m^2) extracted from RAMS and SKIRON/Eta outputs (without NY State emissions), at Dorset during 14-26 August 1997 simulation period. RAMS and SKIRON/Eta outputs are accumulated from the initial time of the simulation

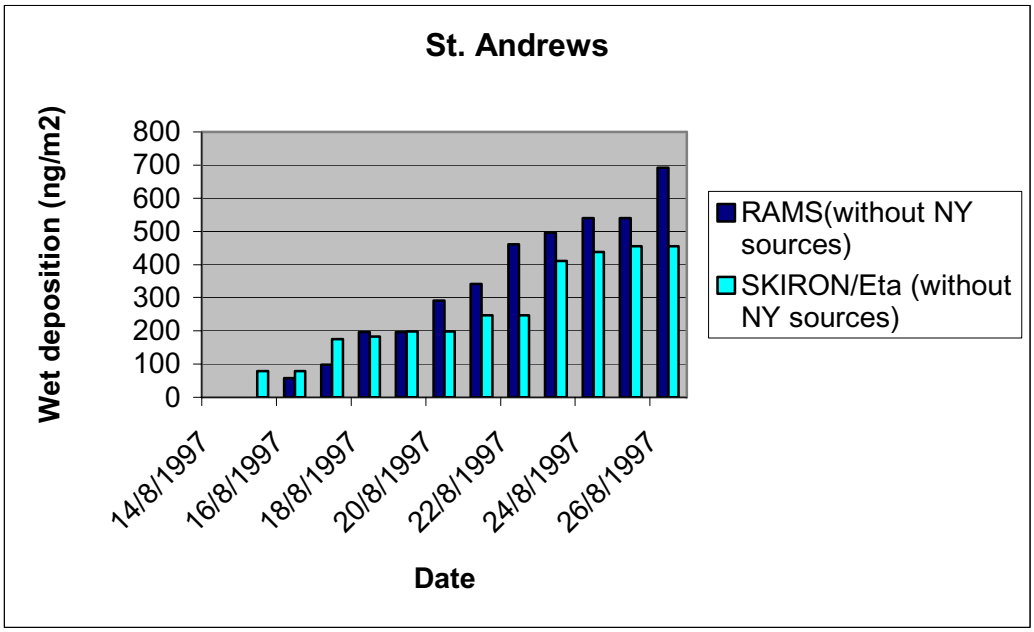

Figure 4.10: Comparison of wet deposition of mercury (ng/m^2) extracted from RAMS and SKIRON/Eta outputs (without NY State emissions), at St. Andrews during 14-26 August 1997 simulation period. RAMS and SKIRON/Eta outputs are accumulated from the initial time of the simulation.

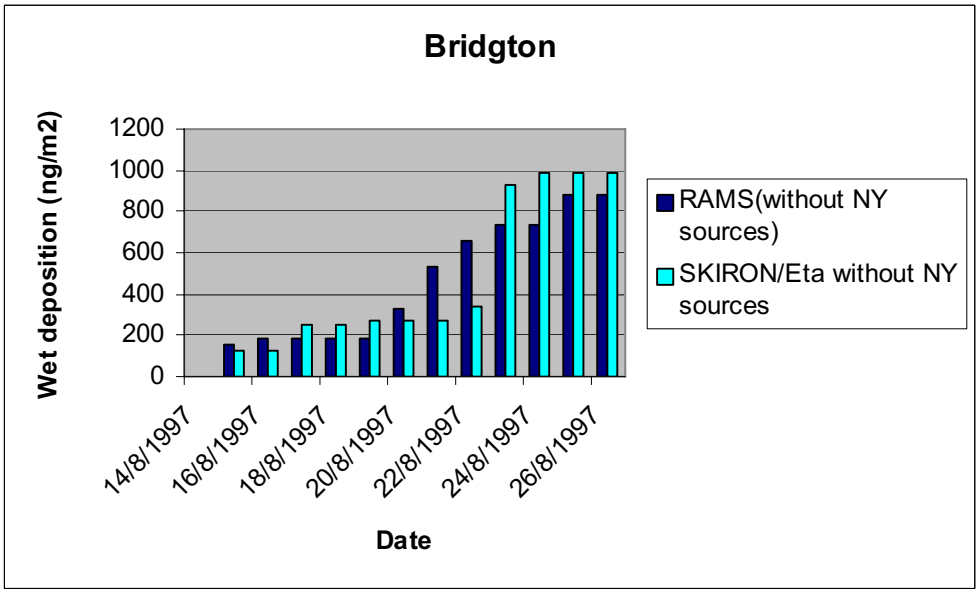

Figure 4.11: Comparison of wet deposition of mercury (ng/m^2) extracted from RAMS and SKIRON/Eta outputs (without NY State emissions), at Bridgton during 14-26 August 1997 simulation period. RAMS and SKIRON/Eta outputs are accumulated from the initial time of the simulation.

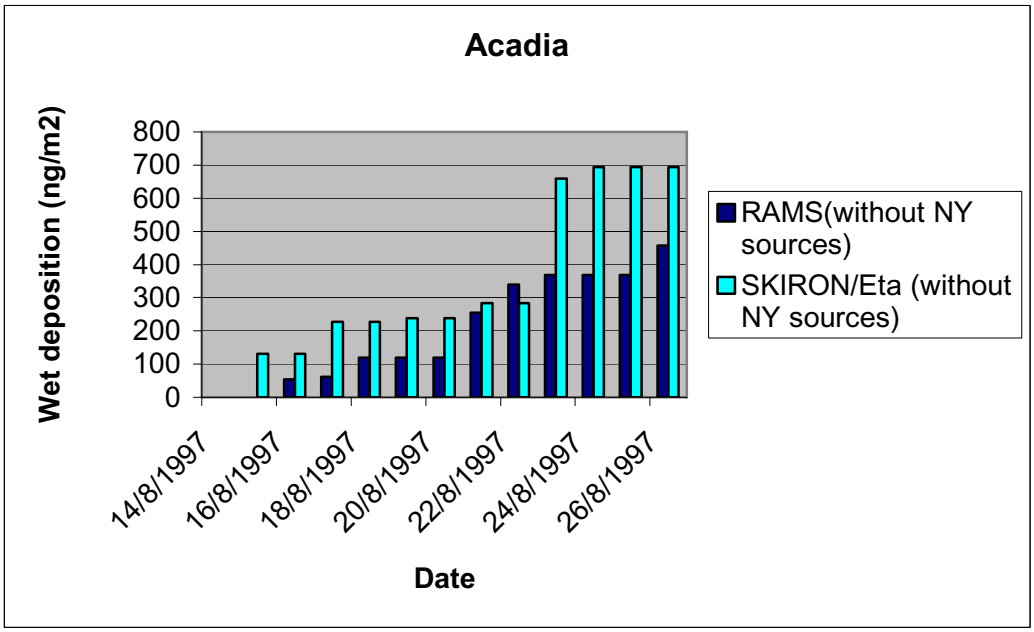

Figure 4.12: Comparison of wet deposition of mercury (ng/m^2) extracted from RAMS and SKIRON/Eta outputs (without NY State emissions), at Acadia during 14-26 August 1997 simulation period. RAMS and SKIRON/Eta outputs are accumulated from the initial time of the simulation.

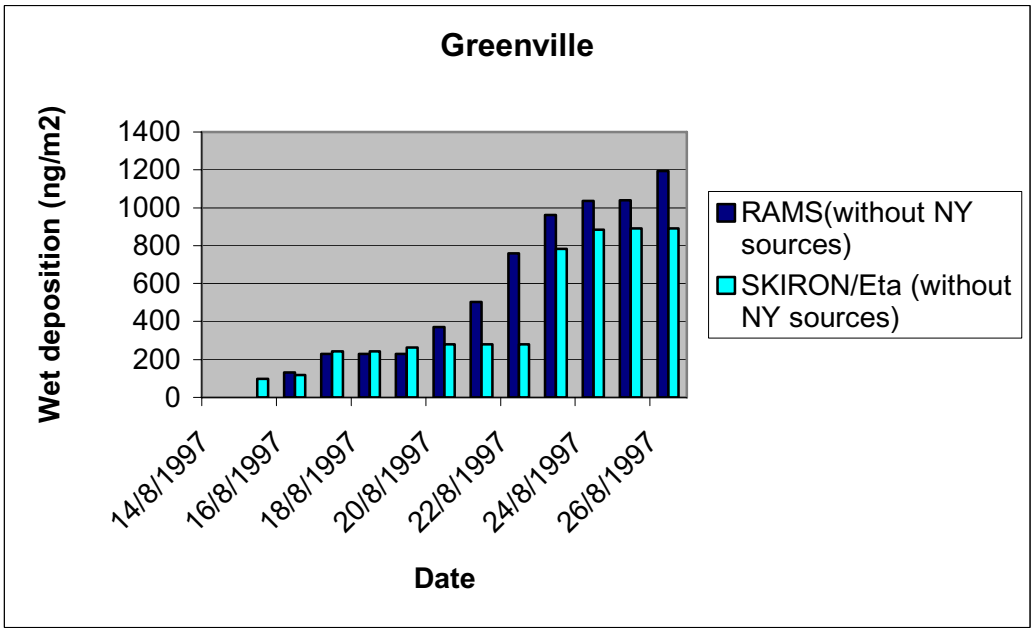

Figure 4.13: Comparison of wet deposition of mercury (ng/m^2) extracted from RAMS and SKIRON/Eta outputs (without NY State emissions), at Greenville during 14-26 August 1997 simulation period. RAMS and SKIRON/Eta outputs are accumulated from the initial time of the simulation

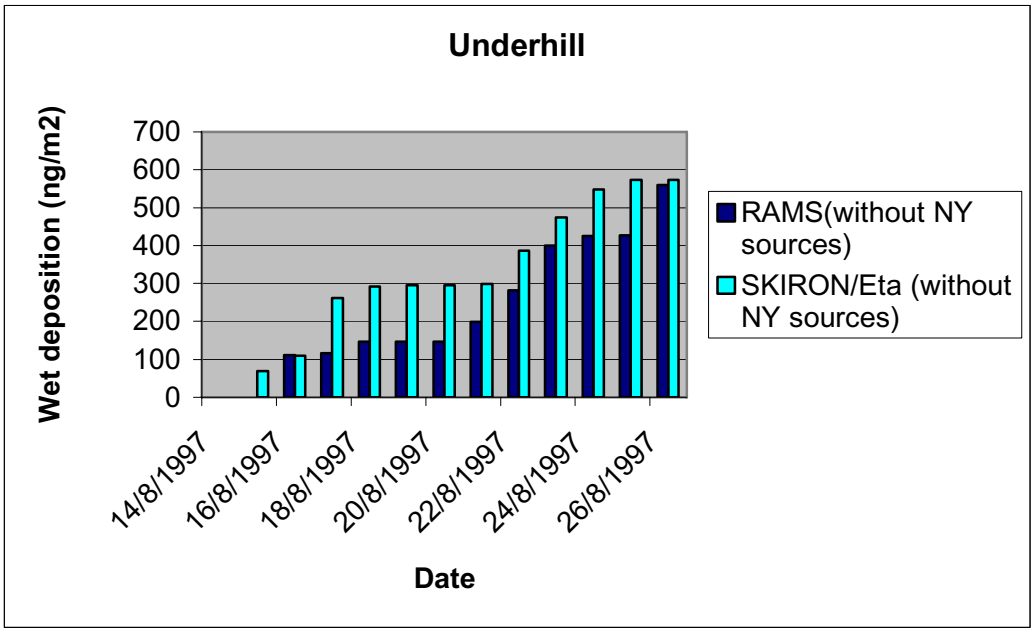

Figure 4.14: Comparison of wet deposition of mercury (ng/m^2) extracted from RAMS and SKIRON/Eta outputs (without NY State emissions), at Underhill during 14-26 August 1997 simulation period. RAMS and SKIRON/Eta outputs are accumulated from the initial time of the simulation

SUMMARY

Parallel development and implementation of the mercury processes in two well-known atmospheric modelling systems has been performed during this project. This allows the inter-comparison of the results and, consequently, the more accurate development of the mercury modelling system. Both RAMS and SKIRON/Eta are 3-D full-physics limited-area models and they have similar capabilities. They can be used for high-resolution simulations and in this way they can satisfactorily represent regional and mesoscale features.

Mesoscale and large-scale precipitation processes are important for the wet deposition of mercury. Also, both atmospheric models include highly accurate turbulence schemes. This is important since the dry deposition of mercury is strongly dependent on turbulence near the surface. Any uncertainties related to wet and dry removal processes were tested extensively.

RAMS includes a detailed cloud microphysical scheme and it has the capability of two-way interactive nesting. Sensitivity tests indicated that a very detailed cloud microphysical scheme is not essential to handle for the mercury removal processes. Either modeling systems can be coupled with oceanographic or lake models in order to describe the mercury path in the water body.

The elemental, reactive and particulate mercury were taken into account in the model development. In both models the most detailed and accurate emission inventory created during the project has been used. Two different emission inventories have been tested for the simulation period. One containing NY State emissions and the other without the emission sources located over NY State. Moreover, both models treat physico-chemical processes, atmospheric reactions, transformations, removal processes and especially the aqueous phase chemistry and gas-to-solid partitioning of elemental mercury.

In general, a satisfactory agreement is evident between observations and model output especially when the NY State emission sources are included. Major problems have been avoided because the mercury process modules are coupled to atmospheric processes on a direct way. However, a systematic model evaluation is difficult unless some other

controlling factors, like emission inventories and observations quality/quantity are not improved significantly.

The difficulties in measuring the wet and dry deposition of mercury make the deposition patterns estimated by the model very useful. The models are also helpful in estimating the mercury concentration due to the lack of reliable and consistent measuring methods. A well-developed numerical model is also much cheaper than a dense observation network that is required for high-resolution estimations of the concentration and deposition. From this aspect, the developed models should be considered as very useful tools for studying the mercury processes and, therefore, be used by policy makers.

This study focused on the regional and synoptic transport of mercury. The representation of mesoscale features was not in the aims of this research. This is the main reason that a relatively coarse resolution of about 36 km was used here. However, the model development presented is able to accurately describe the mercury processes at almost all scales. Very high-resolution simulations with grid spacing of about 5-10 km are required in order to represent mesoscale phenomena. This kind of simulations could resolve mesoscale transport and could provide an understanding of the effects of local versus remote sources. The significant computer resources required for very high-resolution simulations can be made available in the near future, and this will allow the study of the mercury cycle on the meso-scale. Parallel versions of the models are under development at the University of Athens.

Despite the significant modelling effort computed so far, there is still need for further development. The experience we gained so far from the model applications in the Mediterranean and Europe as well for NE USA showed that the Hg budget calculations are more sensitive to the physical rather than the chemical processes. There is a need for a better representation of the gas-to-particle conversions. Most of these processes will be further investigated within the MERCYMS project recently funded by the European Union. The Atmospheric Modelling and Weather Forecasting Group (AMWFG) has undertaken the model development of these processes. A more accurate and systematic way of measuring the various mercury species and a better understanding of the air-water interactions is necessary.

The transport, transformation and deposition processes of mercury in New York State were studied using and comparing two well-known atmospheric models. Since the various mercury species are multi-range transport pollutants the model treatment must

represent these properties of all species accordingly. **At least one-year simulation period is strongly recommended in order quantitatively evaluate the models and to derive reasonable conclusions about the in/out-state contribution to the areas of great concern.**

REFERENCES

Betts, A. K., 1986: A new convective adjustment scheme. Part E. Observational and theoretical basis, *Quart. J. R. Met. Soc.,* **112,** 677-691.

Betts, A. K. and M. J. Miller, 1986: A new convective adjustment scheme. Part II: Single column tests using GATE wave, ATEX and Arctic Air mass data sets, *Quart. J. R. Met. Soc.,* **112,** 693-709.

Brosset, C., 1984: Referenced in: Mercury in the Swedish Environment-Global and Local Sources, National Swedish Environment Protection Board Report SNV-PM 1816, Solna, Sweden, p. 29.

Clark, T. L. and R. D. Farley, 1984: Severe downslope windstorm calculations in two and three spatial dimensions using anelastic interactive grid nesting: A possible mechanism for gustiness. J. Atmos. Sci., 41, 329-350.

Clarkson, T. W., Amin-Zaki L., and S. K. Al-Tikriti 1975: An outbreak of mercury poisoning due to consumption of contaminated grain. Fed.Proc. 34: 2395-2399.

Davies, F., and Notcutt G., 1996: Biomonitoring of atmospheric mercury in the vicinity of Kilauea, Hawaii. Water Air Soil Pollut. 86, 275-281.

Electric Power Research Institute technical report TR-107695, 1996: Mercury in the environment – A research update. Final report, EPRI, Palo Alto, CA.

Fitzgerald, W. F., Engstrom, D. R., Mason, R. P., and Nater, E. A., 1997: The case for atmospheric mercury contamination in remote areas. Env. Sci. Techn., **32**, 1-7.

Forlano, L., Pirrone N., Headgecock I., Kallos G., Kotroni V., and K. Lagouvardos, 1999: Atmosheric transport and deposition fluxes of mercury to the Mediterranean Sea. Proceedings, 5th International Conference May 23-28, 1999, Rio de Janeiro, Brazil. pp124

Giorgi, F., 1986: Development of an Atmospheric Aerosol Model for Studies of Global Budgets and Effects of Airborne Particulate Meterial. PhD Thesis. Georgia Institute of Technology.

Graedel, T. E., and P. J. Crutzen, 1993: Atmospheric change: An earth system perspective. Freeman and company, New York, pp. 446.

Harada, Y., 1966. Congenital (or Fetal) Minamata Disease. In Minamata Disease. Edited by M. Katsanuma. Japan: Kamamoto University, pp.93.

Hicks, B. B., Baldocchi D. D., Hosker R.P. Jr., Hutchison B. A., Matt D. R., McMillen R. T., and L. C. Satterfield, 1985: On the use of monitored air concentrations to infer Dry Deposition, NOAA Technical Memorandum ERL ARL-141, Silver Spring, MD.

Jackson, T. A, 1997: Long-range atmospheric transport of mercury to ecosystems, and the importance of anthropogenic emissions – a critical review and evaluation of the published evidence. Environ. Rev., 5, 99-120.

Janjic, Z. I., 1974: A stable centered difference scheme free of the two-grid-interval noise, *Mon. Wea. Rev.,* **102,** 319-323.

Janjic, Z. I., 1979: Forward-backward scheme modified to prevent two-grid-interval noise and its application in sigma coordinate models, *Contrib. Atmos. Phys.,* **52,** 69-84.

Janjic, Z. I., 1984: Non-linear advection schemes and energy cascade on semi-staggered grids, *Mon. Wea. Rev.,* **112,** 1234-1245.

Janjic, Z. I., 1994: The step-mountain Eta coordinate: Further developments of the convection, viscous sublayer and turbulence closure schemes, *J. Atmos. Sci.,* **122,** 927-945.

Kallos, G., S. Nickovic, A. Papadopoulos, D. Jovic, O. Kakaliagou, N. Misirlis, L. Boukas, N. Mimikou, G. Sakellaridis, J. Papageorgiou, E. Anadranistakis and M. Manousakis 1997: The Regional weather forecasting system SKIRON. Proceedings of the Symposium on Regional Weather Prediction on Parallel Computer Environments, 15-17 October 1997, Athens, Greece. 109-122.

Lindqvist, O., Johansson, K., Aastrup, M., Andersson, A., Bringmark, L., Hovsenius, G., Hakanson, Iverfeldt, A., Meili, M., and Timm, B., 1991: Mercury in the Swedish environment – recent research on causes, consequences and corrective.

Mahrer, Y. and R.A. Pielke, 1977: A numerical study of the airflow over irregular terrain. Beitr. Phys. Atmos., **50**, 98-113.

Marsh, D. O., Mayers G. J., Clarkson T. W., Amin-Zaki L., Al-Tikriti S. K., and M. A. Majeed, 1980. Fetal methylmercury poisoning: Clinical and toxicological data on 29 cases. Ann. Neurol., **7**, 348-353.

Marsh, D. O., Mayers G. J., Clarkson T. W., Amin-Zaki L., Al-Tikriti S. K., and M. A. Majeed, 1981: Dose-Response relationship for human fetal exposure to methylmercury. Clin. Toxicol., **18**, 1311-1318.

Marsh, D. O., Clarkson T. W., Mayers G. J., Amin-Zaki L., and S. K. Al-Tikriti, 1987: Fetal methylmercury poisoning. Arch. Neurol., **44**, 1017-1022.

Mellor, G. L. and T. Yamada, 1974: A hierarchy of turbulence closure models for plenstary boundary layers, *J. Atmos. Sci.,* **31,** 1791-1806.

Mellor, G. L. and T. Yamada, 1982: Development of a turbulence closure model for geophysical fluid problems, *Rev. Geophys. Space Phys.,* **20,** 851-875.

Mesinger, F, 1973: A method for construction of second-order accuracy difference schemes permitting no false two-grid-interval wave in the height field, *Tellus,* **25** 444-458.

Mesinger, F, 1977: Forward-backward scheme and its use in a limited area models, *Contrib. Atmos. Phys.,* **50,** 200-210.

Mesinger, F, 1984: A blocking technique for representation of mountains in atmospheric models, *Riv. Meteor. Aeronaut.,* **44**, 195-202.

Nickovic, S., Jovic D., Kakaliagou O., and Kallos G., 1997: Production and long-range transport of desert dust in the Mediterranean Region: Eta model simulations. Proc. of the 22nd NATO/CCMS Int. Techn. Meeting on Air Pollution Modelling and Its Application, 2-6 June 1997, Clermont Ferrand, France. Edited by Sven-Erik Gryning and Nandine Chaumerliac, Plenum Press, New York, **20**, pp.8.

Nickovic, S., Mihailovic, D., Rajkovic, B., and A. Papadopoulos, 1998: The Weather forecasting System Skiron. Volume II: Description of the model. Univ. of Athens, Dept. of Applied Physics, Athens. pp. 228.

Nickovic, S., Kallos G, Papadopoulos A and Kakaliagou O., 2001: A model for prediction of desert dust cycle in the atmosphere, JGR, **106**, 18113-18129.

Pai, P., Karamchandani, P., and Seigneur, C., 1997: Simulation of the regional atmospheric transport and fate of mercury using a comprehensive Eulerian model. Atm. Env., **31**, 2717-2732

Papadopoulos, A., P. Katsafados, G. Kallos, and S. Nickovic, 2002: "The Poseidon weather forecasting system: An overview". The Global Atmosphere and Ocean Systems (in press).

Petersen, G., Iverfeldt, A., and Munthe, J., 1995: Atmospheric mercury species over central and northern Europe. Model calculations and comparison with observations from the Nordic air and precipitation network for 1987 and 1988. Atm. Env., **29**, 47-67.

Petersen, G., Munthe, J., Bloxam, R. and Kumar, A.V., 1996: A comprehensive Eulerian modelling framework for airborne mercury species: Development and application of a

tropospheric chemistry module. Abstracts of the 4th Intern. Conf. on Mercury as a Global Pollutant. August 4-8, 1996, Hamburg, Germany.

Petersen, G., Munthe, J., Pleijel, K., Bloxam, R. and Kumar, A.V., 1998: A comprehensive Eulerian modelling framework for airborne mercury species: Development and testing of the tropospheric chemistry module (TCM). *Atm. Environ*., **32**, 829-843.

Pielke, R. A., Cotton W. R., Walko R. L., Tremback C. J., Lyons W. A., Grasso L. D., Nicholls M E., Moran M. D., Wesley D. A., Lee T. J., and J. H. Copeland, 1992: A comprehensive meteorological modelling system - RAMS. Meteorol. Atmos. Phys., **49**, 69-91.

Pirrone, N., and G. J. Keeler, 1995: Numerical Modelling of Gas-Particle Partitioning of Atmospheric Mercury in Urban Areas. In Proceedings of the *1995 Annual Meeting of the American Association for Aerosol Research (AAAR)*, October 9-13, 1995, Pittsburgh, Pennsylvania, U.S.A.

Pirrone, N., Keeler G. J., and T. M. Holsen, 1995a: Dry Deposition of Trace Elements over Lake Michigan: A Hybrid-Receptor Deposition Modelling Approach. *Environmental Science and Technology*, 29, 2112-2122.

Pirrone, N., Glinsorn G. and G. J. Keeler, 1995b: Ambient levels and dry deposition fluxes of mercury to lakes Huron, Erie and St. Clair. *Water, Air & Soil Pollut*., **80**, 179-188.

Pirrone, N., Ferrara, R., Hedgecock, I. M., Kallos. G., Mamane, Y., Munthe, J., Pacyna, J. M., Pytharoulis, I., Sprovieri, F., Voudouri, A., Wangberg, I., 2002, Dynamic Processes of Mercury Over the Mediterranean Region:Summary of Results from the MAMCS Project. Atm. Env. (submitted)

Pleijel, K., and J. Munthe, 1995: Modelling the atmospheric chemistry of mercury - The importance of a detailed description of the chemistry of cloud water. *Water, Air & Soil Pollut*., **80**, 317-324.

Schroeder, W., and J. Munthe, 1998 Atmospheric Mercury - An Overview. Atm. Env., **32**, pp 809-822

Seinfeld, J. H. 1986. Atmospheric Chemistry and Physics of Air Pollution. John Wiley & Sons, New York, N.Y.

Sehmel, G.A., 1980: Particle and gas dry deposition: A review. Atmos. Env., **14**, 983-1011.

Shannon, J. D., and E. C. Voldner, 1995: Modeling atmospheric concentrations of mercury and deposition to the Great Lakes. Atmos. Environ., **29**, 1649-1661.

Slinn, S. A., and W.G.N. Slinn., 1981: Modelling of Atmospheric Particulate Deposition to Natural Waters. In: *Atmospheric Pollutants in Natural Waters*, S.J. Eisenreich, Ed., Ann Arbor Science, Ann Arbor, MI. pp. 22-53.

Tripoli, G. J., and W. R. Cotton, 1982: The Colorado State University three-dimensional cloud/mesoscale model. Part I: General theoretical framework and sensitivity experiments. *J. Rech. Atmos*., **16**, 185-220.

Uliasz, M., and R. A. Pielke, 1991: Application of the receptor oriented approach in mesoscale dispersion modelling. In Air Pollution Modelling and Its Application VIII, van Dop, H. and D. G. Steyn, Editors, Plenum Press, New York, 338-408.

Vandal, G. M., Fitzgerald, W. F., Lamborg C. H., and Rolfjus K. R., 1993: The production and evasion of elemental mercury in lakes: a study of Pallette Lake, northern Wisconsin, U.S.A. Proc. 9th International Conference on Heavy Metals in the Environment, pp. 297-300. CEP Consultants Ltd., Heavy Metals Secreatariat, Edinburgh, U.K.

Walko, R. L., and C. J. Tremback, 1996: RAMS - The Regional Atmospheric Modelling System Version 3b: User's Guide. Published by ASTeR, Inc., PO Box 466, Fort Collins, Colorado, 86 pp.

Willams, R. M., 1982: A model for the dry deposition of particles to natural water surfaces. Atmos. Environ., 1933-1938.

Xu, X., Yang., X., Miller, D. R., Helble, J. J., and Carley R. J., 1999: Formulation of bi-directional atmosphere-surface exchanges of elemental mercury. Atmos. Environ., **33**, 4345-4355.

Appendix 1: Summary of Source-Based Mercury Atmospheric Models

Model	ADOM	ASTRAP	CAM	EMERC	ROME	RELMAP	TEAM
Sponsor(s)	AES/OMEE-Canada/ Germany	AES/DOE	SNV/ ELFORSK	German Environmental Protection Agency	EPRI	EPA	EPRI
Developer(s)	AES/ENSR/ OMEE	AES/Argonne Nat'l Laboratory	IVL	GKSS-Germany/ IVL-Sweden	AES/ENSR	EPA	AES/ENSR
Emissions (Sources)	Point and area sources	Point and area sources	Area sources	Point and area sources	Point sources	Point and area sources	Point and area sources
Spatial Resolution (Horizontal & Vertical)	Grid size 127 kmx127 km; domain contains 33x33 grids; 12 vertical layers from 1 m to 10km.	Trajectory model used to calculate air concentration and deposition on regional to continental scale.	Trajectory model.	Grid size 150 km x 150 km.	Trajectory (plume) model with 2-D grid (10 x 10 grids).	Horizontal:1/ 2 deg. long. x 1/3 deg. lat. Vertical : 4 layers, up to 1500 m above ground level.	Projected grid size 100km x 100 km ; domain contains 63x47 grids; 6 vertical layers extending up to 6 km in the vertical
Transport	Eulerian. Horizontal advection and diffusion.	Lagrangian		96-hour backwards trajectories.	Advection with mean wind trajectory.	Puff advection with vertically averaged wind field.	Eulerian. Horizontal advection using a semi-Lagrangian scheme.
Turbulent Diffusion	Vertical advection and diffusion	Horizontal trajectory distribution Vertical: convective mixing.	Well mixed	Horizontal trajectory pathways. Vertical: well mixed planetary boundary layer	1st order or 2nd order closure diffusion.	Horizontal puff expansion. Vertical: well mixed planetary boundary layer during day.	Vertical advection and diffusion
Mercury Transformation	Hg^0 oxidation by O_3 assumed balanced by reduction reactions; $HgCl_2$ scavenged using Henry;s Law	Slow net conversion of Hg^0 to Hg (part.) at rate 0.05% hr.	Aqueous Chemistry. Detailed chemistry of Hg,	No gas phase transformations. Aqueous redox reactions; adsorbion on soot particles.	Gas-phase and aqueous chemistry.	Hg^0 -Hg^2 redox: O_3 oxidation and sulfate reduction;	Gas-phase and aqueous chemistry.

	scavenging coefficients; Hg (part.) scavenged by nucleation		oxidants and inorganic ligands.			considers Hg^2 adsorbion by soot particles.	
Dry Deposition	Deposition to forests.	Deposition velocity of Hg^2 and Hg(part.). Includes elemental Hg.	No deposition for Hg. Deposition for reactants.	No deposition for Hg^0. Dry deposition velocity for Hg^2 and Hg(part.).	Deposition velocities for gases and particulates.	Deposition velocities for Hg^0gas, Hg^2 gas, Hg(part.) and carbon soot.	Deposition velocities for gases and particulates calculated for each grid cell based on land use and input meteorology.
Wet Deposition (Including Cloud & Precipitation)	(See Mercury Transformation above.)	Deposition to surface, and redistribution from mixed layer to free troposphere.	No	Scavenging ratios for Hg^0 , Hg^2 and Hg(part.). Wet deposition proportional to rainfall amount.	Cloud microphysics , rainout and washout.	Precip. scavenging of Hg^2 and Hg(part.) and soot; clouds assumed at top 2 layers when precipitating.	Wet deposition flux is calculated as the product of cloud water concentration of Hg species and the precipitation amount.
Major Applications To Date	Eastern North America episodes; sensitivity analyses.	Great Lakes Region deposition loading.	Sensitivity analysis of chemistry.	North Sea/ Baltic Sea deposition loading and deposition fluxes over Central / Northern Europe.	Power plant plume simulations.	United States.	Simulated the transport and fate of mercury emissions in the contiguous United States; includes detailed model evaluation
Refs.	ERT 1984a,b	Shannon 1985		Petersen 1992a,b; Petersen and Iverfeldt 1993; Petersen et al., 1994a,b	Constantinou and Seigneur 1993; Seigneur et al., 1997	Eder et al. 1986; Bullock et al., 1996	Pai et al.,1997b

Ref.: EPRI TR-107695 3081, 3508, 3297 Final Report, December 1996 pp.3 17 -3 19

APPENDIX 2

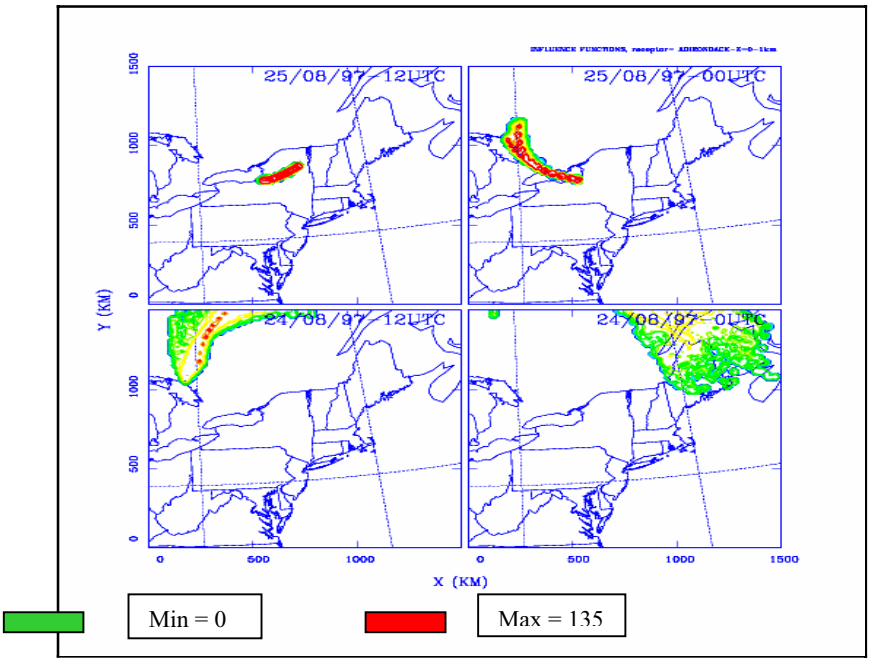

Figure 1: Influence functions calculated 48h backward in time for a receptor area centered at Adirondacks area (44.0N, 74.00W). Simulation started at 1200UTC, August 25, 1997. Each frame presents a 12h interval. Contours are in logarithmic normalized units (number of particles of unit mass per cubic meter).

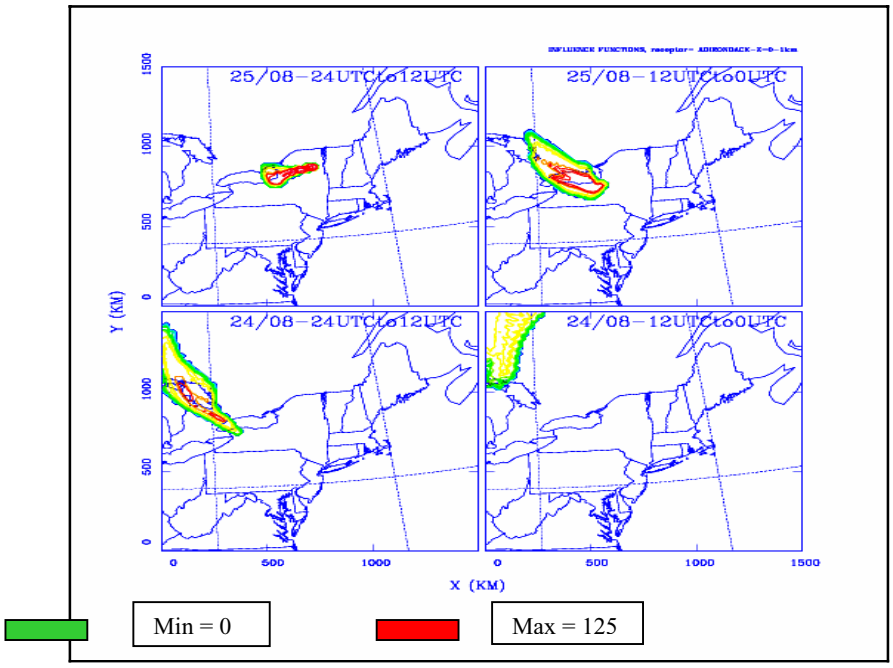

Figure 2: Influence functions calculated 48h backward in time for a receptor area centered at Adirondacks area (44.0N, 74.00W). Simulation started at 2400UTC, August 25, 1997. Each frame presents a 12h interval. Contours are in logarithmic normalized units (number of particles of unit mass per cubic meter).

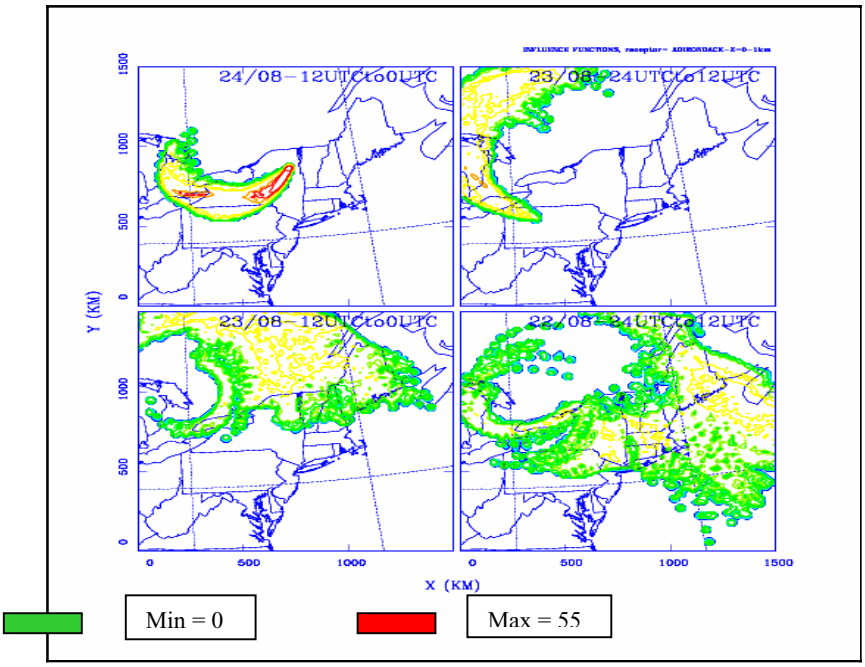

Figure 3: Influence functions calculated 48h backward in time for a receptor area centered at Adirondacks area (44.0N, 74.00W). Simulation started at 1200UTC, August 24, 1997. Each frame presents a 12h interval. Contours are in logarithmic normalized units (number of particles of unit mass per cubic meter).

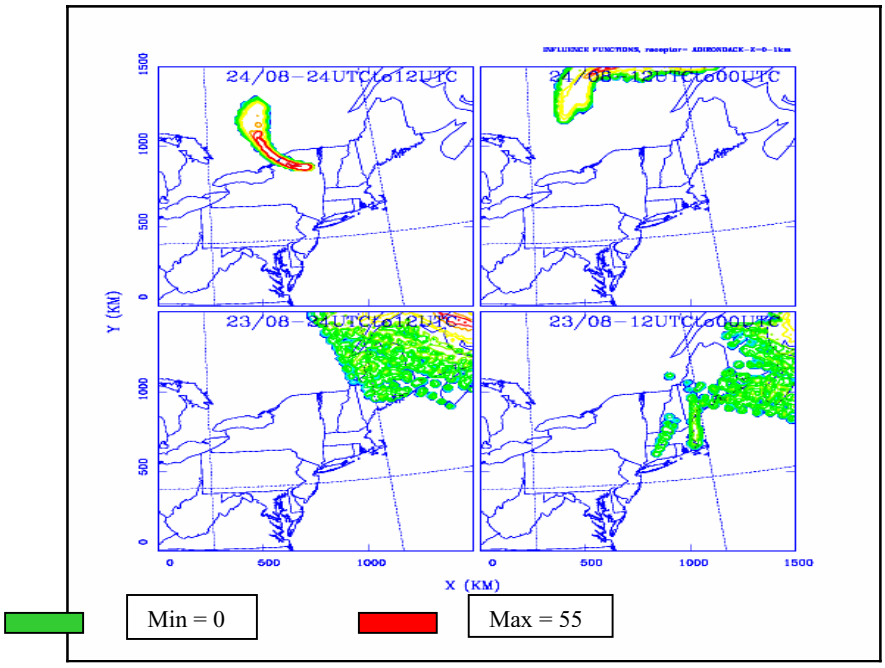

Figure 4: Influence functions calculated 48h backward in time for a receptor area centered at Adirondacks area (44.0N, 74.00W). Simulation started at 2400UTC, August 24, 1997. Each frame presents a 12h interval. Contours are in logarithmic normalized units (number of particles of unit mass per cubic meter).

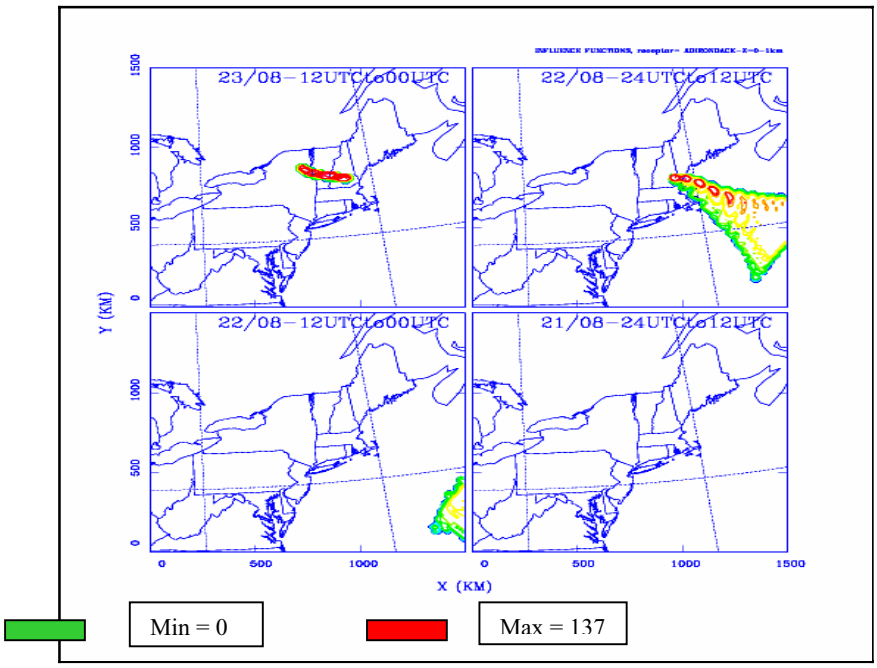

Figure 5: Influence functions calculated 48h backward in time for a receptor area centered at Adirondacks area (44.0N, 74.00W). Simulation started at 1200UTC, August 23, 1997. Each frame presents a 12h interval. Contours are in logarithmic normalized units (number of particles of unit mass per cubic meter).

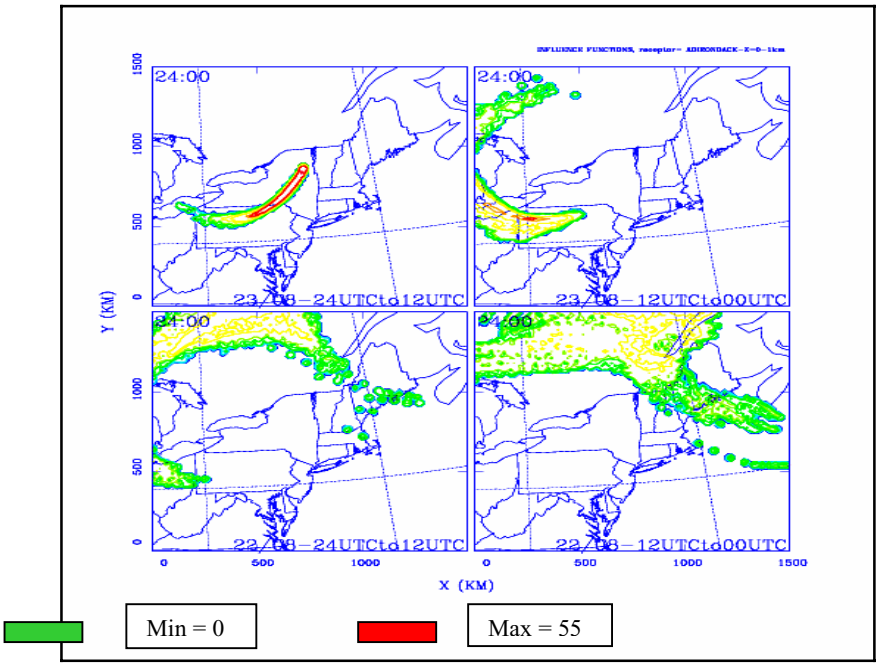

Figure 6: Influence functions calculated 48h backward in time for a receptor area centered at Adirondacks area (44.0N, 74.00W). Simulation started at 2400UTC, August 23, 1997. Each frame presents a 12h interval. Contours are in logarithmic normalized units (number of particles of unit mass per cubic meter).

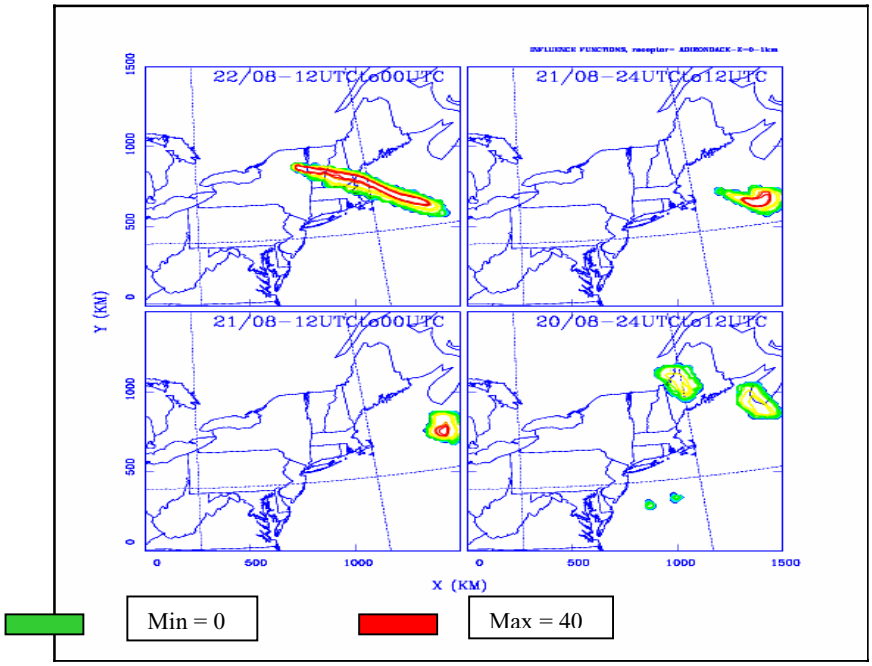

Figure 7: Influence functions calculated 48h backward in time for a receptor area centered at Adirondacks area (44.0N, 74.00W). Simulation started at 1200UTC, August 22, 1997. Each frame presents a 12h interval. Contours are in logarithmic normalized units (number of particles of unit mass per cubic meter).

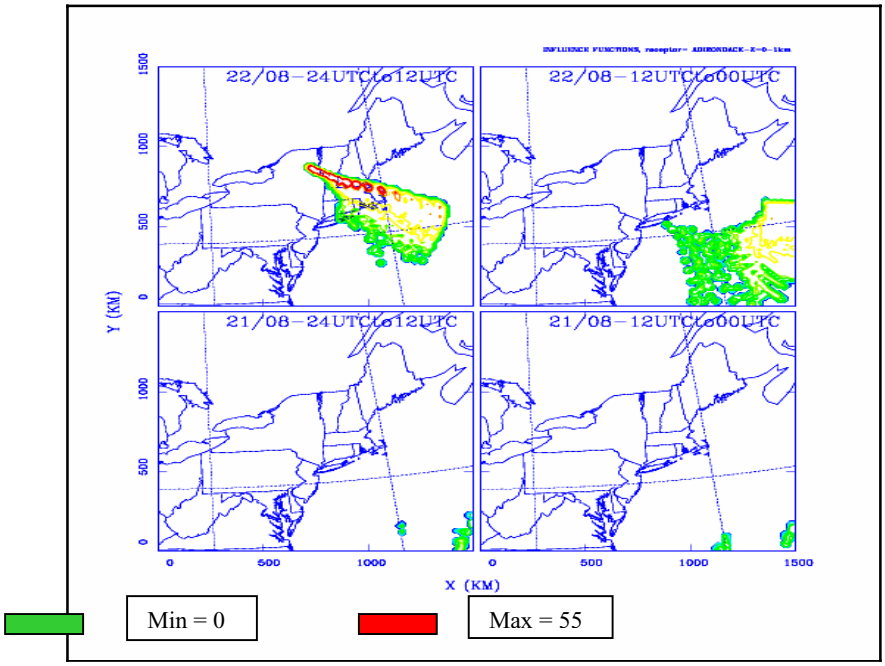

Figure 8: Influence functions calculated 48h backward in time for a receptor area centered at Adirondacks area (44.0N, 74.00W). Simulation started at 2400UTC, August 22, 1997. Each frame presents a 12h interval. Contours are in logarithmic normalized units (number of particles of unit mass per cubic meter).

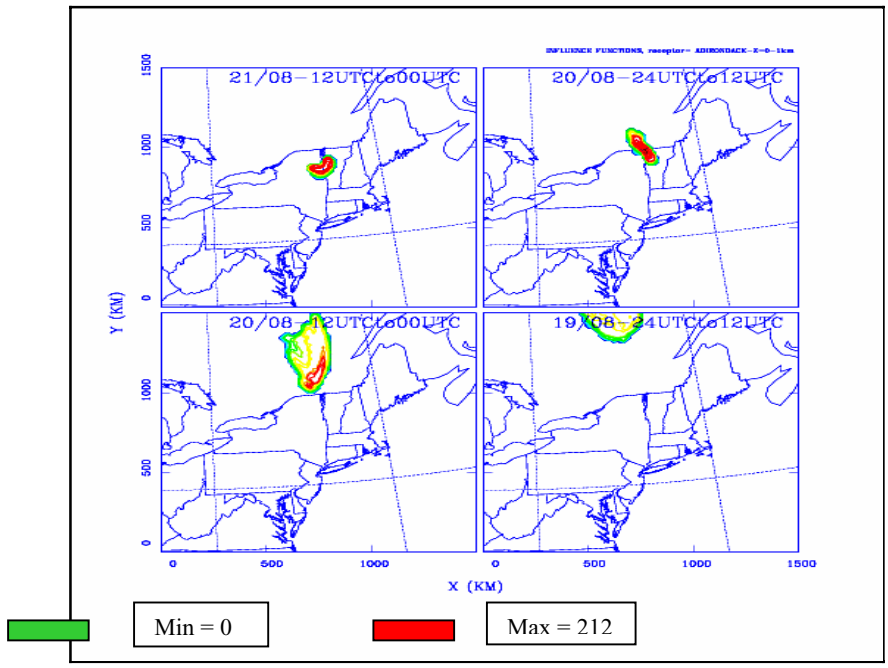

Figure 9: Influence functions calculated 48h backward in time for a receptor area centered at Adirondacks area (44.0N, 74.00W). Simulation started at 1200UTC, August 21, 1997. Each frame presents a 12h interval. Contours are in logarithmic normalized units (number of particles of unit mass per cubic meter).

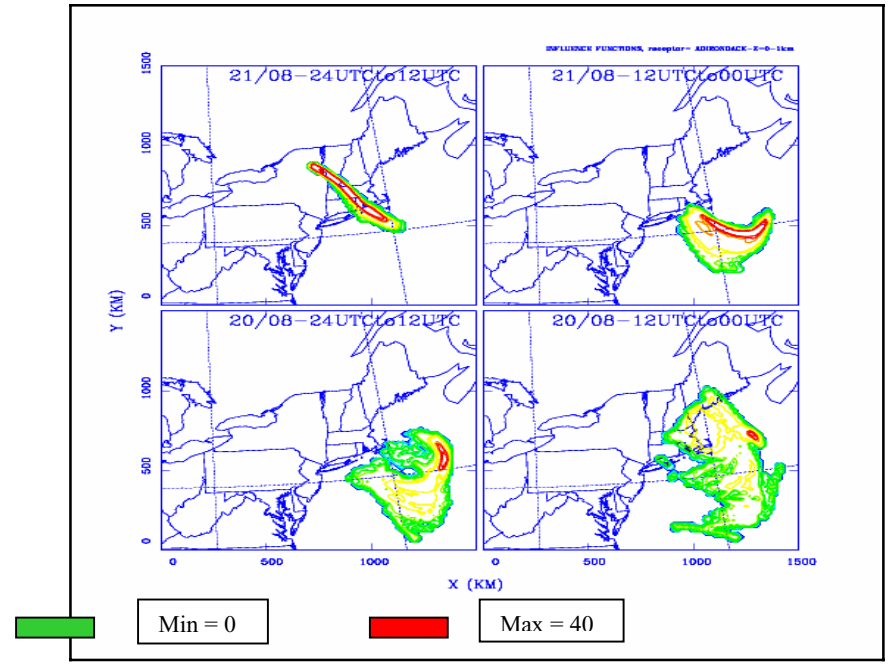

Figure 10: Influence functions calculated 48h backward in time for a receptor area centered at Adirondacks area (44.0N, 74.00W). Simulation started at 2400UTC, August 21, 1997. Each frame presents a 12h interval. Contours are in logarithmic normalized units (number of particles of unit mass per cubic meter).

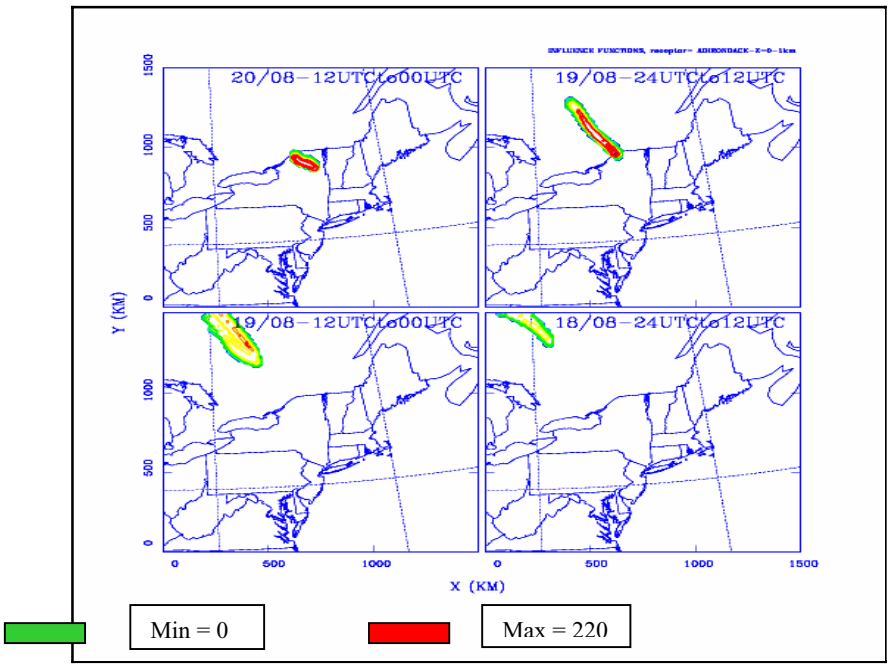

Figure 11: Influence functions calculated 48h backward in time for a receptor area centered at Adirondacks area (44.0N, 74.00W). Simulation started at 1200UTC, August 20, 1997. Each frame presents a 12h interval. Contours are in logarithmic normalized units (number of particles of unit mass per cubic meter).

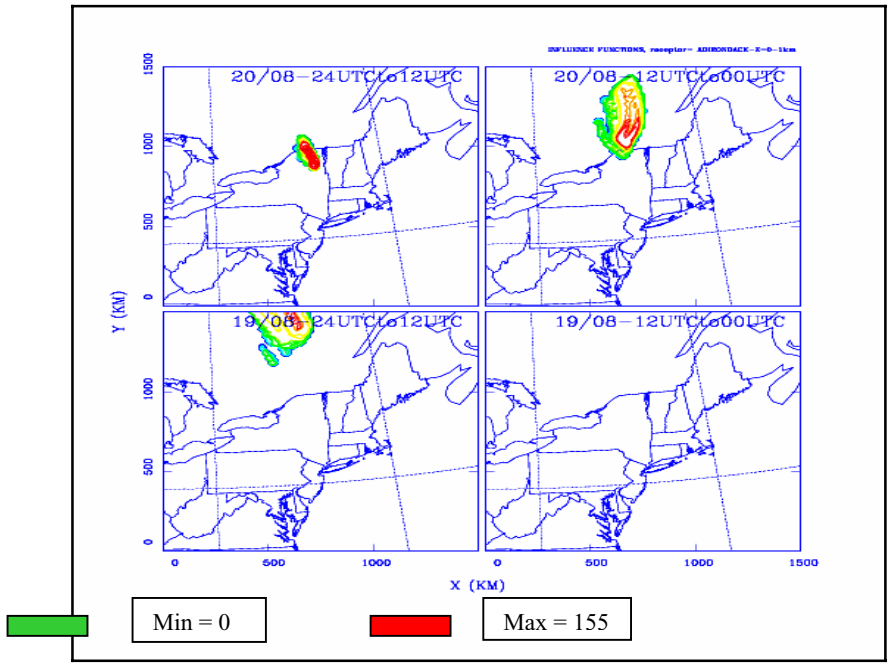

Figure 12: Influence functions calculated 48h backward in time for a receptor area centered at Adirondacks area (44.0N, 74.00W). Simulation started at 2400UTC, August 20, 1997. Each frame presents a 12h interval. Contours are in logarithmic normalized units (number of particles of unit mass per cubic meter).

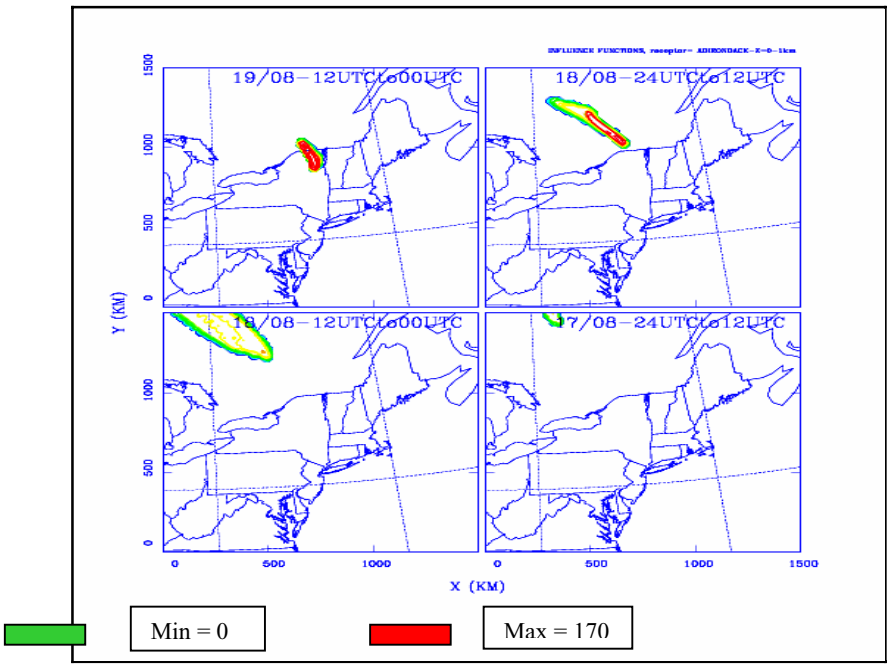

Figure 13: Influence functions calculated 48h backward in time for a receptor area centered at Adirondacks area (44.0N, 74.00W). Simulation started at 1200UTC, August 19, 1997. Each frame presents a 12h interval. Contours are in logarithmic normalized units (number of particles of unit mass per cubic meter).

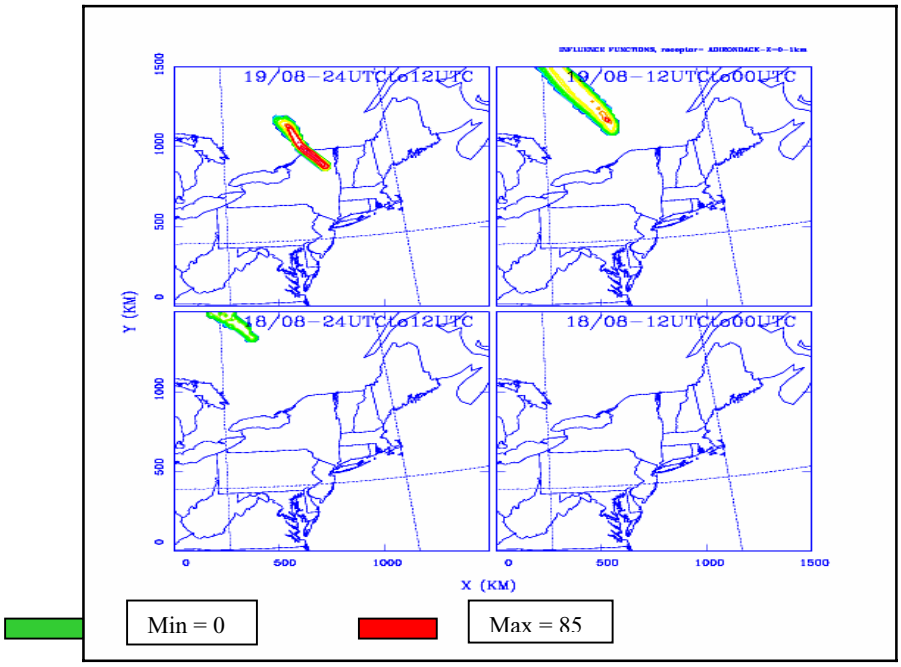

Figure 14: Influence functions calculated 48h backward in time for a receptor area centered at Adirondacks area (44.0N, 74.00W). Simulation started at 2400UTC, August 19, 1997. Each frame presents a 12h interval. Contours are in logarithmic normalized units (number of particles of unit mass per cubic meter).

For information on other
NYSERDA reports, contact:

New York State Energy Research
and Development Authority
17 Columbia Circle
Albany, New York 12203-6399

toll free: 1 (866) NYSERDA
local: (518) 862-1090
fax: (518) 862-1091

info@nyserda.org
www.nyserda.org

Atmospheric Transport and Fate of Mercury and its impacts on New York State

Final Report 05-05

State of New York
George E. Pataki, Governor

New York State Energy Research and Development Authority
Vincent A. DeIorio, Esq., Chairman
Peter R. Smith, President

NYSERDA